DISRUPTION OF SELECTIVE AUTOPHAGY IN COXSACKIEVIRUS B3 INFECTION

by

Junyan Shi

BMSc, Hebei Medical University, 2007

MMSc, Peking Union Medical College, Tsinghua University, 2010

A THESIS SUBMITTED IN PARTIAL FULFILLMENT OF

THE REQUIREMENTS FOR THE DEGREE OF

DOCTOR OF PHILOSOPHY

in

THE FACULTY OF GRADUATE AND POSTDOCTORAL STUDIES

(Pathology and Laboratory Medicine)

THE UNIVERSITY OF BRITISH COLUMBIA

(Vancouver)

July 2015

Abstract

Coxsackievirus infection induces an abnormal accumulation of ubiquitin aggregates that are generally believed to be harmful to the cells and play a key role in the pathogenesis of coxsackievirus-induced myocarditis and dilated cardiomyopathy. Selective autophagy mediated by autophagy adaptor proteins, including sequestosome 1 (SQSTM1/p62) and neighbor of BRCA1 gene 1 protein (NBR1), is an important pathway for disposing of misfolded proteins and damaged organelles. We demonstrated that SQSTM1 was cleaved following CVB3 infection through the proteolytic activity of viral proteinase $2A^{pro}$. The resulting cleavage fragments of SQSTM1 were no longer the substrates of autophagy, and their ability to form protein aggregates was greatly decreased due to incapability of interaction with ubiquitinated proteins. We further tested whether NBR1, a functional homolog of SQSTM1, can compensate for SQSTM1 loss-of-function after viral infection. Of interest, we found that NBR1 was also cleaved after coxsackievirus infection, excluding the possible compensation of NBR1 for the loss of SQSTM1. This cleavage took place at two sites mediated by virus-encoded proteinase $2A^{pro}$ and $3C^{pro}$, respectively. In addition to the loss-of-function, we showed that the C-terminal fragments of SQSTM1 and NBR1 exhibited a dominant-negative effect against native SQSTM1/NBR1, probably by competing for LC3 and ubiquitin chain binding. Apart from the disruption of selective autophagy, CVB3 infection also impaired autophagic flux as confirmed by flux assays with a combination of a tandem fluorescence-tagged LC3 stable cell line and a non-cleavable construct of SQSTM1. Finally, we studied the roles of SQSTM1 and NBR1 in autophagic degradation of depolarized mitochondria (referred to as mitophagy). Following mitochondrial depolarization induced by carbonyl cyanide m-chlorophenylhydrazone (CCCP), a mitochondrial

uncoupler to trigger mitophagy, we demonstrated that NBR1 did not appear to be required for mitochondrial clustering. Deficiency of NBR1 alone or in concert with SQSTM1 did not block the clearance of damaged mitochondria, suggesting that NBR1 is dispensable for mitophagy regardless of the status of SQSTM1. Taken together, the findings in this study suggest novel mechanisms in coxsackieviral pathogenesis: coxsackievirus infection induces abnormal accumulation of ubiquitin conjugates through the disruption of selective degradation of protein aggregates and blockage of autophagic flux.

Preface

All the work presented in this dissertation was primarily accomplished by me with the supervision from Dr. Honglin Luo. Dr. Luo and I conceived the projects and designed the experiments. I performed the majority of the experiments by various techniques except for the *in vitro* cleavage assays and plaque assays. I contributed to all the data analysis. The content of the dissertation is derived from two reviews and two original research papers. A modified portion of the review [**Shi J**, Luo H. Interplay between the cellular autophagy machinery and positive-stranded RNA viruses. *Acta Biochim Biophys Sin (Shanghai)*. 2012, 44(5):375-384.] is incorporated into **Chapter 1**. **Chapter 3** is based on a research paper published in *Autophagy* [**Shi J**, Wong J, Piesik P, Fung G, Zhang J, Jagdeo J, Li X, Jan E, Luo H. Cleavage of sequestosome 1/p62 by an enteroviral protease results in disrupted selective autophagy and impaired NFKB signaling. *Autophagy*. 2013, 9(10):1591-1603.] and a review published in *Future Microbiology* [Garmaroudi FS, Marchant D, Hendry R, Luo H, Yang D, Ye X, **Shi J**, McManus BM. Coxsackievirus B3 replication and pathogenesis. *Future Microbiol*. 2015, 10(4):629-653.]. **Chapter 4** is based on an article published in *Cell Death and Differentiation* [**Shi J**, Fung G, Piesik P, Zhang J, Luo H. Dominant-negative function of the C-terminal fragments of NBR1 and SQSTM1 generated during enteroviral infection. *Cell Death Differ*. 2014, 21(9):1432-1441.]. **Chapter 5** is based on a manuscript entitled "NBR1 is dispensable for PARK2-mediated mitophagy regardless of the presence or absence of SQSTM1" submitted to *Cell Death and Disease* [**Shi J**, Fung G, Deng H, Zhang J, Fiesel F, Springer W, Luo H]. The manuscript is under revision at the time of the online submission of my doctoral dissertation.

During my PhD study, I also conducted additional projects in collaboration with other lab members and contributed to five co-author peer-reviewed articles.

The reuse and reprint of all published work is with permission from journals as indicated. All genes/proteins conform to the recommendations of the HUGO gene nomenclature committee (HGNC).

All CVB3 studies were approved by the University of British Columbia Research Ethics Board (certificate number B14-0190).

Table of Contents

List of Tables

List of Figures

List of Abbreviations

ACTB: actin, beta

ATG: autophagy-related genes

BAF: bafilomycin A1

CC: coiled-coil domain

CCCP: carbonyl cyanide m-chlorophenylhydrazone

CVB3: coxsackievirus type B3

DAPI: 4, 6-diamidino-2-phenylindole

DCM: dilated cardiomyopathy

DMEM: Dulbecco's modified Eagle's medium

DMV: double-membrane vesicle

DPBS: Dulbecco's phosphate-buffered saline

eIF2α/4GI/II: eukaryotic initiation factor 2α, 4GI, or 4GII

FBS: fetal bovine serum

G241E: a SQSTM1 construct with the glycine (G) residue at position 241 replaced with glutamic acid (E)

G3BP: GTPase activating protein (SH3 domain) binding protein

HSC70: heat shock cognate 70 kDa protein 1

IL: interleukin

IRES: internal ribosomal entry site

KEAP1: kelch-like ECH-associated protein 1

KIR: keap1-interacting region

LAC: lactacystin

LAMP2: lysosome-associated membrane protein type 2

LC3: microtubule-associated protein 1 light chain 3 alpha

LIR: microtubule-associated protein 1 light chain alpha-interacting region

MAVS: mitochondrial antiviral signaling protein

MEFs: mouse embryonic fibroblasts

MQC: mitochondrial quality control

NBR1: neighbor of BRCA1 gene 1

NFE2L2: nuclear factor (erythroid-derived 2)-like 2

NFKB: nuclear factor of kappa light polypeptide gene enhancer in B-cells

nt: nucleotides

ORF: open reading frame

PARK2: parkin RBR E3 ubiquitin protein ligase

PB1: Phox/Bem1p domain

PE: phosphatidylethanolamine

PFU: plaque-forming unit

PINK1: PTEN-induced putative kinase 1

RT-qPCR: real-time quantitative reverse transcriptase PCR

SD: standard deviation

si-control: scramble siRNA

si-NBR1: *NBR1* siRNA

si-SQSTM1: *SQSTM1* siRNA

SQSTM1/p62: sequestosome 1

SQSTM1-C: C-terminal fragment of SQSTM1

SQSTM1-N: N-terminal fragment of SQSTM1

TB: tumor necrosis-associated factor 6 binding domain

TLRs: Toll-like receptors

TOMM20: mitochondrial import receptor subunit TOM20 homology

TRAF6: tumor necrosis- associated factor 6, E3 ubiquitin protein ligase

UBA: ubiquitin association domain

UTRs: untranslated regions

VDAC1: voltage-dependent anion channel 1

ZZ: zinc-finger domain

Acknowledgements

I would like to attribute all my research progress to my supervisor Dr. Honglin Luo. She not only impressed me by the knowledge she gained, but also enlightened me by her attitude and enthusiasm to the research. She encouraged me to attend conferences and present to the public, which benefits me greatly through broadening my research horizon and improving my presentation skills.

I give special thanks to my committee meeting members, Dr. Chun Seow, Dr. Decheng Yang, Dr. Colby Zaph, and Dr. Pascal Bernatchez, for their inspiring advices and suggestions. I acknowledge Dr. Eric Jan and Julienne Jagdeo for their help in performing the *in vitro* cleavage assays. I appreciate Dr. Masaaki Komatsu, Dr. Brett Finlay, Dr. Caroline Whitehouse, Dr. Sharon Gorski, and Dr. Wolfdieter Springer for generously providing cell lines or constructs.

I am grateful to the generous support and help from my previous and current lab members, Dr. Tse Yuan Wong (University of San Diego), Jingchun Zhang, Gabriel Fung, Haoyu Deng, and Paulina Piesik.

This research is supported by the Canadian Institutes of Health Research (CIHR) and the CIHR/National Science Foundation of China Joint Initiative. I had been supported by a Doctoral Fellowship from the China Scholarship Council from 2010-2014.

Personally, I give my great appreciation to my parents who brought me to this world and raised me up with so much care and love. They respected my decisions and unselfishly supported me along the years during my study from my hometown to Beijing, and from China to Canada. I owe lots of thanks to my husband and daughter for their understanding in those days when I worked late.

Chapter 1: Introduction

1.1 Myocarditis

1.1.1 Definition and epidemiology

Myocarditis is an inflammatory disease of the myocardium. According to the Dallas criteria, it is defined by the infiltration of immune cells and the presence of necrosis/apoptosis of cardiomyocytes without ischemic injury associated with coronary artery disease [1, 2]. Myocarditis accounts for 8.6-12% of sudden death in adults and about 21% of patients with myocarditis develop chronic dilated cardiomyopathy (DCM) [3, 4, 5, 6, 7, 8]. DCM is characterized by left ventricular dilatation and impaired cardiac output, contributing to arrhythmias, blood clots and ultimately heart failure. The 5-year mortality is as high as 46% in DCM [9]. Myocarditis can be caused by various factors, including infectious agents, immunological factors, and toxins, among which viruses are the primary causative agents of myocarditis in North America and Europe [1, 5, 10]. Enteroviruses, particularly coxsackievirus group B (CVB), such as CVB3 accounts for 30-50% of viral myocarditis in North America [11].

1.1.2 Viral myocarditis is a tri-phasic disease

The understanding of pathophysiology of viral myocarditis comes largely from animal studies. Viral myocarditis exhibits three distinct pathological phases during disease progression [12] (**Figure 1**). The first phase is viral replication. Cardiotrophic viruses enter the cells through receptor-mediated endocytosis. Coxsackie-adenoviral receptor (CAR) is identified as a cell membrane receptor for most enteroviruses [13]. Following viral entry, viruses synthesize viral RNA and protein to assemble viral particles. Meanwhile, the immune response is triggered either

by the direct activation of coreceptor-mediated signaling pathway or by the antigen presented through major histocompatibility complex-restricted pathway [12, 14]. The production of type I interferons (IFNs) plays a key role in the innate antiviral immune response [15]. The double-stranded RNAs (dsRNAs), intermediates of viral replication, are recognized by pathogen recognition receptors (PRRs). PRRs are classified into two groups: Toll-like receptor (TLR) family members (i.e., TLR3 and TLR7/8) and RIG-I-like receptors, including RIG-I, MDA5, and LGP2 [16]. TLR are mostly expressed in immune cells such as macrophages and dendritic cells, while RIG-I-like receptors are ubiquitously expressed [17]. The interaction between dsRNAs and PRRs leads to the production of IFNs through different pathways. Secreted IFNs bind type I IFN receptor (IFNAR) and activate JAK/STAT pathway, which ultimately results in the expression of interferon-stimulated genes (ISGs) [18]. Induction of ISGs is required for the restriction of viral replication and for viral clearance. However, picornaviruses have developed strategies to suppress the host IFN response to favor their own replication. It has been reported that MDA5 and its downstream adaptor protein MAVS are proteolytically targeted by CVB3 protease $2A^{pro}$, debilitating the production of IFN after CVB3 infection [19].

Activation of immune response facilitates the clearance of viruses; however, continuous and exuberant immune response also ensues the second phase of the disease, autoimmunity. It is suggested that autoimmunity may play a greater role in the pathogenesis of viral myocarditis than the primary viral damage [12]. One mechanism by which viruses break host self-tolerance is that virus-mediated damage of cardiomyocytes leads to modification or release of antigenic epitopes usually secluded from the immune system [20, 21]. Another mechanism proposed is antigenic mimicry between host proteins and virus particles [22, 23]. Autoimmunity is mediated by autoreactive T cells, auto-antibodies, and massive cytokines [12]. Auto-antibodies include those

targeting cardiac intracellular antigens (e.g., cardiac myosin heavy chain, cardiac troponin I, adenine nucleotide translocator, and branched-chain alpha-keto dehydrogenase) and antibodies against cardiac cell surface receptors (e.g., β1-adrenergic receptor and M2 muscarinic receptor) [24, 25]. As mediators in immune response, various cytokines are detected in CVB3-infected mouse heart tissues [26]. Patients with myocarditis have marked elevation of tumor necrosis factor alpha (TNF-α), interleukin (IL)-1, and IL-6 [27]. The increased expression of TNF-α, IL-1β, and IL-6 is associated with reduced heart contractility in CVB3-infected mice [28]. Cytokines may contribute to the development of DCM through the activation of matrix metalloproteinases [29].

The chronic sequela of myocarditis is DCM in the third phase. A low-level of viral genomes is present in cardiomyocytes and is attributed to myocyte loss by chronic and persistent activation of immune response [30]. Cardiomyocytes have limited ability of proliferation, leaving the region of damage with replacement of fibroblasts and deposition of collagen, a process described as cardiac remodeling [9]. Cardiac remodeling impairs cardiac contractility and cardiac output [31], resulting in a vicious cycle: cardiac dysfunction in turn leads to further cardiac reconstruction to ensure maximum cardiac output, and ultimately progresses to DCM and heart failure manifested by wall thinning and left ventricle dilatation [32].

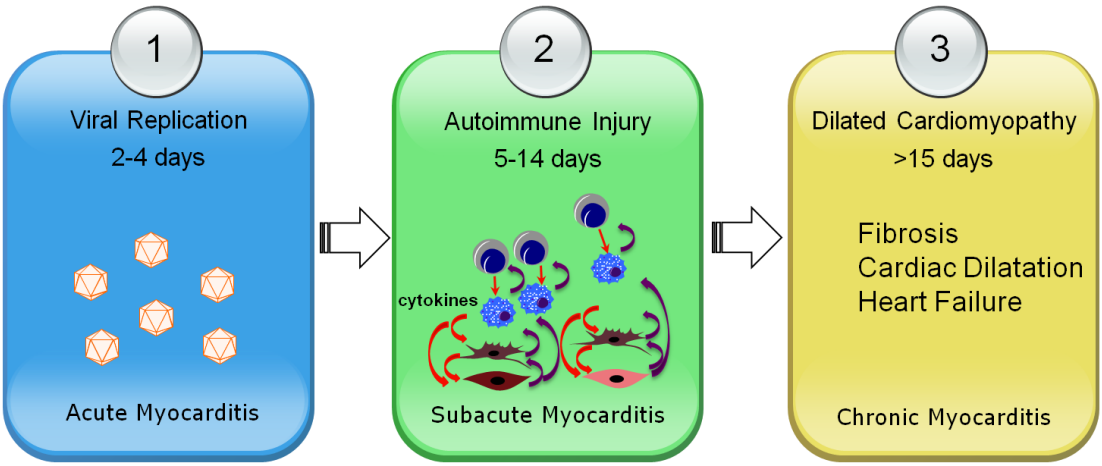

Figure 1. Three phases of viral myocarditis [33].

Viral myocarditis is a tri-phasic disease. Phase 1: Viral replication and direct injury. Phase 2: autoimmune injury mediated by autoreactive T cells, auto-antibodies, and massive cytokines. Phase 3: Dilated cardiomyopathy (DCM). The heart undergoes fibrosis and progresses to cardiac dilatation. Finally, DCM may develop heart failure.

1.1.3 Diagnosis and management of viral myocarditis

The diagnosis of viral myocarditis is based on clinical manifestations and laboratory tests. The majority of cases are asymptomatic, with only 10% of patients display clinical signs and symptoms, such as flu-like syndrome accompanied by fever, chest pain, heart failure, and ventricular dysfunction/dilatation [34, 35]. Laboratory tests may show elevated cardiac fraction of creatine kinase, increased erythrocyte sedimentation rate, raised leukocyte count, and electrocardiographic abnormalities [1, 9, 35]. Due to poor specificity of both clinical manifestations and laboratory tests, the gold standard for the diagnosis of myocarditis is endomyocardial biopsy [1].

The treatment of viral myocarditis varies by clinical presentation. In general, supportive care is the first line of therapy, such as the management of arrhythmia, tissue oxygenation, inotropic therapy, and loop diuretics to lower ventricular filling pressures [1, 9, 36, 37, 38]. Although ribavirin

and interferon alpha shows effectiveness *in vitro* and in mouse models of acute viral myocarditis when applied at the time of viral infection, currently no definite clinical evidence supports antiviral therapy in the management of acute viral myocarditis [38, 39, 40]. Animal studies demonstrate that suppression of cytokine expression by different modulators, such as specific neutralizing antibody or inhibitors, alleviates myocardial damage and improves cardiac function [41, 42, 43]; however, the response to immunosuppression therapy seems dependent on the duration of the disease in patients. A clinical trial demonstrates that patients with acute viral myocarditis do not benefit from immunosuppression [36]; however, patients with chronic symptoms for more than 6 months response positively to immunosuppressive agents [44, 45, 46]. Knockout mice lacking $CD4^+$ and $CD8^+$ T lymphocytes have less severe cellular inflammation and mortality after CVB infection, suggesting that selective manipulation of different subsets of immune cells maybe a more effective intervention [47]. The timing of any treatment is also a critical determinant of efficacy.

1.1.4 Viral myocarditis has emerged as a disease of protein dyshomeostasis

Previous studies have provided valuable insights into the nature of myocarditis; however, currently there is no effective therapeutic available. Other mechanisms underlying myocarditis and the resulting DCM and heart failure remain to be fully understood. Protein homeostasis is important to the overall health of cells, particularly in post-mitotic cells with no or poor regenerative capability, such as the brain and heart. It is well known that the brain suffers from numerous proteinopathies, such as Huntington Disease, Parkinson Disease, prion disease, and amyotrophic lateral sclerosis that are characterized by the accumulation of protein aggregates [48, 49, 50, 51, 52, 53]. Proteotoxicity generated by protein aggregates, or any of the preceding

intermediaries, has been implicated in the pathogenesis of neurodegenerative diseases. Similarly, studies have begun to establish the necessity and sufficiency of proteotoxicity as a major pathogenic factor in the heart [44, 47, 54, 55]. A dramatic induction of ubiquitinated protein aggregates and amyloid oligomers has been observed in the hearts of DCM patients [56, 57, 58]. Cardiomyocyte specific expression of a pre-amyloid oligomer causes heart failure, establishing the cause and effect relationship of protein misfolding and cardiac dysfunction [59]. We previously found that CVB3 infection results in increased accumulation of protein-ubiquitin conjugates both *in vitro* and *in vivo* [60, 61]. Consistently, amyloid oligomers were apparently increased in CVB3-infected mouse hearts (**Figure 2**, unpublished data). The accumulation of misfolded protein aggregates appears to be an uncovered mechanism in the pathogenesis of viral myocarditis. Understanding the formation and clearance of protein aggregates is a pivotal step towards the insight into this disease.

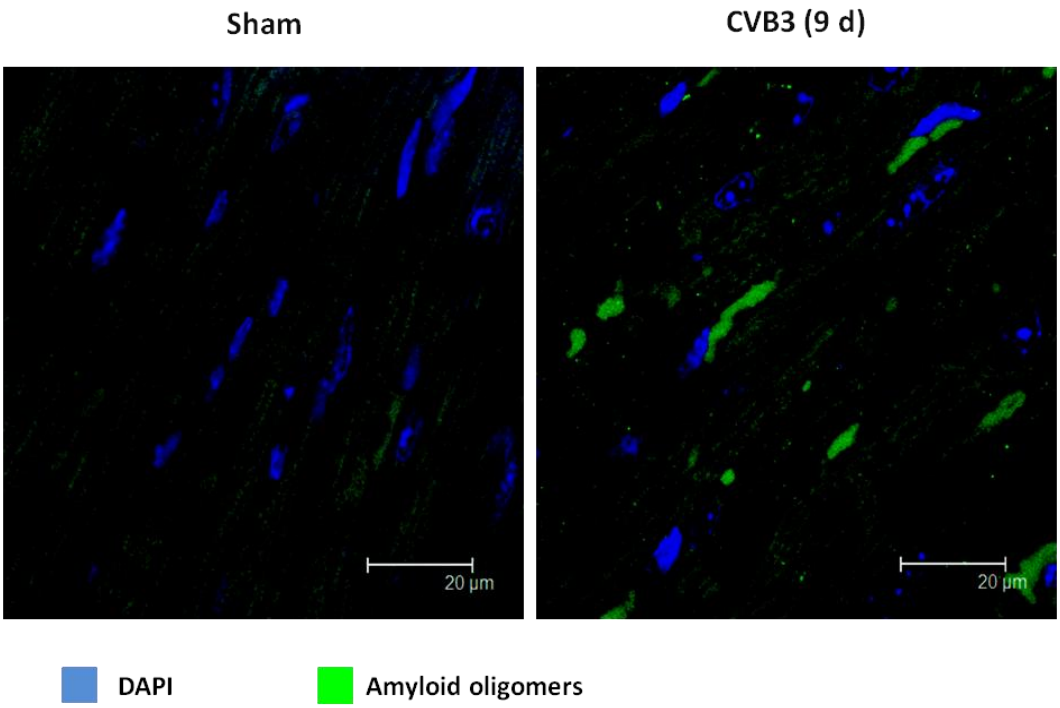

Figure 2. Accumulation of amyloid oligomers in CVB3-infected mouse hearts.

A/J mice were infected with CVB3 [10^5 PFU of Nancy stain] or phosphate-buffered saline (PBS; sham infection). At 9 days (d) after infection mice were sacrificed and heart tissues were harvested. Mouse heart tissues were probed with an antibody against amyloid oligomers (stained in green), and nuclei were counterstained in blue with DAPI.

1.2 Coxsackievirus

1.2.1 Classification

Coxsackievirus belongs to *Enterovirus* genus, *Picornaviridae* family. Coxsackievirus is the second species of enterovirus discovered after poliovirus, named according to the geographical site of isolation in the upstate New York town of Coxsackie [35]. Group A coxsackievirus (CVA) is composed of 23 serotypes, including CVA1-22 and 24. Group B coxsackievirus comprises 6 serotypes, including CVB1-6. A distinction between the two groups is based on the symptoms in

mouse models after virus inoculation. CVA induces flaccid paralysis and affects skeletal and heart muscle, while CVB causes spastic paralysis and widespread damages in the central nervous system (CNS), liver, exocrine pancreas, brown fat, and striated muscle [62]. In the 6 serotypes of CVB, CVB1, 3, and 5 are known to have heart tropism [63]. Virulence of viral infection depends on host factors, such as physical-activity level, sex, age, and genetic background [1].

1.2.2 Structure and functions of viral proteins

CVB3 is a non-enveloped virus containing a single, positive-stranded RNA genome with a 30 nm icosahedral capsid [64, 65]. *Picornaviridae* family shares a conserved genome structure composed of a single open reading frame (ORF) flanked by untranslated regions (UTRs) at both ends. In CVB3, the long 5′UTR (742 nt) is covalently linked to the small viral protein 3B (also known as VPg) and contains cis-acting structural elements, a 5′ terminal domain involved in replication, and an internal ribosomal entry site (IRES) directing translation initiation [66, 67, 68]. IRES element is shared by all picornaviruses but varies in the secondary structures [69, 70]. The short 3′UTR (100 nt) is followed by a polyadenylated tail [65, 68]. The ORF encodes a polyprotein which is subsequently proteolytically cleaved into three primary precursor molecules, P1, P2, and P3. The primary precursors are further cleaved into several intermediates (2BC, 3AB, and 3CD) and 11 mature viral proteins during and after translation. The mature proteins include structural proteins (VP1, VP2, VP3, and VP4) for viral capsid assembly, viral proteinases ($2A^{pro}$ and $3C^{pro}$) that can cleave a number of virus and host proteins, host membrane modifiers (2B and 3A) that can increase plasma membrane permeability and inhibit cellular secretion, an RNA-dependent-RNA polymerase (3D), an ATPase (2C), and a small polypeptide priming RNA synthesis (3B) [33, 71]. The organization of CVB3 viral proteins is illustrated in **Figure 3**.

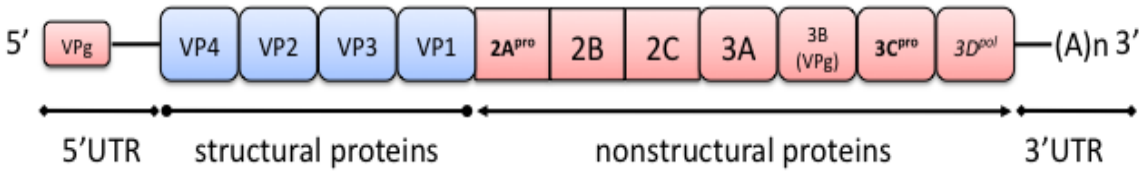

Figure 3. Schematic diagram of coxsackievirus type B3 (CVB3) genome organization.
The open reading frame (ORF) of CVB3 is flanked by 5′ and 3′ untranslated regions (UTRs). The ORF encodes 4 structural viral capsid proteins (VP1-4) and 7 nonstructural proteins (2A, 2B, 2C, 3A, 3B, 3C, and 3D).

1.2.3 Proteolytic cleavage of host proteins by enteroviral proteinases

In addition to cleaving viral precursor polyprotein into mature and functional proteins, enteroviral proteinases also elicit proteolytic cleavage of a number of host proteins sharing the consensus sequences, resulting in the hijack of cellular functions to facilitate viral infection and disruption of host antiviral responses (**Table 1**).

One of the well-characterized cleavage events during viral infection is the cleavage of eukaryotic translation initiation factors 4G (eIF4G) by poliovirus $2A^{pro}$ proteinase [72, 73]. Cleavage of eIF4G disrupts host cap-dependent translation and partially results in host protein translation shut-off, a strategy to facilitate viral IRES-dependent protein synthesis. Viral proteinases also target host anti-viral signaling pathways. For instance, the cleavage of MDA5, mitochondrial antiviral signaling protein (MAVS), and RIG-I by CVB3 proteinase $2A^{pro}/3C^{pro}$ results in the attenuation of type I interferon production and compromise of anti-viral response [19]. Apart from the effects on viral proliferation, the cleavage of host proteins leads to the change of host physiological function. A case in point is the disruption of myocyte contractibility caused by the cleavage of a cardiac-restricted cytoskeletal protein dystrophin (DMD) [74].

Table 1. Host proteins cleaved by enteroviral proteinases $2A^{pro}$ and $3C^{pro}$.

Proteinase	Virus	Function	Protein	Reference
3C	PV	Transcription	Oct-1	75
3C	PV		TBP	76, 77
3C	PV		CREB	78
3C	PV		TFIIIC	79
3C	PV		La	80
2A	CVB3		SRF	81
3C	PV		TP53	82
2A	CVB4	Translation	eIF4GI	83
2A	HRV		eIF4GII	72
3C	PV1, CVB3, HRV		eIF5B	84
2A, 3C	PV		PABP	85
3C	PV, CVB3		G3BP	86, 87
3C	PV		PCBP	88
2A	CVB3	Immune response	MDA5	19
2A, 3C	CVB3		MAVS	19, 89
3C	CVB3		RIG-I	19
3C	CVB3		TRIF	89
3C	PV, HRV		p65-RelA	90
3C	PV		PTB	91
2A	CVB3	Cytoskeleton	DMD	92
2A	HRV2, CVB4		Cytokeratin 8	93
3C	PV, HRV14		MAP-4	94
3C	EV71	RNA or genome processing	CstF-64	95
3C	CVB3		AUF1	96
3C	CVB3		TDP43	97

Abbreviations: PV, poliovirus; CVB, coxsackievirus type B; HRV, human rhinovirus; EV, enterovirus; Oct-1, octamer-binding transcription factor; TBP, TATA-binding protein; CREB, cyclic AMP-responsive element-binding protein; TFIIIC, Pol III DNA-binding transcription factor; SRF, serum response factor; TP53, tumor protein p53; eIF4GI, eIF4GII, and eIF5B, eukaryotic translation initiation factor 4GI, II, and 5B; PABP, poly(A)-binding protein; G3BP, GTPase activating protein (SH3 domain) binding protein; PCBP, poly(rC)-binding protein; MAVS, mitochondrial antiviral signaling protein; TRIF, Toll/IL-1 receptor domain-containing

adaptor inducing interferon-beta;p65-RelA, p65-RelA subunit of the NFKB complex; PTB, polypyrimidine tract-binding protein;MAP-4, microtubule-associated protein 4; CstF-64, nuclear factor CstF-64; AUF1, adenosine-uridine (AU)-rich element RNA binding factor 1; TDP43, transactive response DNA-binding protein 43; DMD, dystrophin.

1.3 Autophagy

1.3.1 Autophagy: mechanism, regulation, and general function

Autophagy is a protein degradation system in eukaryotes. Three types of autophagy have been identified, including macroautophagy, microautophagy, and chaperone-mediated autophagy [98, 99, 100]. The classification is based on how the cargo is delivered to the lysosome. Microautophagy is a process with the direct sequestration of substrates by lysosomes through membrane invagination. In chaperone-mediated autophagy, the substrates with a consensus sequence (KFERQ) are first recognized and translocated to lysosomes by cytosolic chaperone heat shock cognate 70 kDa protein 1 (HSC70) [99, 101], followed by internalization to lysosomes through the interaction of lysosome-associated membrane protein type 2A (LAMP-2A) and LAMP-2A receptor [100].

The process of macroautophagy (hereafter referred to as autophagy) can be divided into four sequential steps (**Figure 4**). Initially, a crescent-shaped double-membrane vesicle (DMV) called an isolation membrane or phagophore is formed to sequester misfolded proteins and damaged organelles (induction and nucleation step). Subsequently, two ends of the phagophore fuse to form a complete DMV termed an autophagosome (elongation step). Finally, the outer membrane of the autophagosome fuses with lysosome to form an autolysosome while the inner membrane and the cargo enwrapped in the autophagosome are degraded by hydrolysis (fusion step). Autophagosomes can also fuse with early or late endosomes to form amphisomes [102].

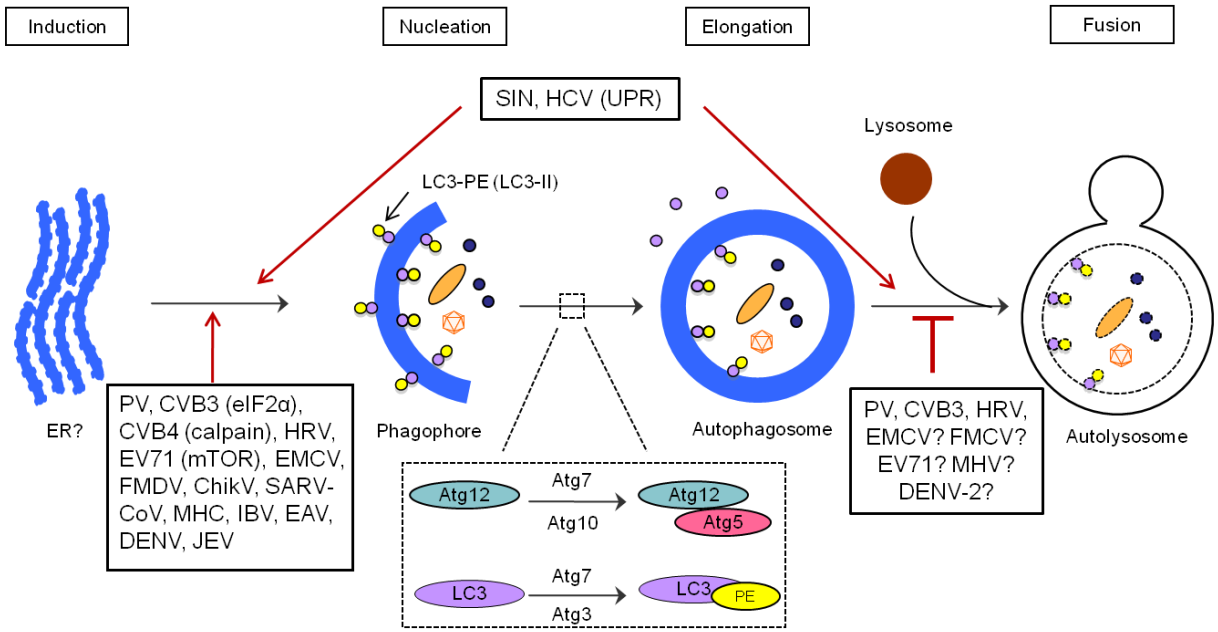

Figure 4. The activation of autophagy pathway by different positive-stranded RNA viruses. The process of autophagy consists of four steps: induction, nucleation, elongation, and fusion with lysosome. Two ubiquitination-like conjugation systems, Atg12-Atg5 and LC3-PE, are essential for the formation of autophagosomes. Positive-stranded RNA viruses induce either complete or incomplete autophagy as indicated. ER stress-induced UPR, eIF2α phosphorylation and the mTOR/p70S6K signaling pathway have been associated with the activation of autophagy in HCV, EV71 and CVB3 infection, respectively. The calpain pathway is required for the activation of autophagy in CVB4 infection. Abbreviations: ER, endoplasmic reticulum; UPR, unfolded protein response; eIF2α, eukaryotic initiation factor 2α; mTOR, mammalian target of rapamycin; p70S6K, p70 ribosomal protein S6 kinase; PE, phosphatidylethanolamine; PV, poliovirus ; CVB, coxsackievirus type B; HRV, human rhinovirus; EV71, enterovirus 71; EMCV, encephalomyocarditis virus; FMDV, foot and mouth disease virus; ChikV, chikungunya virus; SARS-CoV, severe acute respiratory syndrome-coronavirus; MHV, mouse hepatitis virus; IBV, infectious bronchitis virus; EAV, equine arteritis virus; DENV, dengue virus; JEV, Japanese encephalitis virus; SIN, sindbis virus; HCV, hepatitis C virus.

More than 30 autophagy-related (*Atg*) genes have been identified to participate in the autophagic process [103, 104, 105]. The key proteins involved in the formation of autophagosome include: (1) ULK complex, composed of ULK1, ULK2, Atg13, focal adhesion kinase family interacting protein of 200 kDa (FIP200) and Atg101; (2) class III PI3-kinase complex, comprising of Vps34, p150, beclin-1, Atg14 and Ambra1; (3) two ubiquitination-like conjugation systems, composed of Atg4, Atg12, Atg5, Atg16L1, Atg7, Atg10, Atg3, and microtubule-associated protein light chain alpha (LC3) [103, 104, 105]. Other mammalian homologues of LC3 have also been discovered, such as γ-aminobutyric-acid-type-A-receptor-associated protein (GABARAP) and Golgi-associated ATPase enhancer of 16 kDa (GATE16) [106, 107].

The two conjugation systems are essential for the formation of autophagosome (**Figure 4**). For Atg5-Atg12 conjugation, Atg12 is first activated by Atg7 and then transferred to Atg10. Atg12 finally forms a conjugate with Atg5 to activate the formation of the autophagosome [108]. For LC3-phosphatidylethanolamine (PE) conjugation, nascent LC3 is first cleaved by Atg4 to become LC3-I, which is subsequently activated by Atg7 and then transferred to Atg3. Finally, LC3 is conjugated to PE to form a LC3-PE complex (LC3-II), which participates in the formation of autophagosome [108]. Recruitment of LC3 protein to autophagic vesicles has been considered a common trait of autophagosome formation. In addition, conversion from LC3-I to LC3-II has been widely accepted as a marker for detection of autophagosome [109].

Autophagosome formation is also tightly controlled by multiple signaling pathways. Autophagic protein beclin-1 forms the class III PI3-kinase complex with VPS34, a class III PI3-kinase, to facilitate autophagosome formation by providing phosphatidyliositol 3-phosphates to the isolation membrane [110, 111]. The mammalian target of rapamycin (mTOR) and the eukaryotic

initiation factor 2α (eIF2α) kinases also participate in the autophagy process by negatively and positively regulating the formation of autophagosomes, respectively [112, 113].

Autophagy functions as a protein quality control system (**Figure 5**). Thus, defects in autophagy have been associated with several pathological conditions, such as neurodegenerative diseases, myopathy, and cancer [114, 115, 116]. Autophagy has also been implicated in the modulation of infection and immunity. Autophagy serves as a critical component of innate immune response by removing bacteria, viruses and protozoans from the host cells through xenophagy, whose targets are foreign bodies rather than self-molecules [117, 118]. The antigens are then presented through MHC class II molecules, initiating adaptive immune response [119]. In this process, autophagy participates and assists both innate and adaptive immunity to clear the pathogens. However, as opposed to the anti-viral activity, many positive-stranded RNA viruses have successfully developed strategies to hijack autophagy to foster their replication (**Figure 4**). The interplay between autophagy and RNA viruses will be discussed in detail below.

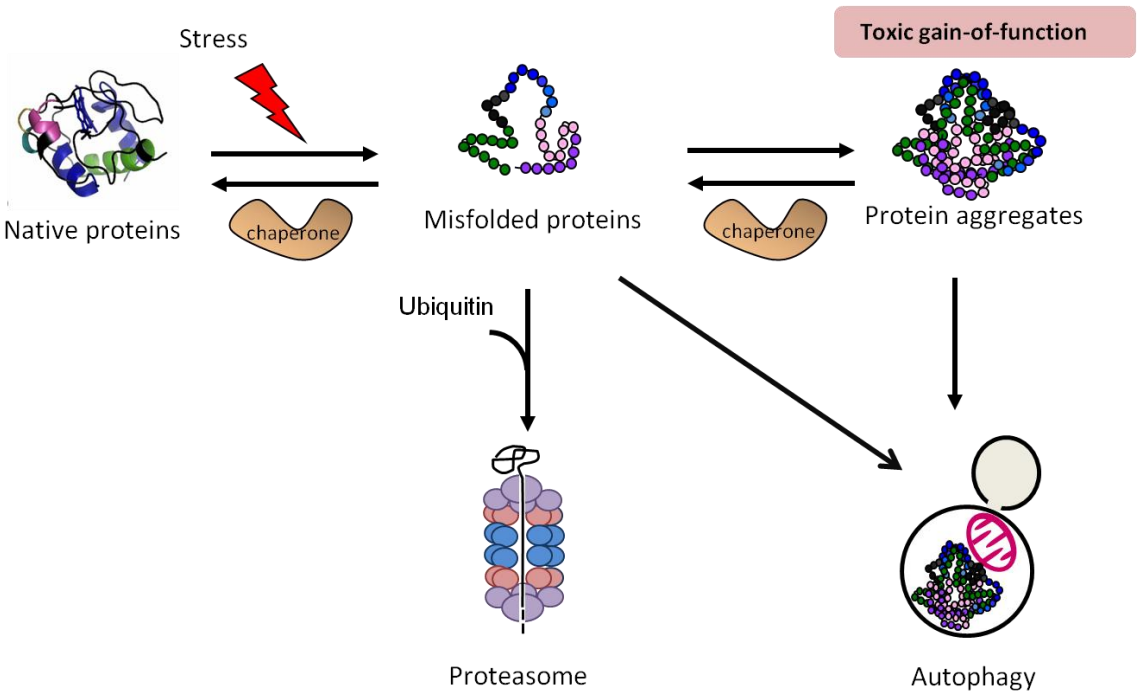

Figure 5. Autophagy in protein quality control.

The protein quality control system consists of molecular chaperones and two protein degradation pathways. Chaperone proteins function as the first line of defense for protein quality control. They help correct protein misfolding and prevent the formation of protein aggregates. Terminally-damaged protein or protein aggregates are delivered to the ubiquitin-proteasome system or autophagy pathway for degradation. The narrow barrel structure of the proteasome prevents the entry of large protein aggregates for degradation. Therefore, the clearance of protein aggregates requires autophagy.

1.3.2 Selective autophagy

Autophagy was traditionally regarded as a non-selective degradation process mainly trigged by starvation. Accumulated evidence in current studies supports the notion that autophagy is highly selective [120, 121, 122]. Different types of selective autophagy have been identified (**Figure 6**). Although the mechanism of cargo recognition is not fully understood, ubiquitination is a

common signal that tags the substrates for selective degradation [123, 124, 125, 126 127]. Selective autophagy is mediated by adaptor proteins that share both a LC3-interacting region (LIR) and an ubiquitin association (UBA) domain. To date, at least five adaptor proteins, e.g., sequestosome 1 (SQSTM1)/p62, neighbor of BRCA1 gene 1 (NBR1), calcium binding and coiled-coil domain 2 (NDP52), TRAF-interacting protein with forkhead-associated domain (T6BP), and optineurin, have been identified [126, 128, 129, 130, 131]. The adaptor proteins interact with ubiquitinated cargo via UBA domain. The interaction between LIR domain and LC3 is crucial for the recruitment of cargo to the inner surface of phagophore [132].

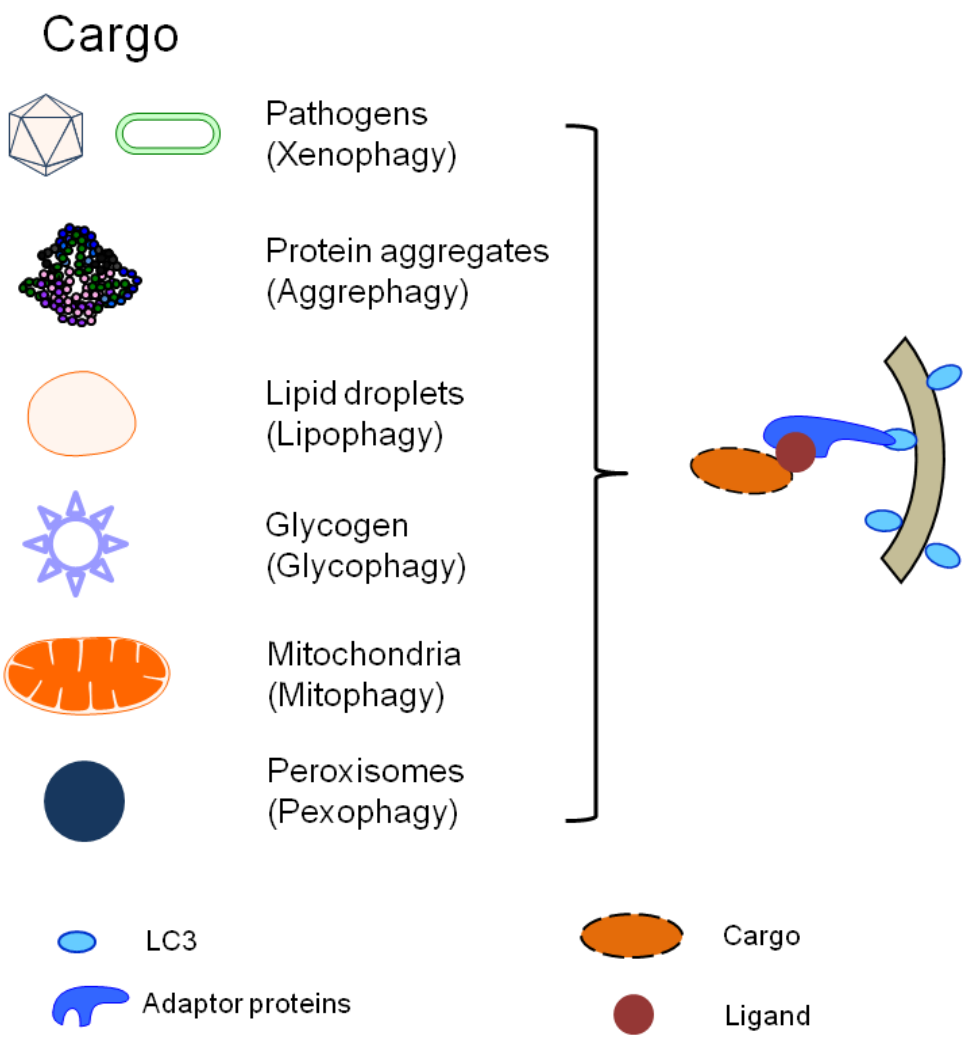

Figure 6. Selective degradation of substrates through autophagy pathway.

Invading pathogens (e.g., bacteria and viruses), intracellular materials (protein aggregates, lipid droplets, and glycogen), and organelles (mitochondria and peroxisomes) can be selectively targeted for autophagic degradation. Autophagy adaptor proteins interact with both LC3 and selective substrates (generally ubiquitinated) to ensure successful cargo loading.

1.3.3 Autophagy in cardiac diseases

As a protein quality control system, a basal level of autophagy is important to maintain normal cardiac function. Cardiac-specific loss of autophagy in adult mice by temporally controlled depletion of *Atg5*, a protein required for autophagy, results in a severe phenotype manifested by cardiac hypertrophy, left ventricular dilatation and contractile dysfunction, as well as increased ubiquitination in mouse hearts at the molecular level [133]. Mice with cardiac-specific deficiency of *Atg5* early in embryogenesis show normal cardiac structure and function up to 10 weeks old. However, *Atg5*-deficient mice develop early-onset cardiac dysfunction and have a shorter life span as compared to control mice, suggesting the importance of constitutive autophagy in maintaining normal cardiac structure and function [134]. Under disease condition, the down-regulated autophagy level in desmin-related myopathy mouse model can be rescued by forced expression of Atg7, another protein required for autophagy, and the characteristic protein aggregates are significantly decreased [135].

The role of autophagy in cardiac function is further addressed by the understanding of human Danon cardiomyopathy, an X-linked disease with deficient lysosome-associated membrane protein type 2 (LAMP2). LAMP2 deficiency results in compromised ability of autophagosome and lysosome fusion, which is attributed to the buildup of glycogen, morphologically abnormal lysosomes, and accumulation of autophagic vacuoles [136, 137, 138, 139].

While autophagy is deemed cytoprotective in aforementioned cases, the process may be detrimental under certain conditions, such as alcoholic cardiomyopathy, ischemia/reperfusion, pressure overload [140, 141, 142, 143]. Thus, delicate regulatory balance is desired to avoid insufficient or excessive autophagy under physiological and pathological conditions.

1.3.4 Autophagy in viral infection

1.3.4.1 Pro-viral effects of autophagy

One of the common features shared by positive-stranded RNA viruses is to assemble and replicate on intracellular membranes [144, 145, 146, 147]. The functions of the membranous structures are proposed to provide a scaffold for anchoring and concentrating the replication complexes to prevent the immune response triggered by dsRNA intermediates and to afford certain lipids required by genome synthesis [148]. The replication complexes are usually composed of viral RNA-dependent RNA polymerase, accessory non-structural proteins with helicase and nucleotide triphosphate activity, viral RNA, and host cell factors.

As parts of the intracellular membranous structures, autophagosomes or amphisomes have been shown to function as scaffolds required for the replication and assembly of certain positive-stranded RNA viruses. Confocal microscopy showed the co-localization of polioviral protein 3A, a critical component of the poliovirus RNA replication complex, with the autophagosome marker LC3 [149]. DENV non-structural protein NS1 and dsRNA were reported to co-localize with LC3 and ribosomal protein L28 [150, 151]. Immuno-electron microscopy also showed co-localization of EV71 capsid protein VP1 with autophagosomes in virus-infected mouse neurons [152]. Confocal and immune-electron microscopy revealed that both non-structural protein 3A and capsid protein VP1 co-localize with autophagosomes during EMCV infection [153]. Co-localizations of non-structural proteins 2B, 2C, and 3A with LC3 and between structural protein VP1 and Atg5 were also reported in FMDV-infected cells [154]. The ultrastructural analysis showed that the ChikV virions locate in the lumen of autophagomes-like vacuoles [155].

Similar to other positive-stranded RNA viruses, HCV infection induces intracellular membrane redistribution. However, controversy exists as to whether autophagosomes serve as

sites for HCV replication. By sucrose gradient analysis, LC3-II was found to co-sediment with HCV RNA and non-structural proteins NS3 and NS5A [156]. However, confocal microscopy showed little evidence of co-localization of LC3 or Atg5 with HCV core, NS3, NS4A/4B, and NS5A proteins [157, 158, 159, 160]. Moreover, it was demonstrated that knockdown of either LAMP2 or Rab7, two critical proteins responsible for the fusion of autophagosome with lysosome, inhibits HCV viral replication [161]. These studies suggest that autophagosome may not be a major site for HCV genome replication.

Although MHV replication complexes were found to be associated with LC3 and Atg12 [162], conflicting results were also reported with regard to the role of autophagy in MHV replication. As opposed to the findings in embryonic stem cell lines that autophagy induced by MHV enhances viral replication, likely through providing a replication site [162], using primary macrophages and murine embryonic fibroblasts it was found that MHV replication does not require the autophagy gene Atg5 [163].

Although direct evidence of the association of viral replication complexes with autophagosomes is lacking for CVB3, blockage of the fusion between autophagosomes and lysosomes using pharmacological inhibitors or knockdown of the genes critical for this fusion increases the accumulation of autophagosomes in virally infected cells and consequently leads to enhanced viral replication [164]. This study provides indirect evidence that the autophagosome is a critical component during CVB3 replication, likely by serving as virus anchoring and replication sites. Similar to the observation in CVB3, inhibition of the fusion between autophagosomes or amphisomes and lysosomes was found to increase the viral yield of DENV-2 [151]. This data together with the discoveries that DENV-2 replication complexes co-localize with LC3 and an endosome marker implies that DENV-2 may use the amphisomes as sites for viral replication [151].

However, this effect seems to be viral serotype-specific. It was found that inhibition of lysosome fusion reduces DENV-3 yields and results in an accumulation of viral NS1 [150]. The mechanisms through which autophagy favors DENV-3 replication remain elusive.

In addition to providing the replication lattice, autophagy has multiple pro-viral roles in viral infections. Currently known pro-viral mechanisms include: promoting viral entry/uncoating and non-lytic release [149, 151, 165, 166, 167], suppressing innate anti-viral immunity [161, 168], regulation of cellular metabolism, and prevention of premature cell death [169, 170, 171].

In summary, the pro-viral functions of autophagy in positive-stranded RNA viral life cycle apparently involve multiple pathways, either direct effects on viral replication or indirect influences on the host immune and non-immune-related activities.

1.3.4.2 Anti-viral effects of autophagy

The autophagy machinery is not always beneficial for positive-stranded RNA viruses. It has been shown that autophagy functions as an anti-viral host defense against SIN infection (**Figure 7**) [172, 173]. In response to SIN infection, mice with beclin-1 overexpression have improved survival rate, reduced viral loads, and attenuated viral pathogenesis as compared to control mice [172]. A study using neuron-specific Atg5 knockout mice showed that disruption of Atg5 gene leads to enhanced susceptibility of the mouse central nervous system to SIN infection [173]. Further investigation demonstrated that loss of Atg5 in SIN-infected neurons results in impaired viral capsid protein clearance, increased SQSTM1 accumulation, and accelerated cell death, without affecting viral growth/spread and type I interferon production [173]. The *in vitro* study showed that SQSTM1 binds directly to viral capsid protein and transports it to autophagosomes for lysosome-mediated degradation [173]. Electron microscopic analysis provided the direct evidence that SIN

virions are captured inside the autophagosome or autolysosome [173]. This study suggests that Atg5 plays a crucial role in protecting against SIN infection in mouse central nervous system by promoting SQSTM1-mediated clearance of viral proteins, rather than modulating innate immune response or viral growth/spread [173]. Further study is required to elucidate the exact mechanisms by which SQSTM1 mediates selective autophagic degradation of SIN capsid protein.

Toll-like receptors (TLRs) play an important role in innate anti-viral immunity against CVB3 infection (**Figure 7**) [174]. It was recently reported that autophagy plays a significant role in TLR-mediated type I interferon signaling during CVB3 infection [175]. It was found that blockage of autophagy by either gene-silencing of LC3-II, beclin-1 or Atg5, or using pharmacological inhibitor 3-MA inhibits TLR3 signaling in response to dsRNA. Interestingly, in contrast to the earlier observation that incomplete autophagy increases CVB3 replication [164], it was demonstrated that complete autophagy is required for the activation of signaling triggered by TLR3, as inhibition of lysosome activity by bafilomycin A1 (BAF) or chloroquine results in decreased type I interferon signaling [175]. The detail mechanisms in relation to a dual function of autophagy in supporting CVB3 replication by providing replication scaffolds and suppressing viral growth by triggering TLR3-mediated innate immune response require further investigation.

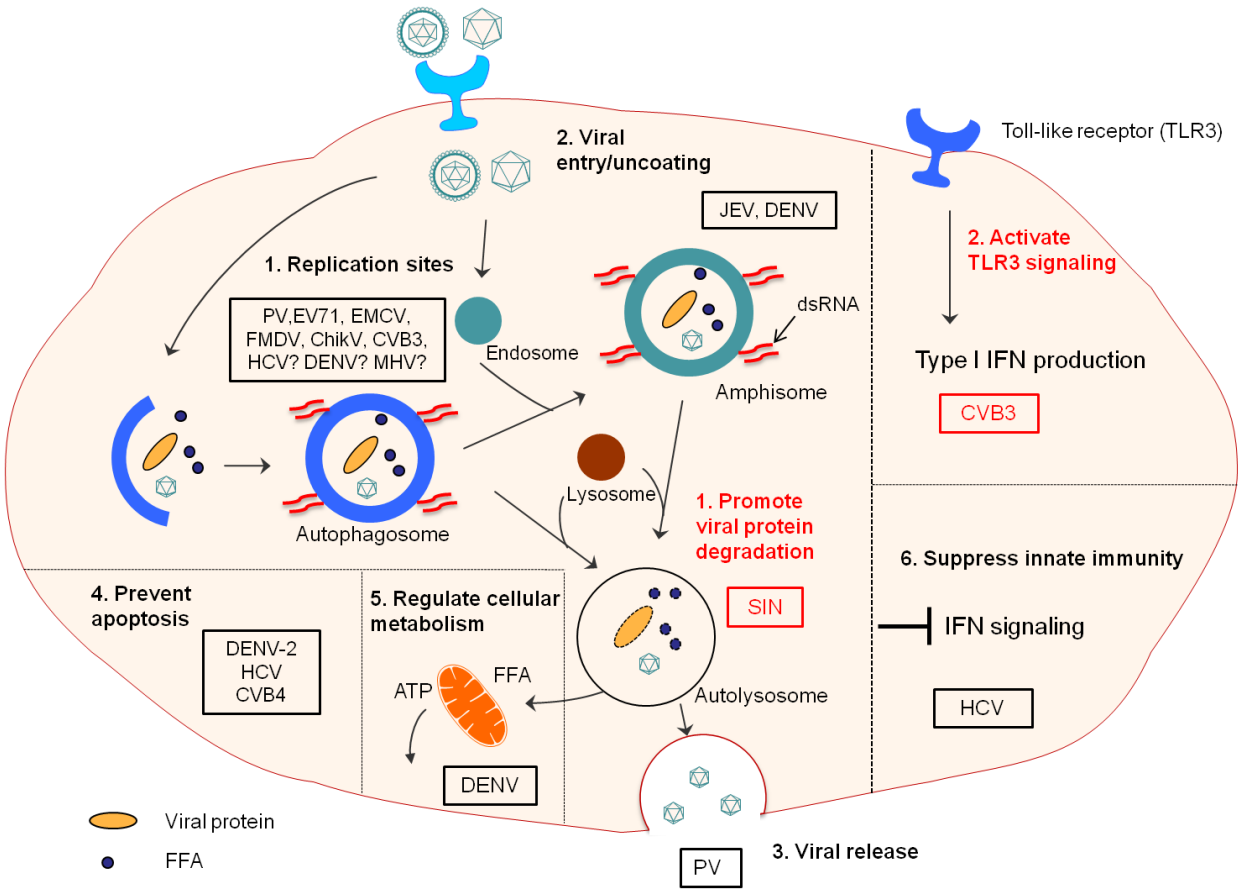

Figure 7. The pro-viral and anti-viral functions of autophagy during positive-stranded RNA viral infection.

Pro-viral functions of autophagy (viruses are indicated in black rectangles): (1) Autophagosomes (PV, EV71, CVB3, EMCV, FMDV, ChikV) or amphisomes (DENV) serve as sites for viral replication; (2) the amphisome is also linked to the entry/uncoating of JEV and DENV; (3) The topological structure of the autophagosome is associated with non-lytic egress of PV particles; (4) Autophagy prevents premature cell death to maintain favorable cellular environment for viral replication (DENV-2, HCV, and CVB4); (5) Autophagy favors DENV replication by selectively degrading lipid droplets to generate ATP for viral replication; (6) Suppression of IFN signaling is related to the pro-viral function of autophagy in HCV infection. Anti-viral functions of autophagy (red rectangles): (1) Autophagy inhibits SIN replication by promoting the clearance of

viral capsid protein; (2) Autophagy is required for TLR3-medicated type-I IFN production during CVB3 infection. Abbreviations : PV, poliovirus ; CVB, coxsackievirus type B; EV71, enterovirus 71; FMDV, foot and mouth disease virus; ChikV, chikungunya virus ; HCV, hepatitis C virus; HRV, human rhinovirus ; EMCV, encephalomyocarditis virus; SIN, sindbis virus ; DENV, dengue virus ; MHV, mouse hepatitis virus ; JEV, Japanese encephalitis virus; FAA, free fatty acid; IFN, interferon; TLR3, toll-like receptor 3.

1.4 Rational, hypothesis, and specific aims

Rational: Previously we observed profound accumulation of ubiquitinated protein aggregates and amyloid oligomers in CVB3-infected mouse hearts, consistent with our observation in cultured cells [60, 61]. It is believed that proteotoxicity generated by protein aggregates or its preceding intermediaries is a major pathogenic factor in the heart. Understanding the mechanism by which excessive protein aggregates are produced is a prerequisite to give further insight into the pathogenesis of viral myocarditis and its sequela DCM. The level of ubiquitinated conjugates is determined by the balance between protein synthesis and degradation. CVB3 infection enhances the expression of ubiquitin enzymes, indicating that increased protein ubiquitination contributes, at least in part, to aberrant accumulation of ubiquitin conjugates [61]. Ubiquitin-proteasome and autophagy are the major protein degradation systems. Both *in vitro* and *in vivo* studies showed that proteasome activity remains unchanged after CVB3 infection, ruling out a possible contribution of proteasome dysfunction to excessive accumulation of ubiquitin conjugates. Moreover, CVB3 infection induces massive autophagosomes in cultured cells [176]. Existing evidence makes it reasonable to speculate whether disruption of autophagy may account for the abnormal accumulation of ubiquitin conjugates.

I **hypothesized** that disruption of autophagy following CVB3 infection results in the impaired degradation of ubiquitin conjugates, contributing to the proteinopathy. My **specific aims** are:

1. To evaluate autophagy activity following CVB3 infection
2. To explore the underlying mechanisms of autophagy disruption
3. To investigate the consequences of compromised autophagy

Chapter 2: Materials and methods

2.1 Cell culture

HeLa cells (American Type Culture Collection, ATCC® CCL-2™) and pWPI-EGFP-Myc-Parkin/PARK2 stably expressing HeLa cells (generously provided by Dr. Wolfdieter Springer, Mayo Clinic, United States) were maintained in Dulbecco's modified Eagle's medium (DMEM) supplemented with 10% fetal bovine serum (FBS), 100 μg/ml penicillin, and 100 μg/ml streptomycin. *Sqstm1*$^{-/-}$ MEFs (a generous gift from Dr. Masaaki Komatsu, Tokyo Metropolitan Institute of Medical Science, Japan) were cultured in DMEM supplemented with 10% FBS, 100 μg/ml penicillin, 100 μg/ml streptomycin, 1× non-essential amino acids (Life Technologies, 11140-050), and 1× sodium pyruvate (Life Technologies, 11360-070) at 32.5°C, supplied with 5% CO_2.

2.2 CVB3 infection

HeLa Cells and *sqstm1*$^{-/-}$ MEFs were infected with CVB3 (Kandolf strain) at multiplicity of infections (MOI) of 10 and 40, respectively, for 1 h in DMEM without FBS, and then washed in Dulbecco's PBS (DPBS) and maintained in the culture medium containing DMEM and 10% FBS for a variety of time points as indicated.

2.3 Plasmids, siRNAs, and transient transfection

The Flag-tagged SQSTM1 construct (a generous gift from Dr. Brett Finlay, University of British Columbia, Canada) was used as a template to generate a series of SQSTM1 deletion mutants, site-directed SQSTM1-G241E mutant, and SQSTM1 truncations (SQSTM1-C and

SQSTM1-N). Plasmids expressing C-terminal NBR1 fragments (Flag-2A-NBR1-C and Flag-3C-NBR1-C) were established from a HA-NBR1 template generously provided by Dr. Caroline Whitehouse, King's College London, United Kingdom. The small interfering RNAs (siRNAs) against human SQSTM1 (L-010230-00-0005) and NBR1 (L-010522-00-0005) were purchased from Dharmacon. NBR1 siRNA against mouse was purchased from Santa Cruz Biotechnology (sc-149849). Cells were transfected with DNA plasmids or siRNAs using Lipofectamine® 2000 (Life Technologies, 11668-019) for 24-48 h according to the manufacturer's instructions.

2.4 Nuclear protein extraction

Cells were washed and harvested in DPBS, followed by centrifugation at 13,000 g for 2 min. The cell pellet was collected and incubated in TD buffer (25 mM Tris, pH 8.0 and 2 mM $MgCl_2$) on ice for 5 min. After addition of 5% NP-40 and subsequent centrifugation at 8, 000 g for 5 min, the supernatant fraction was removed and the remaining pellet fraction was incubated in BL buffer (10 mM Tris, pH 8.0, 0.4 M LiCl, and 20% glycerol) on ice for 10 min. The mixture was centrifuged at 18,000 g for 25 min, and the supernatant fraction containing nuclear protein was collected.

2.5 Western blot analysis

Cells were washed in cold DPBS and lysed in Modified Oncogene Science lysis buffer (MOSLB) (50 mM NaPyrophosphate, 50 mM NaF, 50 mM NaCl, 5 mM EDTA, 5 mM EGTA, 100 µM Na_3VO_4, 10 mM HEPES, and 0.1% Triton X-100). Protein concentration was measured by the Bradford assay (Bio-Rad Laboratories, #500-0006) or BCA protein assay (Thermo

Scientific, 23227), and 20-40 μg of protein was loaded for SDS-PAGE. Western blotting was performed according to a standard protocol as previously described [177].

2.6 Subcellular fractionation

HeLa cells were washed in cold DPBS and lysed in DPBS containing 1% Triton X-100 and complete proteinase inhibitors on ice for 30 min with vortex every 10 min. After centrifugation at 15,000 g for 30 min at 4 °C, the supernatant fractions were collected as Triton X-100-soluble fractions. The pellets were washed with DPBS containing 1% Triton X-100, and further solubilized in DPBS containing 2% SDS and complete proteinase inhibitors (Roche, 11836170001) at 60 °C for 1 h with vortex every 20 min. After centrifugation at 15,000 g for 30 min at 4 °C, the supernatant fractions were collected as Triton X-100-insoluble fractions.

2.7 Real-time quantitative reverse transcriptase PCR (RT-qPCR)

Total RNA was extracted using the RNeasy Mini kit (Qiagen, 74104). cDNA was synthesized using the SuperScript III First-Strand Synthesis kit following the manufacturer's protocol (Life Technologies, 18080-051). NBR1 or SQSTM1 was amplified in a 20 μl PCR reaction system composed of 100 ng of cDNA template, 1 μl of 20×TaqMan probe [Life Technologies, #4331182, Hs01061917_g1 (SQSTM1), Hs00245918_m1(NBR1), Hs02758991_g1 (GAPDH)], and 2×TaqMan Universal Master Mix II with UNG (Life Technologies, #4440038). The PCR reactions were performed on a ViiA 7 Real-Time PCR System (Applied Biosystems) with the following condition: 50 °C, 2 min; 95 °C, 10 min; 40 cycles of 95 °C, 15 sec and 60 °C, 1 min. Samples were run in triplicate concurrently with a 10× serial dilution of sample cDNA as a standard.

2.8 CVB3 proteinases $2A^{pro}$ and $3C^{pro}$ *in vitro* cleavage assay

Coxsackieviral proteinases $2A^{pro}$, $2A^{pro}$ mutant, and $3C^{pro}$ were purified as previously described [85]. HeLa cells were collected into the cleavage reaction buffer (20 mM Hepes, pH 7.4, 150 mM KOAc, and 1 mM DTT) and grinded with a dounce homogenizer for 30-50 strokes on ice. Cell lysates were centrifuged to remove the debris. Purified $2A^{pro}$, $2A^{pro}$ mutant, or $3C^{pro}$ was incubated with 50 μg of HeLa cell extracts in the cleavage reaction buffer at 37 °C for increasing periods of time as indicated. The reaction was stopped by addition of SDS-PAGE sample buffer.

2.9 Plaque assay

Virus titers in the supernatant fraction were measured by the plaque assay as previously described. In brief, cell supernatant fractions were serially diluted in DMEM and overlaid on 90-95% confluent HeLa cell monolayer. After 1 h incubation, the medium was replaced with complete medium with 10% FBS and 0.75% agar. After 72 h infection, cells were fixed in Carnoy's fixative (75% ethanol-25% acetic acid) containing 1% crystal violet. Plaques formed on the monolayer were counted manually and viral titers were calculated as plaque forming units (PFU)/ml.

2.10 NFKB luciferase activity assay

HeLa cells were co-transfected with various SQSTM1 constructs (empty vector, Flag-SQSTM1-WT, Flag-SQSTM1-N, or Flag-SQSTM1-C), inducible NFKB-responsive firefly luciferase construct, and constitutively-expressing renilla luciferase construct, with a ratio of 5:4:1 after optimization, for 48 h. NFKB luciferase activity was measured using the dual-luciferase® reporter assay system according to the manufacturer's protocol (Promega, E1960).

2.11 Immunofluorescence and confocal laser-scanning microscopy

Cells were fixed with 4% paraformaldehyde diluted in DPBS for 15 min at room temperature, permeabilized with 0.25% Triton X-100 in DPBS for 10 min, and blocked with 1% bovine serum album in DPBS plus Tween 20 for 30 min. Coverslips were incubated with primary antibodies at 4 °C overnight. After washing for 5 min × 3 times, secondary antibodies were added and incubated for 1 h at room temperature in the dark. The cover slips were washed for 5 min × 3 times after decanting secondary antibodies and cells were counterstained with DAPI (4, 6-diamidino-2-phenylindole, Vector Laboratories, H-1200). Images were taken with a Nikon eclipse TE300 fluorescence microscope or a Leica SP2 AOBS confocal fluorescence microscope.

2.12 Immunoprecipitation

Cell lysates were prepared using lysis buffer containing 50 mM Tris HCl, pH 7.4, 150 mM NaCl, 1 mM EDTA, 1% Triton X-100, and proteinase inhibitor cocktail (Roche, 04693132001). Immunoprecipitation was carried out using EZview™ Red ANTI-FLAG® M2 Affinity Gel (Sigma-Aldrich, F2426) following the manufacturer's protocol and with controls recommended by the protocol.

2.13 Reagents

The following antibodies were used in the study: anti-C-terminal SQSTM1 (PROGEN Biotechnik GmbH, GSQSTM1-C), anti-N-terminal SQSTM1 (PROGEN Biotechnik GmbH, GSQSTM1-N), anti-FLAG (Santa Cruz Biotechnology, sc-807), anti-NFE2L2 (Santa Cruz Biotechnology, sc-13032), anti-histone H1 (Santa Cruz Biotechnology, sc-10806), anti-G3BP1

(Santa Cruz Biotechnology, sc-98561), anti-N-terminal NBR1 (Santa Cruz Biotechnology, sc-130380), anti-cleaved caspase-3 (Asp175) (Cell Signaling, 9661S), anti-ubiquitin (Sigma-Aldrich, U5379), anti-ACTN/α-actinin (Sigma-Aldrich, A5044), anti-ACTB/β-actin (Sigma-Aldrich, A5316), anti-VP1 (DakoCytomation, M706401-1), anti-HA (Roche, 11867423001), and anti-GFP (Life Technologies, A-6455), anti-cytochrome c (H-104) (Santa Cruz Biotechnology, sc-7159), anti-TOMM20 (FL-145) (Santa Cruz Biotechnology, sc-11415), anti-Parkin/PARK2 (Prk8) (Cell Signaling, #4211), anti-VDAC (Cell Signaling, #4866), anti-MAVS (Cell Signaling, #8348), anti-PINK1(N3C3) (GeneTex, GTX107851), and anti-LC3B (Novus Biologicals, NB100-2220). The chemicals used in this study include: general caspase inhibitor benzyloxycarbonyl-Val-Ala-Asp-fluoromethylketone (Z-VAD-FMK) (EMD Millipore, #219007), VECTASHIELD mounting medium with DAPI (4', 6-diamidino-2-phenylindole) (Vector Laboratories, H-1200), fluorophore-labeled secondary antibodies (Life Technologies), Lipofectamine® 2000 (Life Technologies, #11668-019), complete proteinase inhibitor tablets (Roche, #11836170001), carbonyl cyanide m-chlorophenylhydrazone (CCCP) (Santa Cruz Biotechnology, sc-202984), BAF (LC Laboratories, B-1080), and lactacystin (LAC) (Sigma-Aldrich, L6785).

2.14 Statistical analysis

All data presented are representative of at least three independent experiments. Results are presented as mean ± standard deviation (SD). Unpaired Student's t-test was performed. $P < 0.05$ was considered to be statistically significant. Densitometric analysis of Western blot images was performed using NIH ImageJ software. Cells were counted using NIH ImageJ or Image-Pro Plus 5.1 software.

Chapter 3: Cleavage of sequestosome 1/p62 results in disrupted selective autophagy

3.1 Background

The replication of positive-sense RNA viruses is associated with membranous structures [178]. Previous studies demonstrated the colocalization of viral RNA replication complexes with autophagosome membrane during poliovirus infection, suggesting a pro-viral mechanism for autophagy by generating the membrane scaffold for viral RNA replication [179, 180]. To benefit most from the replication lattice, it was proposed that viruses might block the fusion of autophagosomes with endosomes/lysosomes. The disruption of autophagy is beneficial to viruses through enhancing the accumulation of autophagosomes, preventing their own destruction through the autophagy machinery, and limiting host innate antiviral response via interaction between viral RNA and the single-stranded RNA sensor Toll-like receptor-7, which is present in late endosomes and lysosomes [179, 181, 182]. Although definite evidence is lacking, this hypothesis is supported by the observation of abundant large-sized autophagosomes in CVB3-infected pancreata [182]. These giant autophagosomes are believed to be formed by the coalescence of smaller autophagosomes due to the blockage of autophagosome-lysosome fusion [182].

The whole process of autophagy, referred to as autophagic flux, can be monitored by various methods, among which SQSTM1 is a widely used marker as it inversely correlates with autophagic flux through autophagic degradation [183, 184, 185]. In addition, SQSTM1 is a key receptor protein in mediating selective autophagy [122, 186, 187]. SQSTM1 contains multiple functional domains, including an N-terminal Phox/Bem1p (PB1) domain, LIR, and a C-terminal

UBA domain [122, 186, 187]. The PB1 domain not only allows SQSTM1 to bind to other PB1-containing proteins, such as atypical protein kinase C, mitogen-activated protein kinase kinase 5, and caspase 8, but also enables SQSTM1 to self-oligomerize and form aggregates, which is crucial for its degradation by autophagy [188]. The UBA domain of SQSTM1 interacts directly with lysine 48- and 63-linked polyubiquitin chains, whereas the LIR domain of SQSTM1 allows it to bind to LC3, a critical process required for SQSTM1 recruitment into the phagophore [122, 186, 187]. Through interaction with these important domains, SQSTM1 targets ubiquitinated protein aggregates for autophagic degradation [122, 186, 187].

Apart from selective autophagy, SQSTM1 also plays an essential role in regulating multiple signaling pathways. The best-studied function of SQSTM1 as a scaffold protein is its role in activating the NFKB pathway. SQSTM1 activates the NFKB pathway by binding to atypical protein kinase C, receptor (TNFRSF)-interacting serine-threonine kinase 1, or TRAF6 (tumor necrosis- associated factor 6, E3 ubiquitin protein ligase) through its PB1, zinc finger (ZZ), or TRAF6 binding (TB) domains, respectively [189, 190, 191]. Recent studies also suggest an antioxidative role of SQSTM1 by competitive binding to KEAP1 (kelch-like ECH-associated protein 1), the negative regulator of transcription factor NFE2L2, resulting in the stabilization of NFE2L2 and subsequent upregulation of antioxidant genes [192, 193].

Given the functional importance of SQSTM1 in multiple cellular processes, e.g., as a marker to evaluate autophagic flux, as an adaptor protein in selective autophagy, and as a mediator in anti-viral signaling pathway, we focus on SQSTM1 in association with viral infection.

3.2 Specific aims

The purpose of this chapter is to elucidate whether CVB3 infection results in impaired autophagic flux.

The **SPECIFIC AIMS** include:

Aim 1. To test protein expression level of SQSTM1 following CVB3 infection

Aim 2. To elucidate the underlying mechanisms responsible for the reduction of SQSTM1

Aim 3. To explore the effects of SQSTM1 cleavage on selective autophagy

Aim 4. To evaluate whether autophagic flux is suppressed following CVB3 infection

3.3 Results

3.3.1 Cleavage of SQSTM1 following CVB3 infection.

To evaluate autophagic flux following CVB3, we first examined protein expression of SQSTM1 in HeLa cells, a well-characterized model in viral studies. Western blotting showed the decreased abundance of full-length SQSTM1 (more than 70% reduction at 7 h post-infection as compared to sham infection), accompanied by the appearance of ~30-kDa fragments using antibodies against either the C or N terminus of SQSTM1, implicating virus-associated cleavage of SQSTM1 (**Fig. 8A**). To determine whether SQSTM1 is transcriptionally downregulated during CVB3 infection, we conducted real-time quantitative PCR to measure the mRNA expression of *SQSTM1*. As shown in **Fig. 8B**, mRNA levels of *SQSTM1* were unaltered following CVB3 infection, suggesting that the reduced protein expression of SQSTM1 is not due to decreased mRNA expression.

To verify the cleavage of SQSTM1, cells were transiently transfected with a Flag-tagged SQSTM1 construct, followed by CVB3 infection. Western blotting revealed the cleavage

products of transfected SQSTM1 (**Fig. 8C**), which corresponded well with the observation of endogenous SQSTM1 cleavage (**Fig. 8A**), confirming that SQSTM1 is cleaved after CVB3 infection.

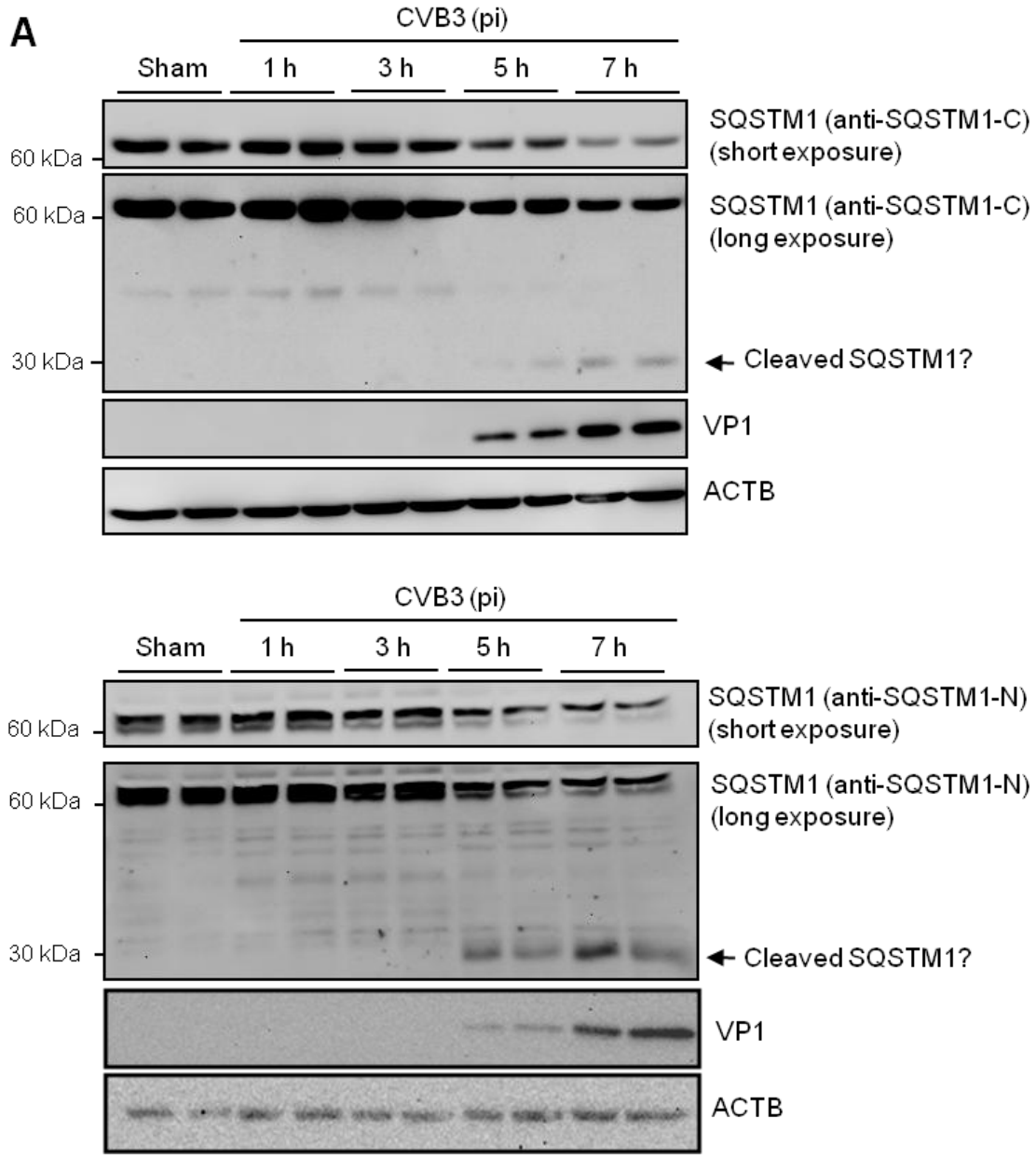

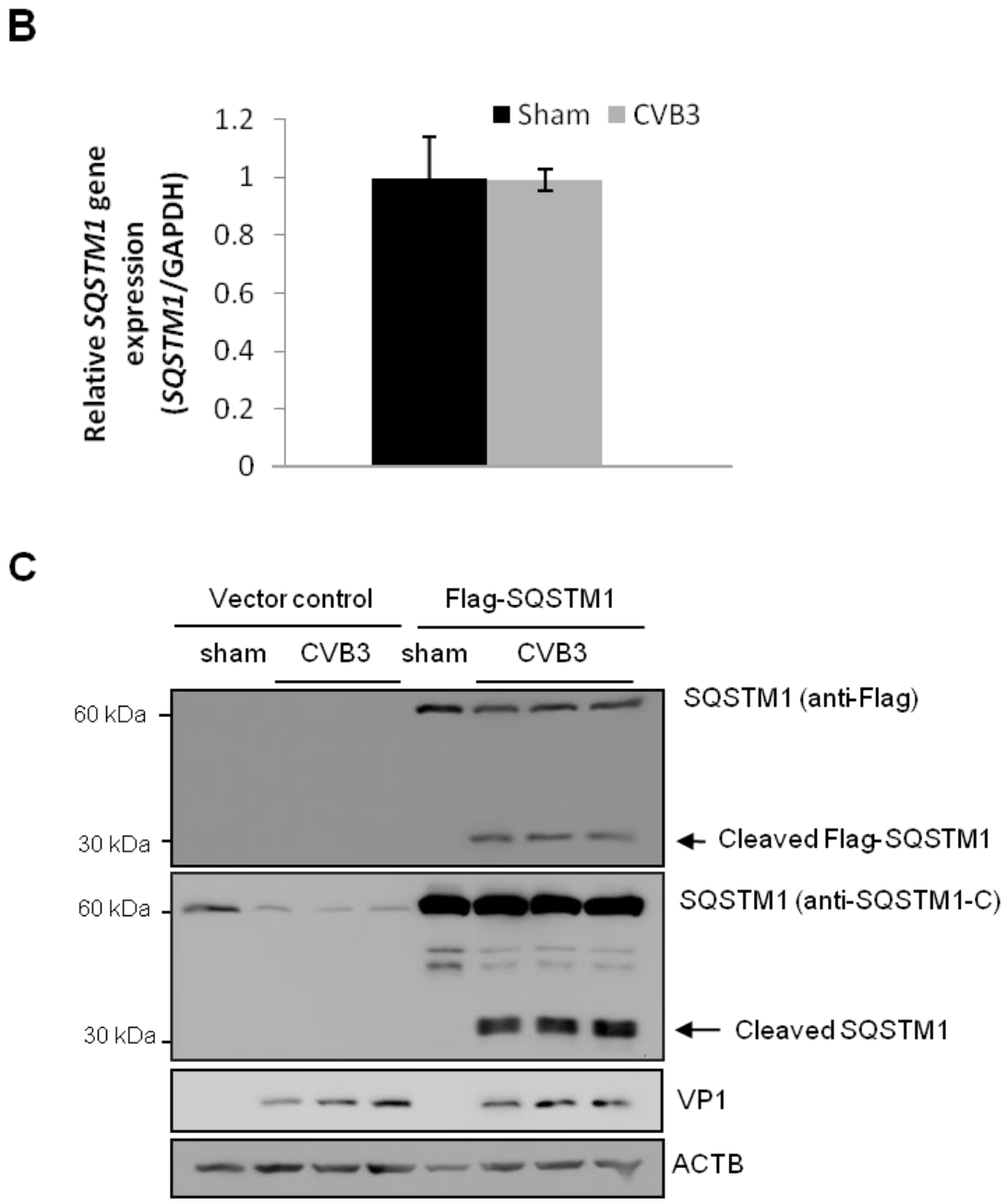

Figure 8. Cleavage of SQSTM1 after CVB3 infection.

(A) Protein expression of SQSTM1 after CVB3 infection. HeLa cells were either sham-infected or infected with CVB3 for the indicated time points. Western blot analysis was performed to examine protein expression of SQSTM1, viral capsid protein VP1, and ACTB/β-actin (loading control). Antibodies against either the C terminus (upper panel) or N terminus of SQSTM1

(lower panel) were used for detection of SQSTM1 as indicated. (B) mRNA expression of SQSTM1 after CVB3 infection. HeLa cells were infected with CVB3 for 7 h or sham-infected with PBS. Gene levels of SQSTM1 were measured by real time quantitative PCR and normalized to *GAPDH* mRNA (mean ± SD, n=3). (C) Cleavage of SQSTM1 after CVB3 infection. HeLa cells were transiently transfected with either an empty-vector control (pcDNA3) or a plasmid expressing N-terminal Flag-tagged SQSTM1 for 24 h, followed by sham or CVB3 infection for 7 h. Western blotting was performed to examine the presence of SQSTM1 cleavage products by detecting N-terminal Flag-SQSTM1 (top) or C-terminal SQSTM1 (middle). ACTB/β-actin (bottom) was used as the loading control. pi, post-infection.

3.3.2 Identification of the SQSTM1 cleavage site.

A compilation of verified substrates has revealed a core consensus sequence [L/I/M•X•T/S•X | G•X•X•X] for enteroviral proteinase $2A^{pro}$ and [A•X•X•Q | G•P•X•X] for enteroviral proteinase $3C^{pro}$ (L, leucine; I, isoleucine; M, methionine; T, threonine; S, serine; A, alanine; Q, glutamine; G, glycine; P, proline; X stands for any amino acid; |, stands for the scissile site). To identify the cleavage site of SQSTM1, we constructed a series of deletion and point mutation plasmids based on the consensus sequences and the predicted sizes of the cleavage fragments. We found that the G241E [the glycine (G) residue at position 241 was replaced with glutamic acid (E)] and Δ236-240 deletion mutants were uncleavable after CVB3 infection, suggesting that SQSTM1 is cleaved at glycine 241 (**Fig. 9A and B**). This cleavage takes place within the TB domain, resulting in the separation of the N-terminal PB1 and ZZ domains from the C-terminal LIR, KEAP1-interacting region (KIR), and UBA domains **(Fig. 9C)**. Amino acid sequence alignments of SQSTM1 with other known viral proteinase $2A^{pro}$ substrates at the cleavage region revealed a similar cleavage motif, indicating that $2A^{pro}$ is likely responsible for SQSTM1 cleavage.

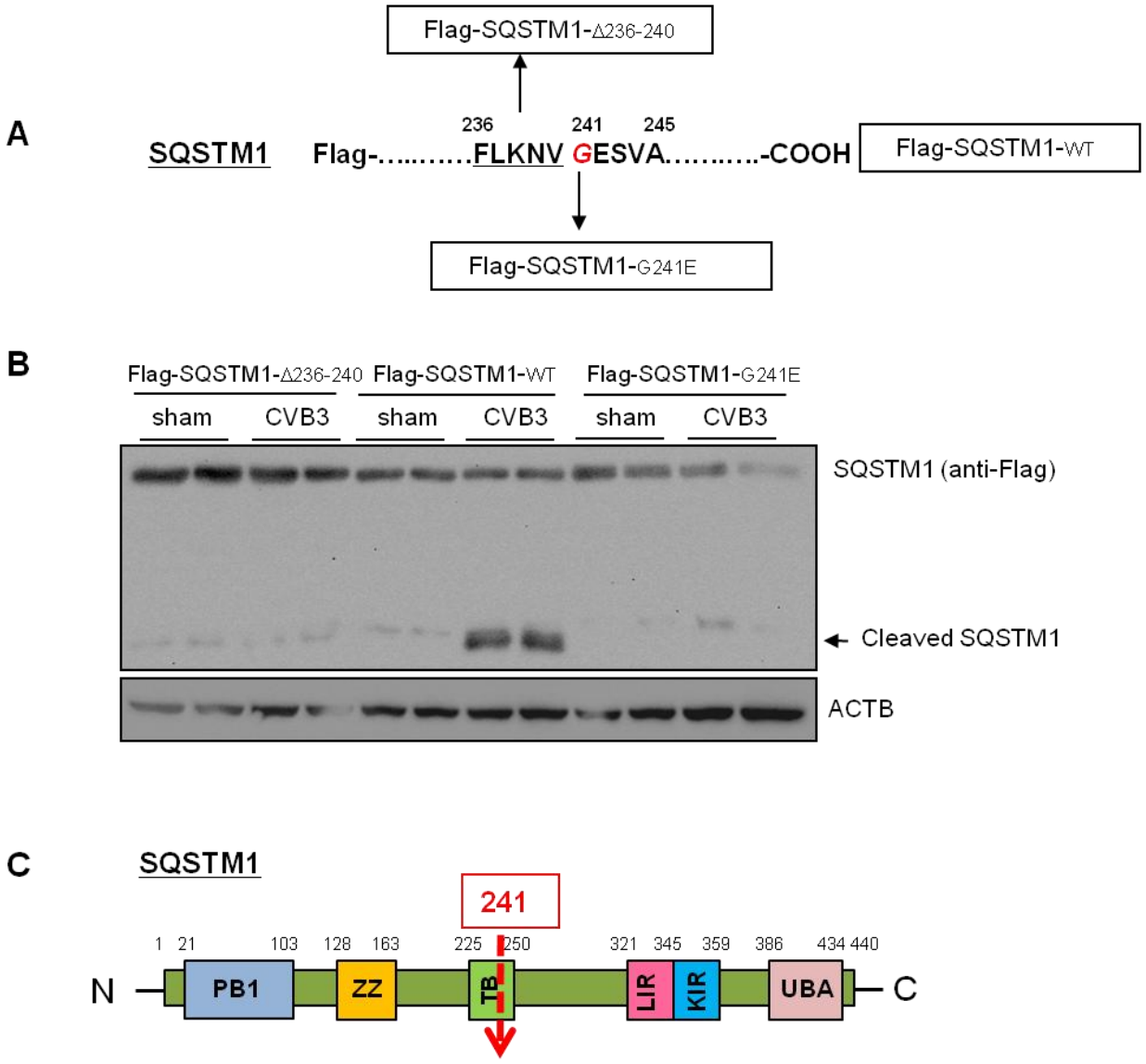

Figure 9. Identification of the cleavage site on SQSTM1.

(**A**) Diagrammatic illustration of the SQSTM1 constructs used in this study. The Flag-SQSTM1-wild-type (WT), Flag-SQSTM1-Δ236-240 (missing amino acids 236 to 240), and Flag-SQSTM1-G241E [glycine (G) at amino acid 241 was replaced by glutamic acid (E)] constructs are displayed. (**B**) Identification of the SQSTM1 cleavage site. HeLa cells were transiently transfected with Flag-SQSTM1-WT, Flag-SQSTM1-Δ236-240 or Flag-SQSTM1-G241E for 24 h, followed by sham or CVB3 infection for 7 h. Western blotting was performed to detect various forms of SQSTM1 using anti-Flag antibody. ACTB/β-actin was examined as a loading

control. **(C)** Schematic diagram of SQSTM1 structural domains and the identified cleavage site. PB1, Phox/Bem1p domain; ZZ, zinc-finger domain; TB, TRAF6 binding domain; LIR, LC3-interacting region; KIR, KEAP1-interacting region; UBA, ubiquitin association domain.

3.3.3 Viral proteinase $2A^{pro}$ is responsible for CVB3-induced SQSTM1 cleavage.

To examine whether viral proteinase $2A^{pro}$ induces SQSTM1 cleavage, we performed *in vitro* cleavage assays. As shown in **Fig. 10A**, in the presence of purified $2A^{pro}$, SQSTM1 protein in HeLa cell lysates was cleaved, generating cleavage products of SQSTM1 with molecular weights similar to those observed in CVB3-infected cells. This result indicates that SQSTM1 cleavage during CVB3 infection is mediated through the action of $2A^{pro}$. It is noted that the *in vitro* cleavage efficiency was not as potent as shown in cells (**Figs. 8 and 9).** This is likely due to the fact that *in vitro* purified $2A^{pro}$ generally has low activities.

We also explored whether viral proteinase $3C^{pro}$ contributes to SQSTM1 cleavage. **Fig. 10B** showed that incubation with purified $3C^{pro}$ resulted in the cleavage of G3BP1 [GTPase activating protein (SH3 domain) binding protein 1], a known substrate for $3C^{pro}$ [86]. However, SQSTM1 remained intact after treatment with $3C^{pro}$.

In vitro proteolytic cleavage assays have shown that SQSTM1 is a substrate of caspases [194]. To determine whether caspase activation is responsible for CVB3-mediated cleavage of SQSTM1, we pretreated cells with z-VAD (50 μM), a general caspase inhibitor. **Fig. 10C** showed that caspase inhibition did not prevent SQSTM1 cleavage, indicating that cleavage of SQSTM1 is caspase-independent.

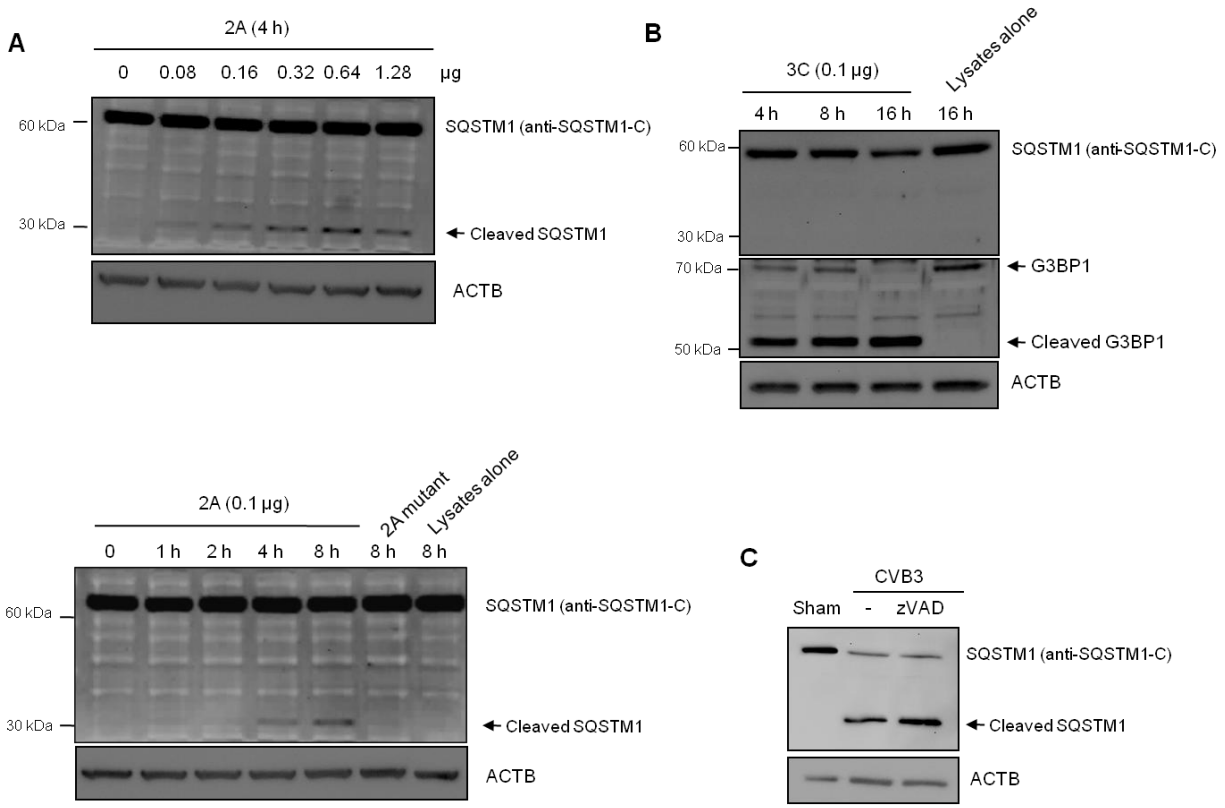

Figure 10. Viral proteinase 2A^{pro} is responsible for CVB3-induced SQSTM1 cleavage.

(A, B) Effect of viral proteinase 2A^{pro} and 3C^{pro} on SQSTM1 cleavage. An *in vitro* cleavage assay was conducted as described in Materials and Methods. HeLa cell extracts (50 μg) were incubated with purified 2A^{pro} (A), 2A^{pro} mutant (A) or 3C^{pro} (B) for increasing concentrations or period of time as indicated. Protein levels of SQSTM1 (using anti-C-terminal SQSTM1 antibody), G3BP1 (a known substrate for enteroviral proteinase 3C), and ACTB/β-actin (loading control) were analyzed by Western blotting. (C) Effect of caspase inhibition on CVB3-induced cleavage of SQSTM1. HeLa cells were infected with CVB3 for 7 h in the presence or absence of zVAD (50 μM), a pan caspase inhibitor. Western blotting was performed to examine protein expression of SQSTM1 using anti-C-terminal SQSTM1 antibody and ACTB/β-actin (loading control). "–", vehicle-treated.

3.3.4 Stability and binding activities of SQSTM1 cleavage fragments.

To determine whether the resulting cleavage products of SQSTM1 are targets of autophagy, cells were treated with BAF, an inhibitor of lysosomal degradation. Upon BAF treatment, protein expression of noncleaved SQSTM1 was increased as expected (**Fig. 11A**). However, protein levels of both N- and C-terminal fragments of SQSTM1 (**Fig. 11A**) remained unchanged, indicating that they were not degraded through autophagy. Similar results were observed using another autophagy inhibitor, NH_4Cl (data not shown).

We further explored the functional consequences of SQSTM1 cleavage. As alluded to earlier, SQSTM1 contains multiple structural domains, including those involved in selective autophagy of polyubiquitinated substrates. To determine whether the C-terminal fragment of SQSTM1, which contains intact LIR and UBA domains, is capable of binding to LC3 and polyubiquitin chain, HeLa cells were co-transfected with Flag-SQSTM1-WT, Flag-SQSTM1-C, or Flag-SQSTM1-N together with GFP-LC3 (**Fig. 11B**) or HA-ubiquitin (**Fig. 11C**). Immunoprecipitation was conducted to assess the physical association between SQSTM1-WT/N/C and LC3 (**Fig. 11B**) or polyubiquitin chain (**Fig. 11C**). We showed that full-length SQSTM1 is capable of binding to both LC3 and polyubiquitinated proteins (**Fig. 11B and C**), in line with previous reports [125, 130, 188, 195]. Interestingly, we observed that the C-terminal fragment of SQSTM1 retained its ability to bind to LC3 (**Fig. 11B**) but lost its association with ubiquitinated proteins (**Fig. 11C**). As expected, the N-terminal fragment of SQSTM1, which lacks both LIR and UBA domains, failed to interact with LC3 and ubiquitin chain (**Fig. 11B and C**).

To determine whether the N-terminal fragment of SQSTM1, which possesses a complete PB1 domain for self-oligomerization, is able to bind to full-length SQSTM1, we utilized two

SQSTM1 constructs labeled with Flag and GFP, respectively. HeLa cells were co-transfected with GFP-SQSTM1-WT together with Flag-SQSTM1-WT, Flag-SQSTM1-N, or Flag-SQSTM-C, and immunoprecipitation assay revealed that SQSTM1-N maintained its function in interacting with SQSTM1-WT, likely through its PB1 domain (**Fig. 11D**). Both empty vector and SQSTM1-C failed to bind to full-length SQSTM1 (**Fig. 11D**).

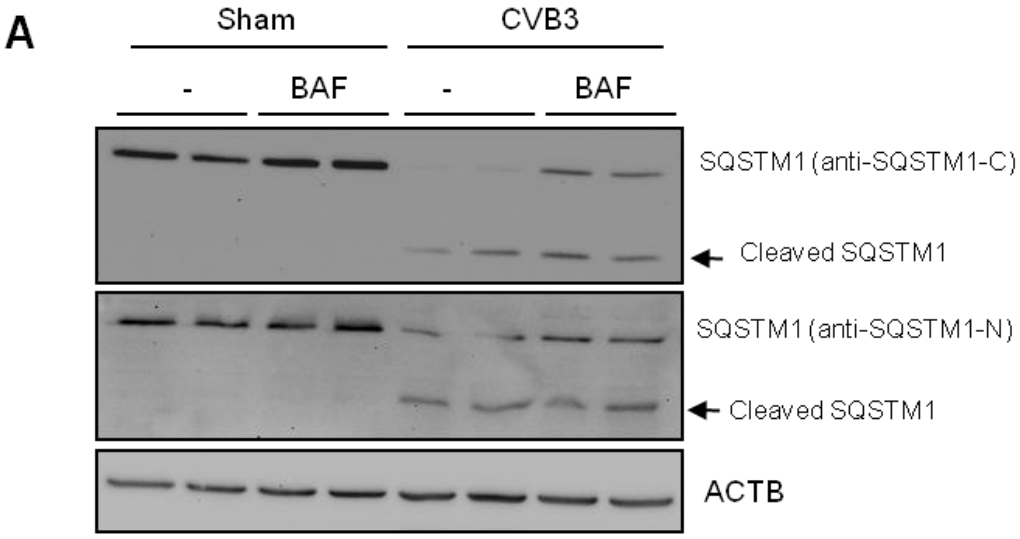

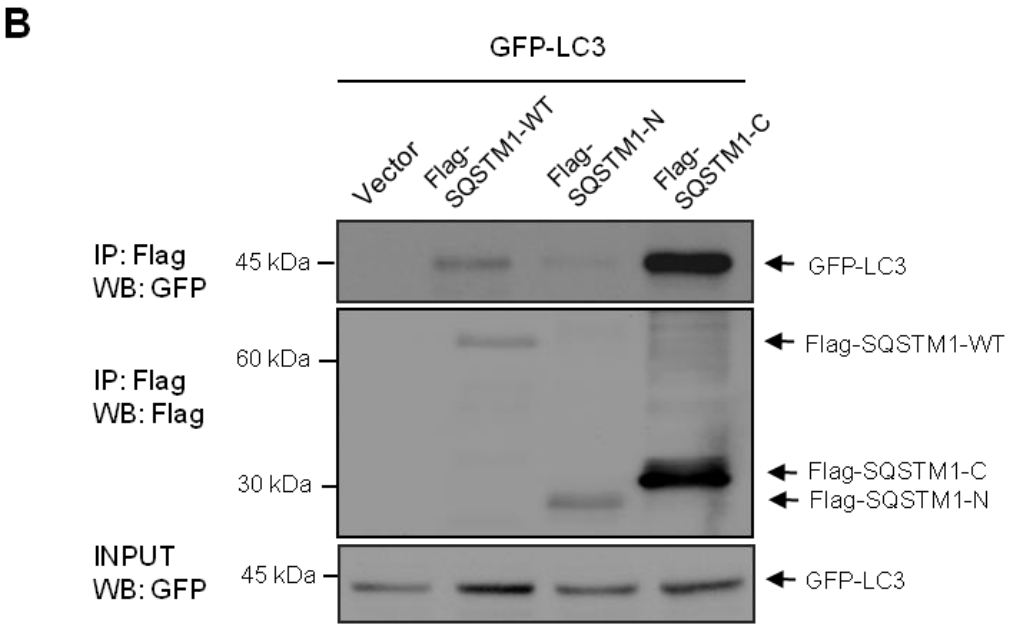

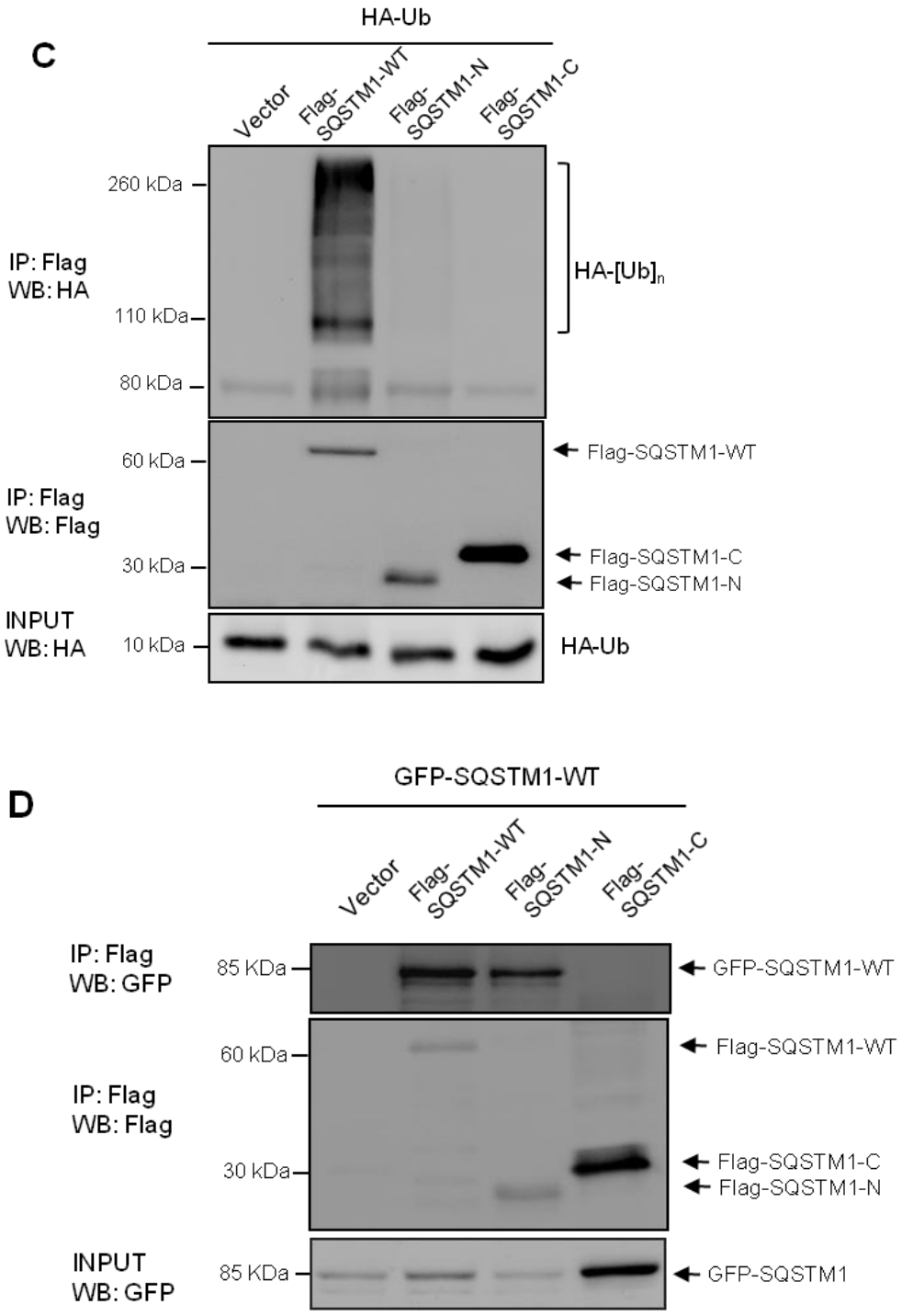

Figure 11. Stability and binding activities of SQSTM1 cleavage fragments.

(A) Stability of SQSTM1 cleavage fragments. HeLa cells were either sham-infected or infected with CVB3 for 7 h in the presence or absence of bafilomycin A_1 (BAF, 200 nM), an inhibitor of

lysosomal degradation. Western blotting was performed to examine protein levels of full-length and cleaved SQSTM1, with ACTB/β-actin as a loading control. "–", vehicle-treated. (B, C) Interaction of SQSTM1 truncations with LC3 and ubiquitin. HeLa cells were transiently transfected with Flag-SQSTM1-N, Flag-SQSTM1-C, Flag-SQSTM1-WT, or an empty vector, together with GFP-LC3 (B) or HA-ubiquitin (HA-Ub) (C) for 24 h, followed by treatment with bafilomycin A_1 (200 nM) for 8 h. Immunoprecipitation and Western blotting were conducted to assess the physical association between SQSTM1-WT or SQSTM1-C with LC3 (B) or ubiquitin (C) as indicated. (D) Interaction of SQSTM1-N with full-length SQSTM1. HeLa cells were transiently transfected with Flag-SQSTM1-N, Flag-SQSTM1-C, Flag-SQSTM1-WT, or an empty vector, together with GFP-SQSTM1-WT for 24 h, followed by bafilomycin A_1 treatment as described above. Immunoprecipitation and immunoblot were performed to examine the interaction between GFP-SQSTM1-WT and Flag-SQSTM1-WT, or Flag-SQSTM1-N, or Flag-SQSTM1-C, with the indicated antibodies.

3.3.5 Subcellular distribution of SQSTM1 cleavage fragments.

Next, we assessed the subcellular localization of the truncated SQSTM1 mutants. We first examined whether SQSTM1-N and SQSTM1-C are able to form aggregates. As shown in **Fig. 12A**, SQSTM1 punctate structures representing protein aggregates were observed in ~91.01% of SQSTM1-WT-transfected cells, as compared to ~31.13% and ~7.34% in SQSTM1-N- and SQSTM1-C-transfected cells, respectively. These results indicate that the ability to form aggregates was significantly imparied for SQSTM1-N and almost lost for SQSTM1-C.

We then examined whether SQSTM1 truncations interact with LC3 and ubiquitin. Confocal microscopy images revealed the punctate colocalization of transfected SQSTM1-WT with LC3 (53.38%, **Fig. 12B** upper panels) and SQSTM1-WT with ubiquitin (91.59%, **Fig. 12C** upper panels), in agreement with previous reports [125, 130, 188, 195]. However, in cells expressing SQSTM1 truncations, the colocalization ratio was considerably decreased, i.e., 0.57% and 8.77% between

LC3 and SQSTM1-N and SQSTM1-C, respectively, as well as 11.94% and 10.12% between ubiquitin and SQSTM1-N and SQSTM1-C, respectively (**Fig. 12B and C**). These results indicate that the association between SQSTM1-N and SQSTM1-C with LC3 and ubiquitin within the punctate structures was disrupted.

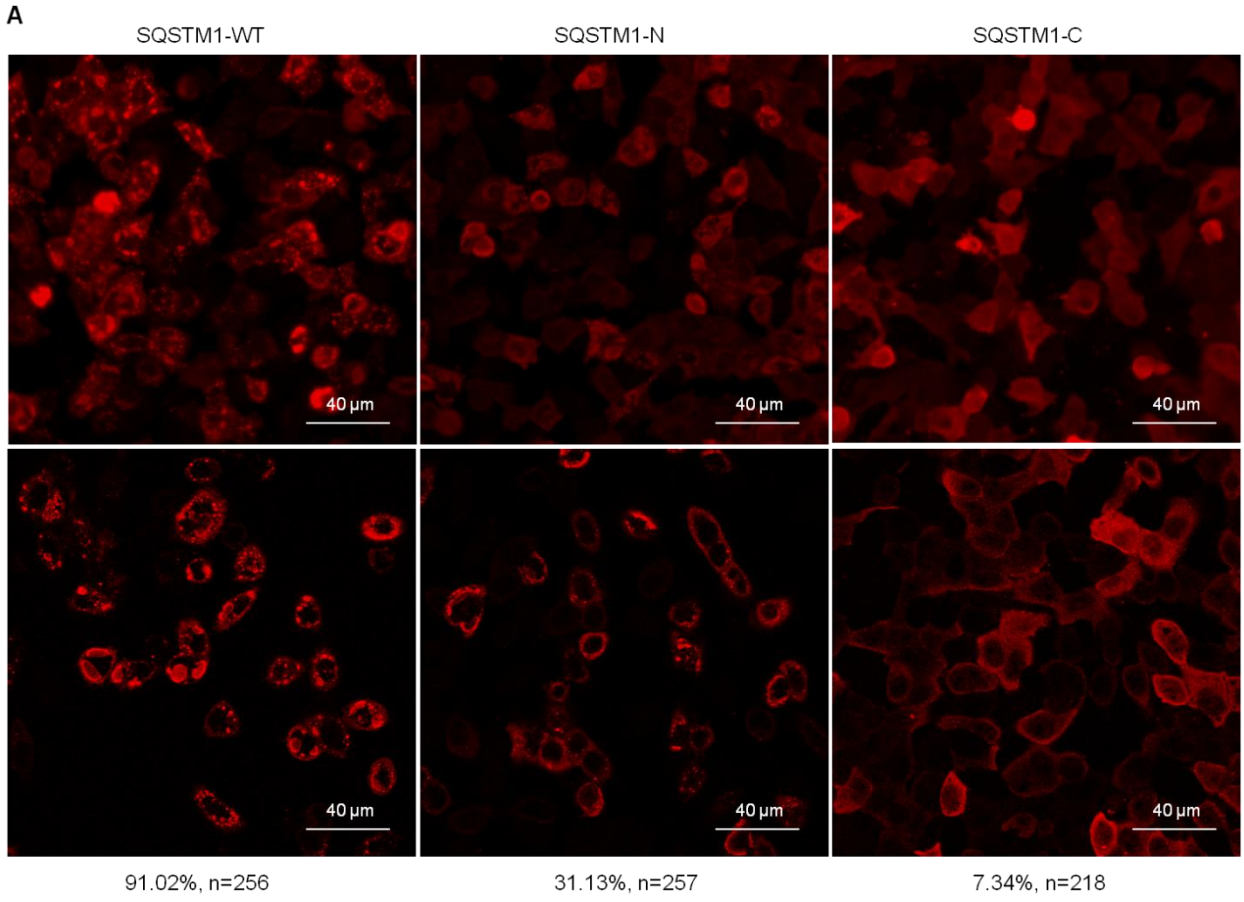

B

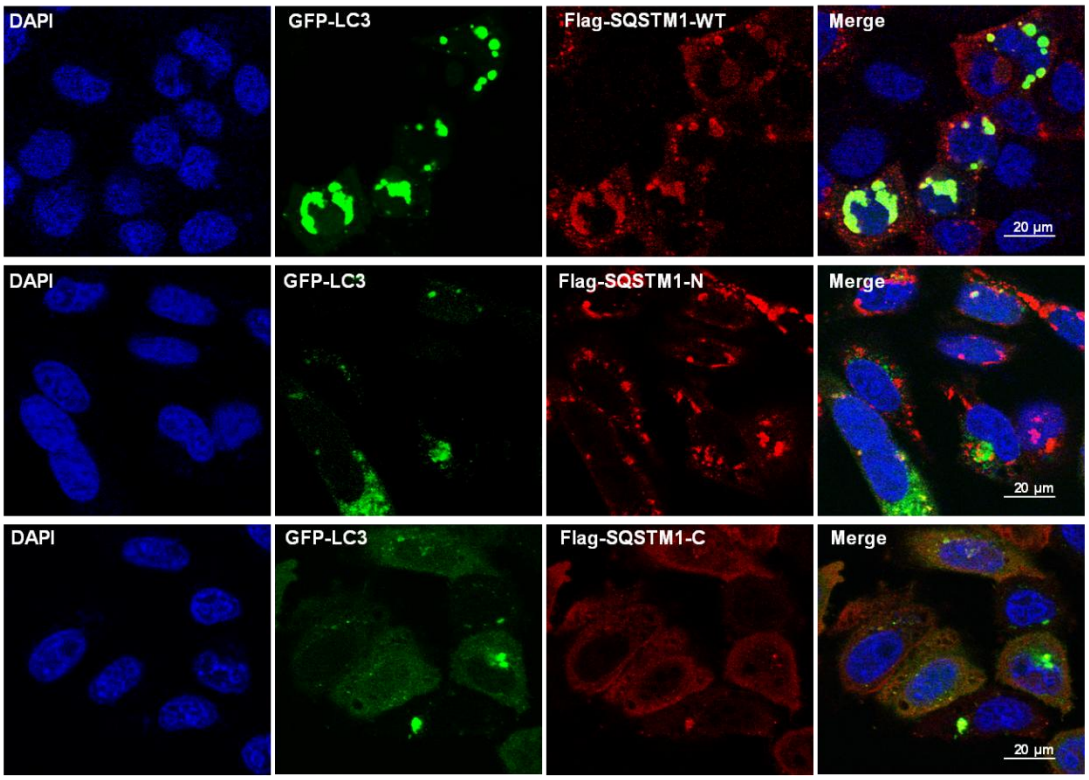
DAPI
GFP-LC3
Flag-SQSTM1-WT
Merge
20 μm
53.38%, n=133
DAPI
GFP-LC3
Flag-SQSTM1-N
Merge
20 μm
0.57%, n=175
DAPI
GFP-LC3
Flag-SQSTM1-C
Merge
20 μm
8.77%, n=114

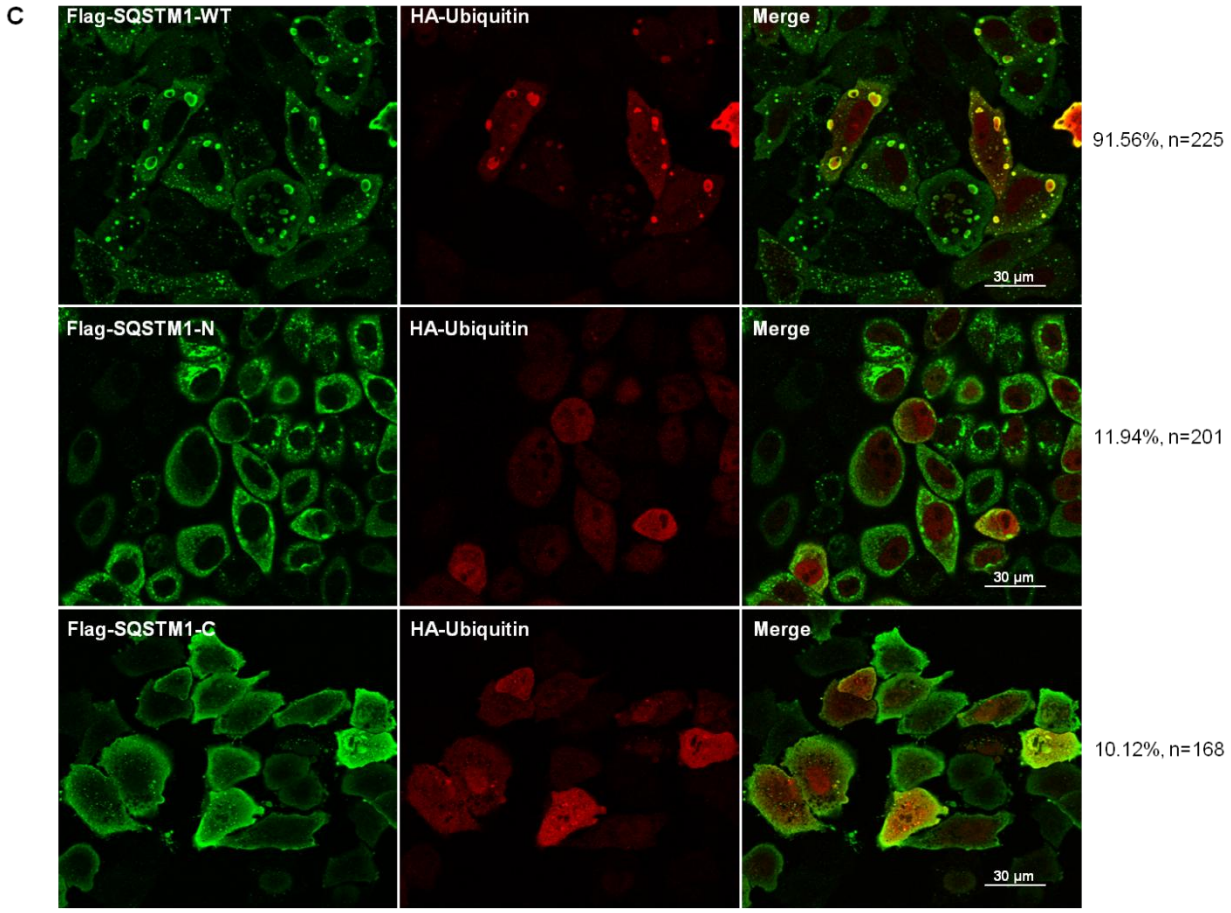

Figure 12. Cellular localization of SQSTM1 cleavage fragments.

(**A**) Subcellular distribution of SQSTM1 truncations. HeLa cells were transiently transfected with Flag-SQSTM1-WT, Flag-SQSTM1-C or Flag-SQSTM1-N construct for 24 h, followed by 8 h treatment with bafilomycin A_1 (200 nM). Immunocytochemical staining was performed using anti-Flag antibody. Cell images were captured using a fluorescence microscope (upper panels) and a confocal microscope (lower panels). The percentage of cells with punctate SQSTM1 staining over the total number of SQSTM1-positive cells (n) was calculated and presented. (**B, C**) Colocalization of SQSTM1 truncations with LC3 or ubiquitin. HeLa cells were transfected with GFP-LC3 construct (**B**) or HA-ubiquitin (**C**), together with Flag-SQSTM1-WT, Flag-SQSTM1-N, or Flag-SQSTM1-C. Immunocytochemical staining was carried out using anti-Flag (**B**) or anti-Flag/anti-HA (**C**) antibody and cell images were captured by confocal

microscopy. The nucleus was counterstained with DAPI. The percentage of cells with puncta colocalization over the total number of cotransfected cells (n) is displayed.

3.3.6 Effects of SQSTM1 cleavage products on the formation of insoluble ubiquitin conjugates.

A role for SQSTM1 has been implicated in the formation of inclusion bodies and aggresomes [123, 190]. The major components of inclusion bodies and aggresomes are misfolded proteins and ubiquitin conjugates, which are present in the insoluble fractions of the cell lysates and are normally targeted as substrates for autophagic degradation. To examine the effects of the cleavage fragments of SQSTM1 on the abundance of insoluble ubiquitin conjugates, HeLa cell were transfected with SQSTM1-WT, SQSTM1-N, or SQSTM1-C plasmid. Cell lysates were fractionated as Triton X-100-soluble and -insoluble parts. We found that the levels of ubiqutinated proteins in Triton X-100-soluble fractions appeared no different among the groups (**Fig. 13,** upper panels). We further demonstrated that SQSTM1-WT facilitated the formation of insoluble ubiquitin conjugates, whereas SQSTM1-N and -C fragments lost this property of native SQSTM1 (**Fig. 13,** lower panels), suggesting that cleavage of SQSTM1 results in defects in the removal of ubiquitined protein aggregates through the autophagy pathway.

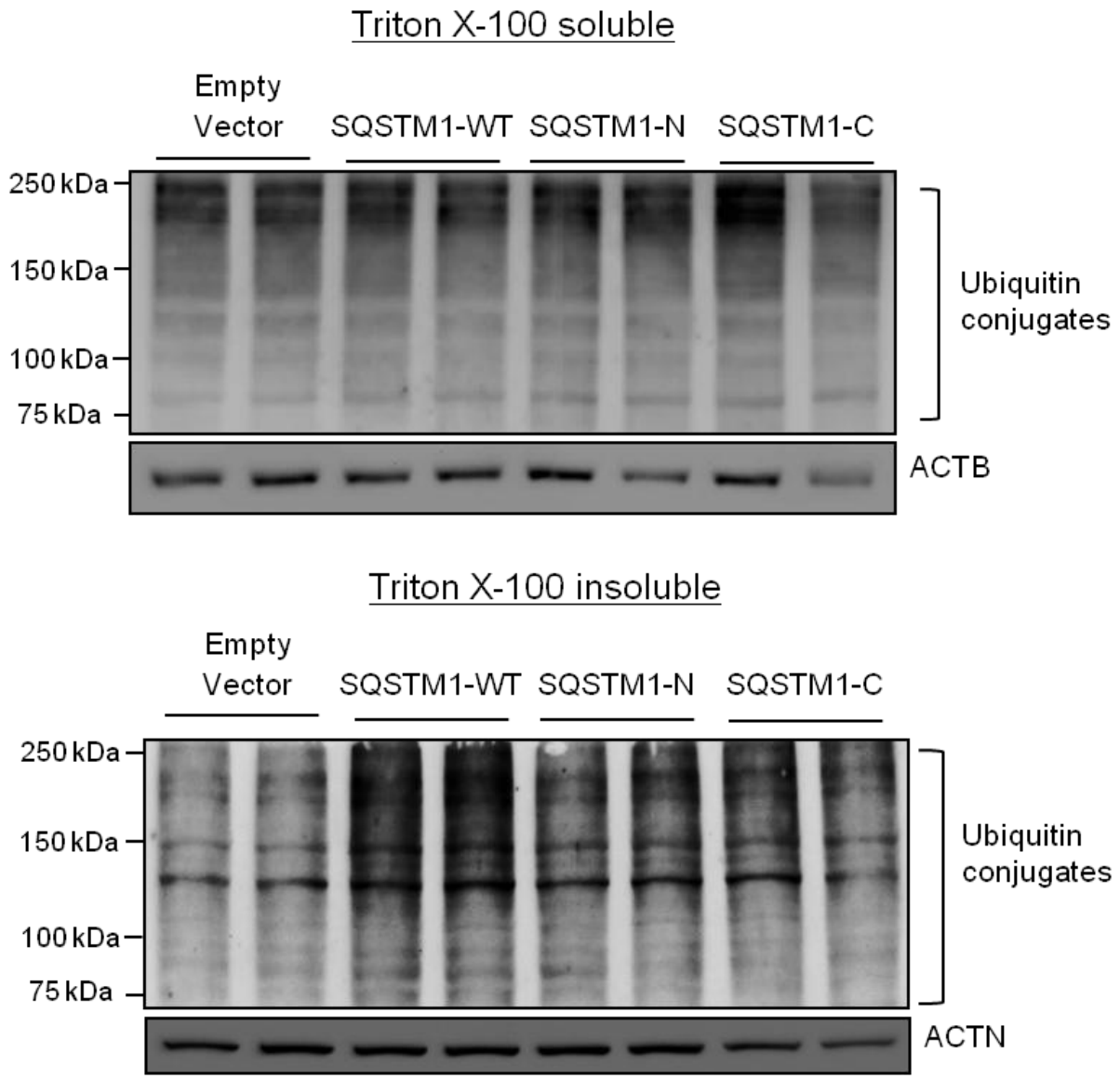

Figure 13. Effects of SQSTM1 cleavage products on the formation of insoluble ubiquitin-conjugates.

HeLa cells were transiently transfected with Flag-SQSTM1-WT, Flag-SQSTM1-N or Flag-SQSTM1-C construct for 48 h, followed by isolation of Triton X-100-soluble and -insoluble fractions as described in Materials and Methods. The levels of ubiquitin-conjugates in Triton X-100-soluble and -insoluble fractions were analyzed by Western blotting using anti-ubiquitin

antibody. ACTB/β-actin and ACTN/α-actinin were used as loading controls for Triton X-100-soluble and -insoluble fractions, respectively.

3.3.7 Effects of SQSTM1 cleavage products on NFKB activity and NFE2L2 expression.

As mentioned in the Introduction, full-length SQSTM1 is capable of activating transcription factor NFKB [189, 190, 191]. To investigate whether cleavage fragments sustain this function of SQSTM1, HeLa cells were transfected with SQSTM1-WT, SQSTM1-N, or SQSTM1-C plasmid, together with an NFKB firefly luciferase reporter construct and a renilla luciferase construct for 48 h, followed by luciferase and renilla luminesence detection. **Fig. 14A** showed that NFKB activity was significantly increased in cells overexpressing SQSTM1-WT. However, in SQSTM1-N or SQSTM1-C transfected cells, NFKB activity remained unchanged.

It was previously reported that overexpression of SQSTM1 results in stabilization of antioxidant transcription factor NFE2L2 by competing for NFE2L2-KEAP1 interaction via its KIR domain [192, 193]. KEAP1 is a component of the CUL3/cullin 3 ubiquitin ligase, targeting NFE2L2 for ubiquitination and then proteasomal degradation.[9,10] To explore the effects of SQSTM1 truncations on protein levels of NFE2L2, we transfected SQSTM1-WT, SQSTM1-N and SQSTM1-C into HeLa cells and examined NFE2L2 abundance in the nuclear fractions. Arsenite-treated HeLa cells were used as positive controls. Results presented in **Fig. 14B** revealed that overexpression of SQSTM1-WT resulted in increased levels of NFE2L2. We further showed that SQSTM1-C which possesses an intact KIR domain retained this function of SQSTM1-WT (**Fig. 14B**). As expected, SQSTM1-N was unable to promote NFE2L2 upregulation (**Fig. 14B**).

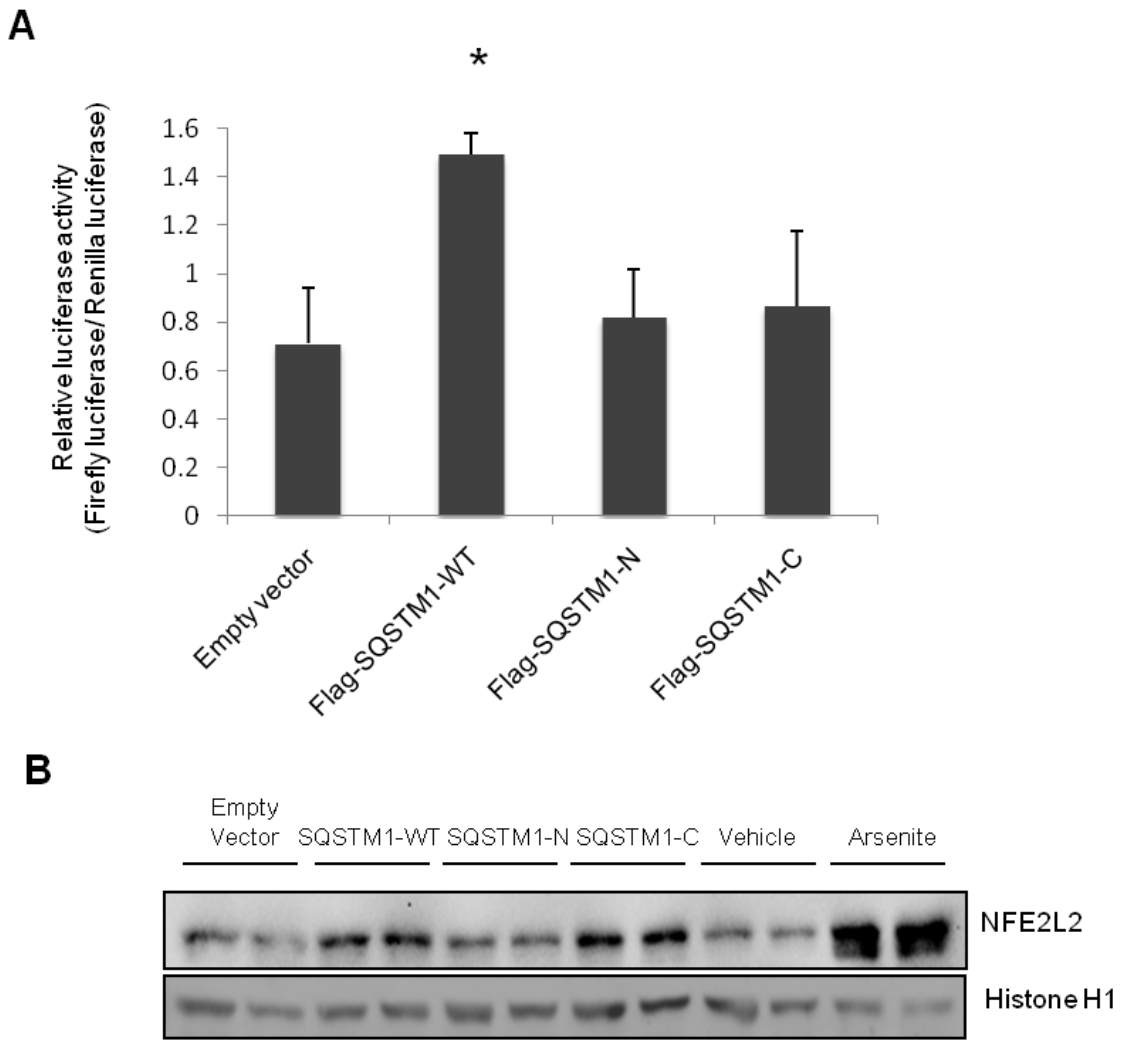

Figure 14. Effects of SQSTM1 cleavage fragments on NFKB activities and NFE2L2 protein levels.

(A) Effects of SQSTM1 truncations on NFKB luciferase activities. HeLa cells were transfected with Flag-SQSTM1-WT, Flag-SQSTM1-N, Flag-SQSTM1-C, or an empty vector for 48 h. NFKB luciferase activity was measured as described in Materials and Methods. Results are presented as mean ± SD (n=3). *$p < 0.01$ compared to vector control. (B) Effects of SQSTM1 truncations on protein levels of NFE2L2. HeLa cells were transfected with Flag-SQSTM1-WT, Flag-SQSTM1-N, Flag-SQSTM1-C, or an empty vector for 48 h. Cells treated with 10 μM sodium arsenite for 18 h were used as a positive control. Cell fractionation was performed and

the nuclear fractions were subjected to Western blot analysis with the antibodies specified. Histone H1 was probed as a loading control for nuclear proteins.

3.3.8 Roles of SQSTM1 in viral replication and release.

Previous research has demonstrated that SQSTM1-mediated selective autophagy is a host defense mechanism against Sindbis viral infection [173]. To determine whether SQSTM1 plays a role in CVB3 replication and release, we overexpressed or knocked down SQSTM1. **Fig. 15A and B** showed that neither overexpression nor knockdown of SQSTM1 affected viral protein expression and viral progeny release, suggesting that loss of SQSTM1 may not contribute directly to successful viral replication.

We further examined the impact of SQSTM1 mutants on viral replication and release. Considering that HeLa cells express basal levels of SQSTM1 protein, which may interfere with the effect of transfected SQSTM1 truncations or cleavage-resistant mutant, we utilized *sqstm1*$^{-/-}$ mouse embryonic fibroblasts (MEFs) for this study. MEFs were transfected with Flag-SQSTM1-WT, Flag-SQSTM1-N, Flag-SQSTM1-C, Flag-62-G241E or an empty vector for 24 h, followed by CVB3 infection for 18 h. **Fig. 15C** showed that viral protein expression and progeny production were not apparently changed among different MEF groups, indicating that cleavage of SQSTM1 may not have a direct benefit to coxsackieviral replication and release.

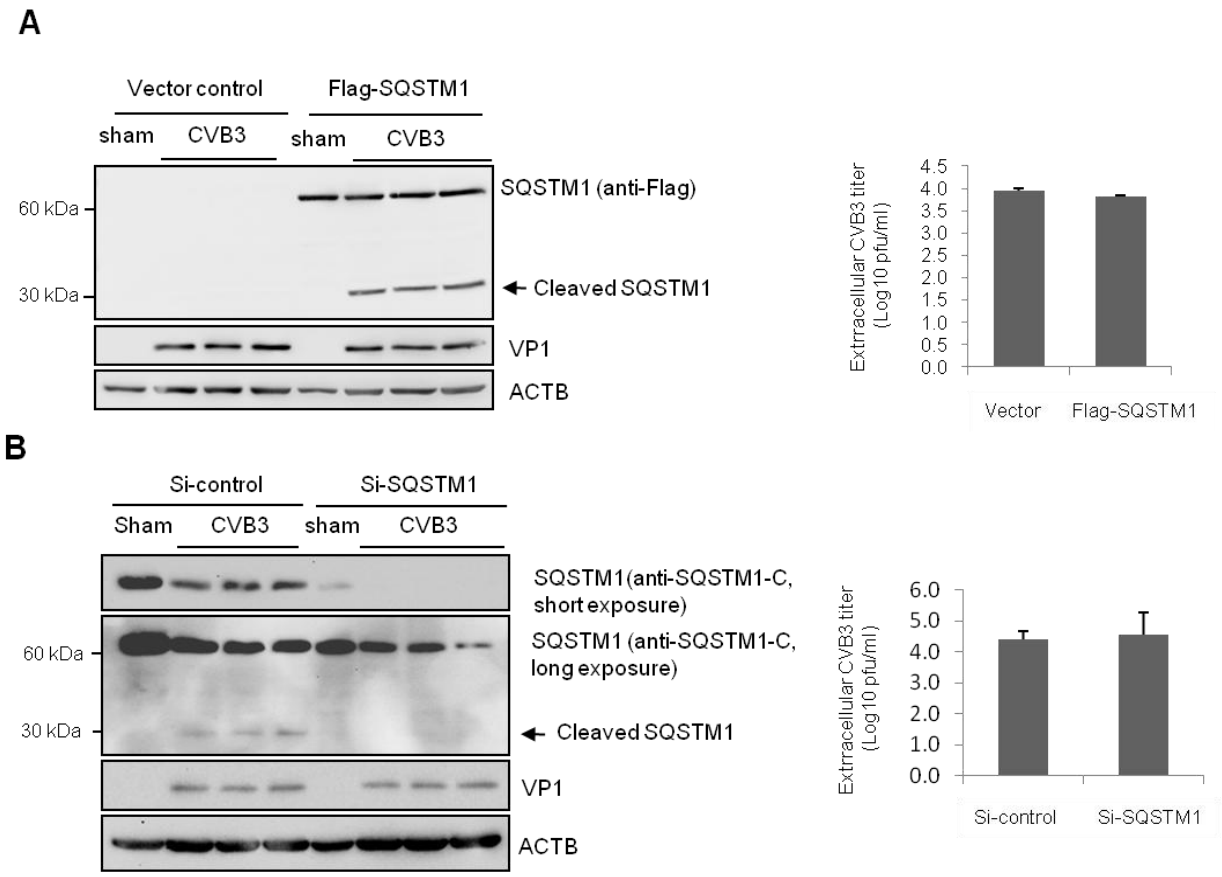
A
Vector control
Flag-SQSTM1
sham
CVB3
sham
CVB3
60 kDa
30 kDa
SQSTM1 (anti-Flag)
Cleaved SQSTM1
VP1
ACTB
Extracellular CVB3 titer (Log10 pfu/ml)
4.5
4.0
3.5
3.0
2.5
2.0
1.5
1.0
0.5
0.0
Vector
Flag-SQSTM1
B
Si-control
Si-SQSTM1
Sham
CVB3
sham
CVB3
60 kDa
30 kDa
SQSTM1(anti-SQSTM1-C, short exposure)
SQSTM1 (anti-SQSTM1-C, long exposure)
Cleaved SQSTM1
VP1
ACTB
Extracellular CVB3 titer (Log10 pfu/ml)
6.0
5.0
4.0
3.0
2.0
1.0
0.0
Si-control
Si-SQSTM1

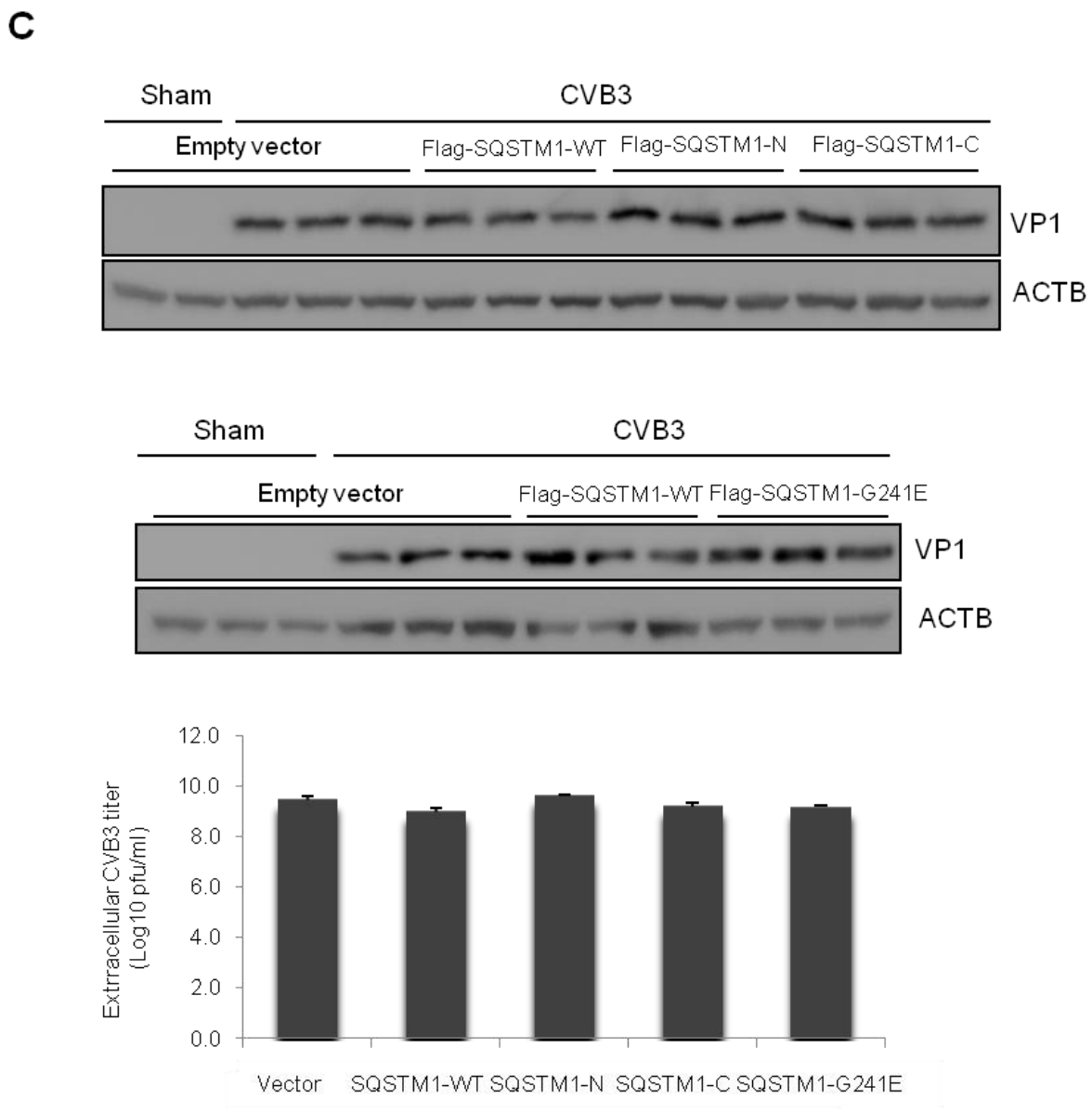

Figure 15. Effects of SQSTM1 cleavage on viral replication and release.

(**A**) Effects of overexpression of SQSTM1-WT on viral replication in HeLa cells. Cells were transiently transfected with either a control vector or an Flag-tagged SQSTM1 construct for 24 h, followed by CVB3 infection for 7 h. Western blotting was performed to examine protein expression of VP1, SQSTM1, and ACTB/β-actin (loading control). A plaque assay was employed to measure extracellular viral titers (mean ± SD, n=3). (**B**) Effects of knockdown of endogenous SQSTM1 on viral replication in HeLa cells. Cells were transfected with *SQSTM1*

siRNA (si-SQSTM1, 100 nM) or scramble siRNA (si-control) for 48 h, followed by CVB3 infection for 7 h. Western blot analysis and plaque assay were performed as described above. **(C)** Effects of various forms of SQSTM1 mutants on viral replication and release in *sqstm1*$^{-/-}$ MEFs. MEFs were transfected with Flag-SQSTM1-WT, Flag-62-G241E, Flag-SQSTM1-C, Flag-SQSTM1-N or an empty vector (control) for 24 h, followed by CVB3 infection for 18 h. Western blot analysis (upper two panels) and plaque assay (lower panel) were performed as described above.

3.3.9 Monitoring Autophagic flux during CVB3 infection.

As we found that the protein level of SQSTM1 is also regulated by proteinase 2A^{pro}-mediated proteolytic degradation, SQSTM1 does not serve as an accurate marker of autophagic flux during CVB3 infection. We therefore utilized an mRFP-EGFP-LC3 stably expressing HEK293 cell line to monitor autophagic flux. The conversion of fluorescence in the tandem fluorescent-tagged cell line is very instrumental to track autophagy dynamics [196, 197, 198]. Unlike mRFP, EGFP is unstable in low-pH environment and is quenched in the acidic lysosomes upon autophagosome-lysosome fusion. Thus, yellow fluorescence (overlap of green and red signals) represents autophagosomes, while red only fluorescence represents autolysosomes [185]. The mRFP-EGFP-LC3 stable HEK293 cells were infected with sham or CVB3 in the presence or absence of BAF, a vacuolar-type H+ ATPase inhibitor to block autophagosome and lysosome fusion. Starvation is a potent stimulator of autophagy with enhanced autophagic flux [185]. Therefore, starvation in combination with BAF treatment was used as a positive control to show the blockage of autophagic flux. Confocal images showed that BAF has no effects on the colocalization of EGFP-LC3 and mRFP-LC3 puncta after CVB3 infection (Rr Ratio of CVB3: CVB3+BAF=0.89: 0.89) as compared to control groups where colocalization of EGFP-LC3 and mRFP-LC3 puncta were dramatically enhanced after BAF treatment (Rr Ratio of Sham: Sham+

BAF=0.31: 0.84; Starvation: Starvation+ BAF=0.37: 0.86) (**Fig. 16A**), suggesting that autophagic flux is impaired during CVB3 infection. Similar results were obtained in HeLa cells transiently transfected with the mRFP-EGFP-LC3 construct (data not shown). Consistent with the immunofluorescence data, Western blotting demonstrated that LC3-II protein level did not further increase upon BAF treatment after CVB3 infection, unlike that in starvation or sham group (**Fig. 16B**).

To further confirm the blockage of autophagic flux, we utilized the non-cleavable form of SQSTM1 (SQSTM1-G241E). Stable HEK293 cells were transfected with SQSTM1-G241E, followed by starvation or CVB3 infection. As expected, starvation results in autophagic degradation of SQSTM1-G241E (**Fig. 16C**). In contrast, non-cleavable SQSTM1-G241E was accumulated (**Fig. 16D**) after CVB3 infection, confirming that autophagic flux is blocked.

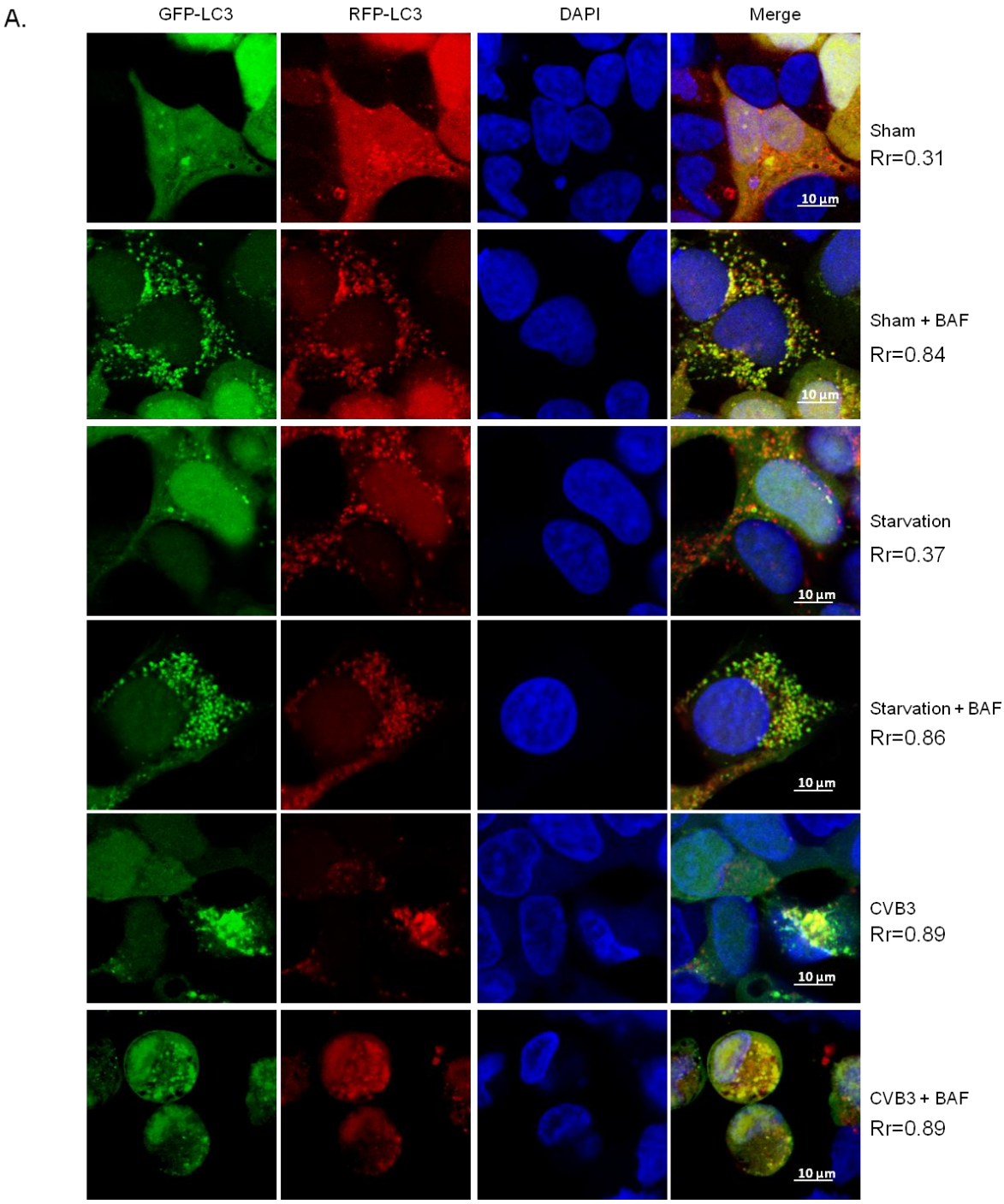
A.
GFP-LC3
RFP-LC3
DAPI
Merge
Sham
Rr=0.31
Sham + BAF
Rr=0.84
Starvation
Rr=0.37
Starvation + BAF
Rr=0.86
CVB3
Rr=0.89
CVB3 + BAF
Rr=0.89
10 μm

B.

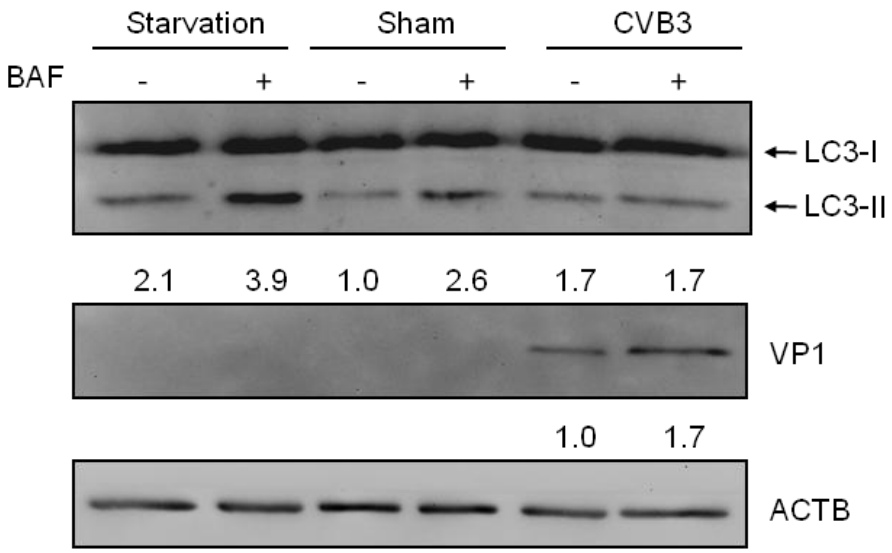
Starvation
Sham
CVB3
BAF
- + - + - +
LC3-I
LC3-II
2.1 3.9 1.0 2.6 1.7 1.7
VP1
1.0 1.7
ACTB

C.

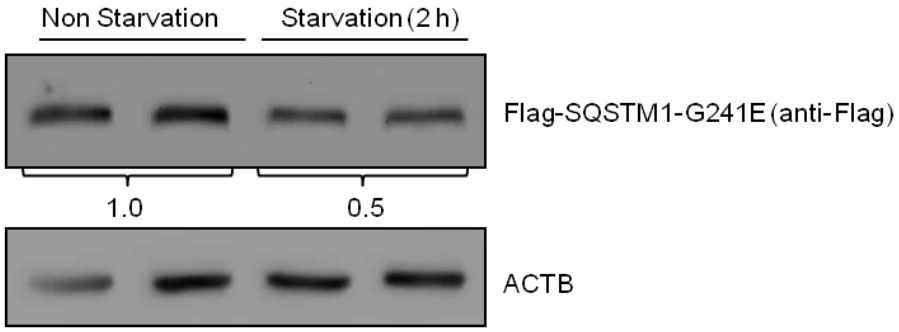
Non Starvation
Starvation (2 h)
Flag-SQSTM1-G241E (anti-Flag)
1.0 0.5
ACTB

D.

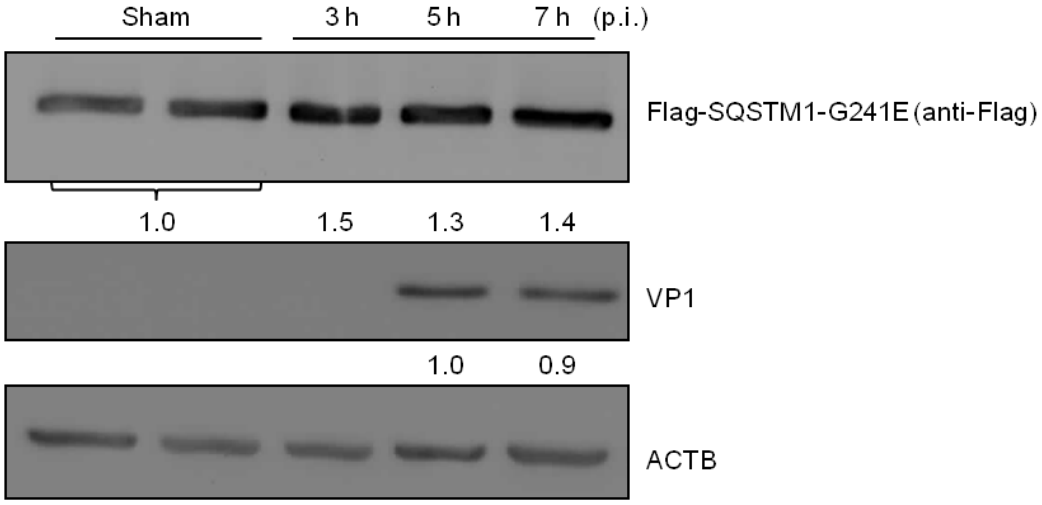
Sham
3 h
5 h
7 h (p.i.)
Flag-SQSTM1-G241E (anti-Flag)
1.0 1.5 1.3 1.4
VP1
1.0 0.9
ACTB

Figure 16. Autophagic flux during CVB3 infection.

(**A and B**) mRFP-EGFP-LC3 stable HEK293 cells were sham- or CVB3-infected at MOI=20 for 7 h in the presence or absence of vacuolar-type H+ ATPase bafilomycin (BAF, 20 μM) since 1 h post infection (p.i.). Cells were serum starved (DMEM without 10% FBS) in the presence or absence of BAF for 6 h. The nucleus was counterstained with DAPI. Cell images were captured by confocal microscopy. Colocalization between GFP-LC3 and mRFP-LC3 puncta was quantified using Image-Pro Plus 5.1 software and presented as Pearson Correlation (Rr, Rr=1, perfect colocalization; Rr=0, random/no colocalization) (**A**). Protein expression of autophagy markers LC3-I, II, and viral capsid protein VP1 were tested by Western blotting. ACTB was probed as a loading control. Densitometric analysis was performed using ImageJ software. The numbers presented were relative protein density over references (where indicated as 1.0) after normalization to ACTB (**B**). (**C and D**) HeLa cells were transiently transfected with non-cleavable Flag-SQSTM1-G241E, in which glycine (G) residue at position 241 was replaced with glutamic acid (E) residue. Twenty-four hours post transfection, cells were treated with starvation (**C**) or CVB3 infection (**D**) for indicated periods of time. Exogenous expression of Flag-SQSTM1-G241E was measured by Western blotting using anti-Flag antibody. Quantification was performed as described above.

3.4 Discussion

Our previous study demonstrated that CVB3 infection induces dramatic increase of autophagosomes and autophagy marker protein LC3-II [164]. Given that autophagy is a dynamic process basically composed of induction and degradation, the accumulation of autophagosomes and LC3-II could be attributed to enhanced production, impaired degradation, or both. We previously showed the activation of autophagy upstream signaling pathway, suggesting that enhanced production contributes at least partly to the accumulation of autophagosomes [164]. However, whether autophagy pathway is complete after CVB3 infection remains unknown. Several studies utilized SQSTM1 as a marker of autophagic degradation in enteroviral infections

and found a reduction of SQSTM1 [199, 200, 201]. Similarly, our study also found the decreased protein level of SQSTM1; however, the decline of SQSTM1 is not due to enhanced autophagic degradation, but due to CVB3 proteinase $2A^{pro}$-mediated proteolytic cleavage. Thus, cautions should be taken when using SQSTM1 to measure autophagic flux during viral infection. Using a combination of different techniques, including a tandem fluorescent-tagged cell line and a non-cleavable SQSTM1-based method, we provide solid evidence supporting that autophagy flux is suppressed following CVB3 infection. However, we did not observe any megaphagosomes that were found in pancreatic cells [182], implying that the formation of megaphagosomes may be cell-specific.

CVB3 infection not only impairs autophagic flux, but also disrupts selective autophagy. The protein degradation system acts as a critical component of protein quality control by removing terminally misfolded proteins/aggregates. Increasing evidence has revealed that aberrant protein degradation plays an important role in the development of many human diseases. Misfolded protein aggregates are frequently detected in neurodegenerative, liver, and heart diseases and are thought to be toxic to cells [57, 202, 203]. We have previously demonstrated an abnormal accumulation of ubiquitin conjugates in CVB3-infected cells and tissues, suggesting that defective protein degradation may contribute to viral pathogenesis [60, 61, 204]. However, the underlying mechanisms regarding how protein conjugates are formed during CVB3 infection remain largely undetermined.

Although the functional role and the precise mechanism of SQSTM1 in selective autophagy still need rigorous evaluation, SQSTM1 has been suggested to act as an autophagy receptor targeting ubiquitinated proteins for autophagosome-lysosome degradation. When autophagy is deficient, SQSTM1 and ubiquitin conjugates accumulate to form aggregates that are often

observed in pathological inclusion bodies [205]. In this study, we explored autophagic flux during CVB3 infection and the link between CVB3 infection and SQSTM1-mediated selective autophagy. Our major findings in the present study are: (1) receptor protein SQSTM1 is cleaved in the course of CVB3 infection; (2) CVB3-encoded proteinase $2A^{pro}$ is responsible for the cleavage of SQSTM1; (3) cleavage of SQSTM1 occurs within the TB domain, leading to the dissociation of the N-terminal PB1 and ZZ domains from the C-terminal UBA, LIR, and KIR domains; (4) SQSTM1 truncations lose the function of full-length SQSTM1 in mediating selective autophagy; and (5) cleavage products of SQSTM1 retain the activity of SQSTM1 in stabilizing NFE2L2, but fail to regulate NFKB activation; (6) Autophagic flux is suppressed during CVB3 infection.

In our previous publication, we showed that SQSTM1 protein levels were not apparently decreased in the course of CVB3 infection using anti-N-terminal SQSTM1 antibody [164]. There are three possible explanations for the discrepancy between the current finding and the earlier report. First, the western blot might be overexposed in the previous study, so the difference in protein expression was not clearly visible. Second, due to the difference in cell and experimental conditions, the amount of produced viral proteinases might vary between experiments. Third, we found that the binding affinity and the specificity of different batches of anti-SQSTM1-N antibody were different.

It is known that SQSTM1 facilitates the formation of ubiquitinated protein aggregates (also known as SQSTM1 bodies or sequestosomes) prior to delivering them to the phagophore for degradation [123, 206]. Two structural domains of SQSTM1, PB1 and UBA, play critical roles in this process of selective autophagy [188]. It was reported that self-oligomerization via the PB1 domain is required for the formation of ubiquitin-positive inclusions [207, 208]. In addition, recognition and

recruitment of the substrate protein through its UBA domain also participate in this process [188]. Our findings in the present study showed that the number of cells with punctate structures is considerably lower in SQSTM1-N- or SQSTM1-C-expressing cells (31.13% and 7.34%, respectively) as compared to SQSTM1-WT-expressing cells (91.02%), supporting the notion that both the PB1 and UBA domains are required for SQSTM1- mediated protein aggregate formation.

Immunoprecipitation assay demonstrated the physical interaction between SQSTM1-C and LC3; however, immunocytochemical staining showed that the colocalization rate of SQSTM1-C and LC3 within the punctate structures was largely reduced as compared to the association between SQSTM1-WT and LC3 (8.77% versus 53.38%). This observation appears to be a reflection of the reduced ability of SQSTM1-C to form protein aggregates.

SQSTM1 is degraded via the autophagic pathway together with ubiquitinated proteins. As a result of CVB3 infection, we found that both N- and C-terminal cleavage fragments of SQSTM1 are not degraded through the autophagic pathway. While this finding is not surprising for SQSTM1-N, it is interesting to note that SQSTM1-C that contains intact LIR and UBA domains is also resistant to lysosome-mediated degradation. This discovery indicates that other functional domain(s) at the N terminus of SQSTM1 are also required for the recruitment and/or degradation of SQSTM1. Indeed, it was recently reported that self-oligomerization of SQSTM1 mediated by its PB1 domain is crucial for its localization to phagophores [207]. It is therefore reasonable to think that the SQSTM1-C fragment is unable to be recruited to the autophagosome formation site due to the lack of the PB1 domain.

Another interesting observation in this study is that while the SQSTM1-C fragment contains a complete UBA, pull-down assay failed to detect the presence of polyubiquitinated proteins.

Immunostaining also revealed that the percentage of cells with punctate colocalization of SQSTM1-C and ubiquitin was considerably lower than that in SQSTM1-WT-expressing cells (10.12% versus 91.59%). It was previously shown that the interaction between the TB domain of SQSTM1 and TRAF6 is required for polyubiquitination of the substrate proteins associated with the UBA domain of SQSTM1 [189, 195]. The binding partner of the TB domain, TRAF6, is a RING finger ubiquitin ligase that catalyzes lysine 63 (K63)-linked ubiquitination of target proteins [209]. Thus, it is speculated that failure to discover the association between SQSTM1-C and ubiquitin conjugates is a result, at least in part, of the absence of the TB domain and its associated ubiquitin ligase.

SQSTM1 has been identified as a key regulator of the NFKB signaling. Among the three functional domains (PB1, ZZ, and TB) that were previously reported to be involved in the activation of the NFKB pathway [210, 211]. The TB domain of SQSTM1 appears to be the major driver for NFKB activation. It was shown that interaction between the TB domain of SQSTM1 and the TRAF6 protein facilitates K63-linked auto-ubiquitination of TRAF6 and subsequent NFKB activation [189, 191]. In this study, we discovered that SQSTM1 is cleaved at amino acid 241 within the TB domain (amino acids 225 to 250). It is therefore plausible to assume that an incomplete TB domain results in loose association of SQSTM1 with, or complete dissociation of SQSTM1 from, TRAF6, which corresponds with our observation that both N- and C-terminal fragments of SQSTM1 are incapable of activating NFKB. It is well documented that NFKB pathway plays a critical role in antiviral innate immunity and cell survival [212]. Inability to activate this pathway may represent a viral strategy to stymie the host defense mechanism. Future investigation is warranted to further understand the role of cleavage of SQSTM1 in innate immunity using animal models.

Apart from its function in protein quality control, autophagy also plays a crucial role in viral infectivity [213]. Autophagy is traditionally considered as a host defense mechanism for clearing pathogens [214, 215]. However, some viruses can subvert this host antiviral machinery to promote their own replication [213]. We demonstrate that CVB3 infection induces the formation of double-membrane structures termed autophagosomes [164]. Blockage of autophagy effectively inhibits viral replication, whereas induction of autophagosome formation promotes viral replication, suggesting that the autophagosome is an important cellular apparatus required for CVB3 replication [164]. However, in this study, we found that neither knockdown nor overexpression of various forms of SQSTM1 has an effect on viral replication and release, indicating that inhibition of SQSTM1 function is unlikely a viral strategy to establish efficient viral replication in host cells.

Chapter 4: Dominant-negative function of the C-terminal fragments of NBR1 and SQSTM1 generated during CVB3 infection

4.1 Background

NBR1 is a functional homolog of SQSTM1 in mediating selective autophagy. Despite the difference of its primary sequence and size from those of SQSTM1, NBR1 shares a similar domain structure with SQSTM1, both containing PB1, ZZ, LIR, and UBA domains [216] (**Figure. 17**). Depending on the characteristics of the substrates, NBR1 and SQSTM1 work either independently or cooperatively with each other. It was reported that autophagic clearance of bacteria, such as Salmonella and Listeria, requires SQSTM1, but not NBR1 [217]. In contrast, NBR1 alone is sufficient to target peroxisomes to lysosomes for degradation in the absence of SQSTM1, but SQSTM1 increases the efficiency of NBR1-mediated pexophagy[218]. NBR1 can also work in concert with SQSTM1 to remove ubiquitinated cargo [124, 216]. The observation that deletion of SQSTM1 fails to induce the accumulation of ubiquitinated proteins implies a possible compensatory role for NBR1 when the function of SQSTM1 is compromised [131, 190].

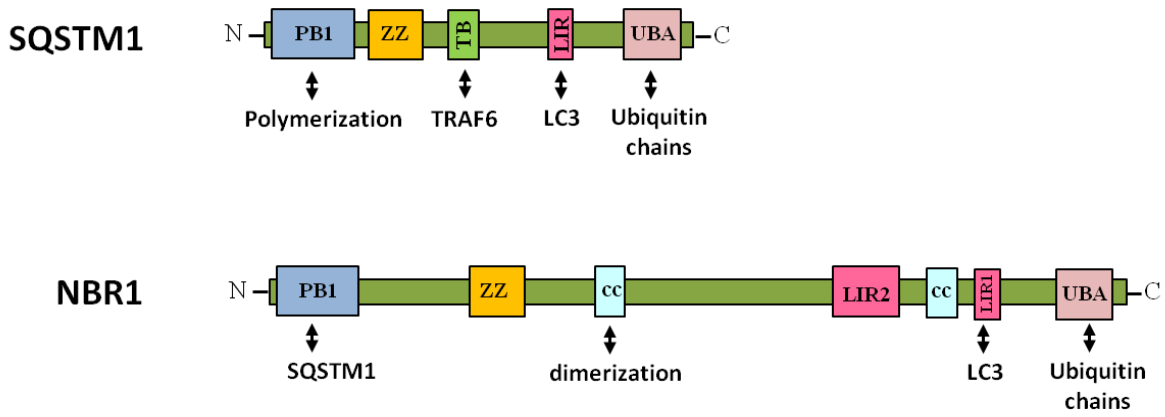

Figure 17. Domain architecture of SQSTM1 and NBR1.

SQSTM1 and NBR1 are different in size, but share similar functional domains. PB1, Phox and Bem1 domain; ZZ, zinc-finger domain; TB, TRAF6-binding domain; LIR, LC3-interacting region; UBA, ubiquitin-associated domain; CC, coiled-coil domain. N-terminal PB1 domain, C-terminal LC3, and UBA domains form the structural basis for selective degradation of ubiquitin-tagged substrates through autophagy pathway.

4.2 Specific aims

The purpose of this chapter is to determine whether NBR1 could compensate for the compromised functions of SQSTM1 following coxsackievirus infection.

The **SPECIFIC AIMS** include:

Aim 1. To test whether NBR1 is cleaved following CVB3 infection

Aim 2. To identify the proteinases responsible for NBR1 cleavage and the cleavage sites

Aim 3. To study the functional alterations of the cleavage fragments of SQSTM1 and NBR1, with a particular focus on the gain-of-functions

4.3 Results

4.3.1 Cleavage of NBR1 following CVB3 infection.

We have previously demonstrated that SQSTM1 is cleaved during coxsackievirus infection, resulting in the disruption of the function of SQSTM1 [219] . Since NBR1 may play a compensatory role for the loss of SQSTM1, we examined NBR1 expression after CVB3 infection. We found that NBR1 was also potentially cleaved after CVB3 infection, generating at least two cleavage fragments (~100kDa and ~50kDa, respectively) using an anti-N-terminal NBR1 antibody (**Fig. 18A**). mRNA expression of NBR1 appeared unaltered after CVB3 infection (**Fig. 18B**).

To verify the cleavage of NBR1, cells were transiently transfected with an HA-tagged NBR1 construct, followed by CVB3 infection. The cleavage products of exogenous NBR1 detected by an anti-HA antibody (**Fig. 18C**) corresponded well with those of the endogenous NBR1 (**Fig. 18A**), confirming that NBR1 is cleaved after CVB3 infection.

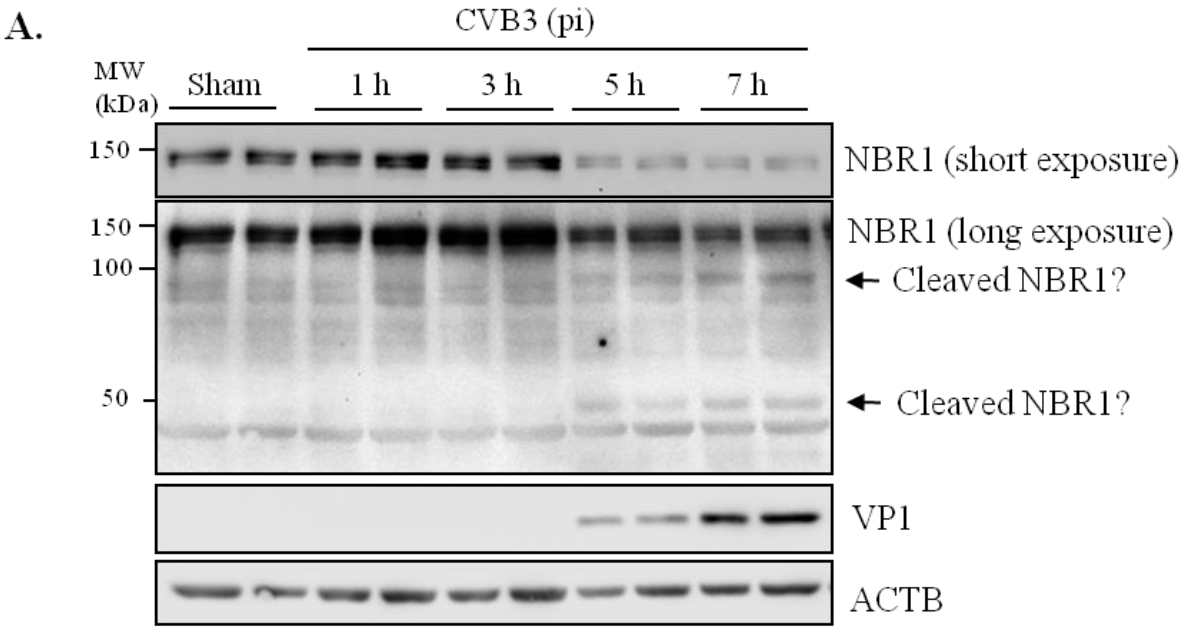

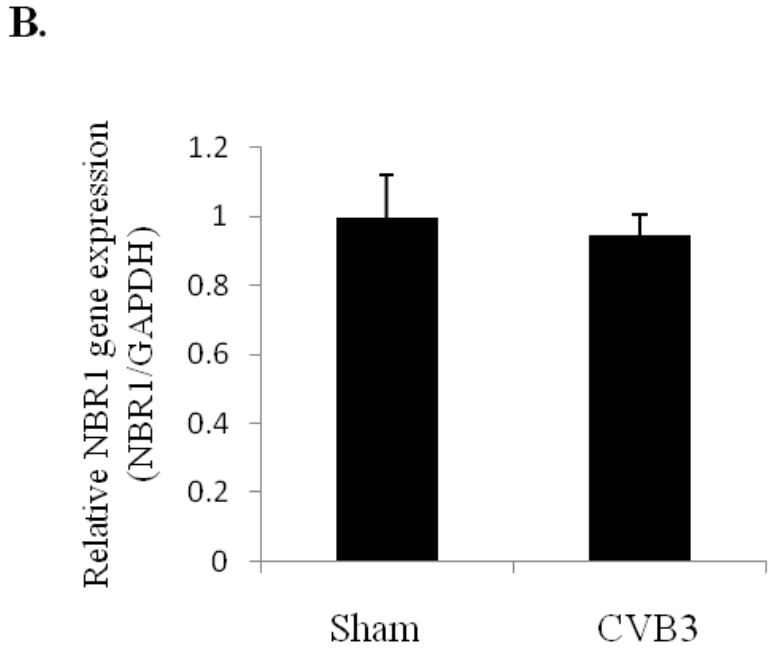

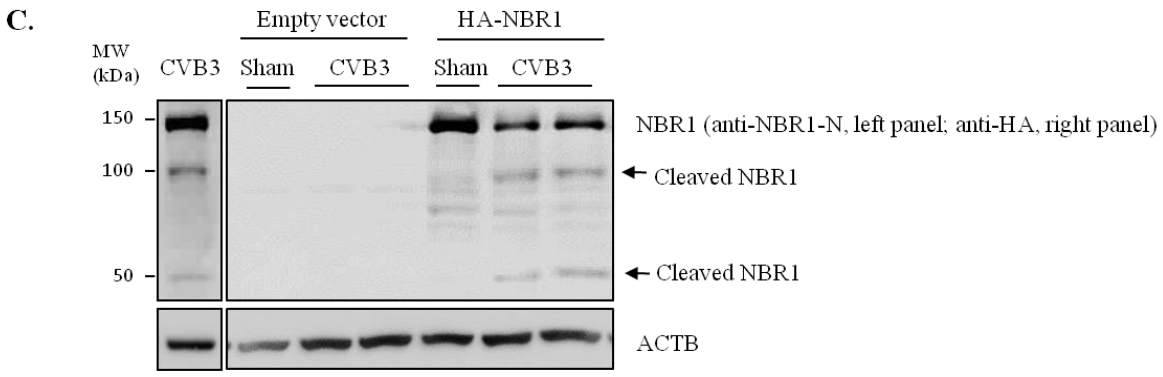

Figure 18. Cleavage of NBR1 following CVB3 infection.

(A) Protein level of NBR1 after CVB3 infection. HeLa cells were sham-infected with PBS or infected with CVB3 for indicated times at a multiplicity of infection (MOI) of 10. Western blot analysis was performed to examine the expression of NBR1 using anti-N-terminal NBR1 antibody which recognizes amino acids 1~150 (Santa Cruz Biotechnologies), viral capsid protein VP1, and ACTB/β-actin (loading controls). **(B)** mRNA expression of NBR1 after CVB3 infection. HeLa cells were either sham-infected or infected with CVB3 for 7 h. mRNA expression of NBR1 was examined by real time quantitative PCR and normalized to GAPDH mRNA (mean ± SD, n=3). **(C)** Cleavage of NBR1 after CVB3 infection. HeLa cells were transiently transfected with a plasmid expressing HA-tagged NBR1 for 24 h, followed by CVB3 infection for 7 h. Western blotting was carried out to examine expression levels of exogenous NBR1 using anti-HA antibody which recognizes the N terminus of NBR1. For size comparison, Western blotting of endogenous NBR1 using anti-N-terminal NBR1 antibody was presented on the left lane. Protein expression of ACTB/β-actin was measured as the loading control. pi, post-infection.

4.3.2 Cleavage of NBR1 is mediated by coxsackieviral proteinases $2A^{pro}$ and $3C^{pro}$.

To explore whether coxsackievirus proteinases are responsible for NBR1 cleavage, we performed *in vitro* cleavage assays using purified coxsackieviral $2A^{pro}$ and $3C^{pro}$. We showed that incubation of cell lysates with purified $2A^{pro}$ and $3C^{pro}$ resulted in the time-dependent

generation of NBR1 cleavage products of ~50kDa and ~100kDa, respectively, similar to those observed in CVB3-infected cells (**Fig. 19A & B**). $2A^{pro}$ mutant failed to induce the cleavage of NBR1 (**Fig. 19A**). These results suggest that the cleavage of NBR1 is mediated by both coxsackieviral $2A^{pro}$ and $3C^{pro}$.

As CVB3 infection results in caspase activation [220], we further examined whether caspase activation plays a role in the cleavage of NBR1. **Fig. 19C** showed that treatment with a pan caspase inhibitor Z-VAD-FMK inhibited CVB3-induced caspase-3 cleavage, but did not block the production of NBR1 cleavage fragments, indicating that cleavage of NBR1 is independent of caspase activity.

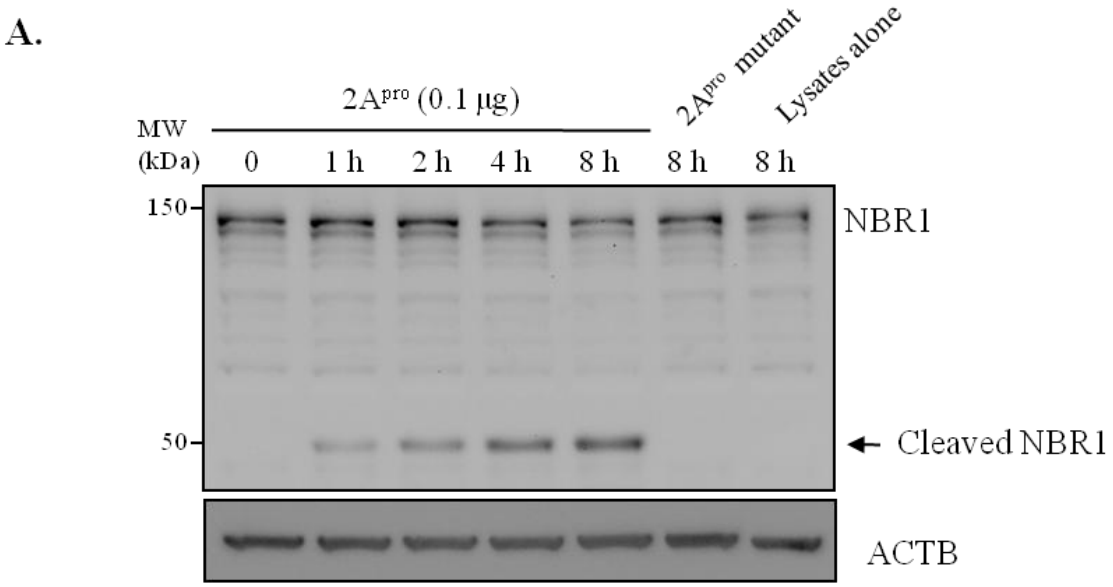

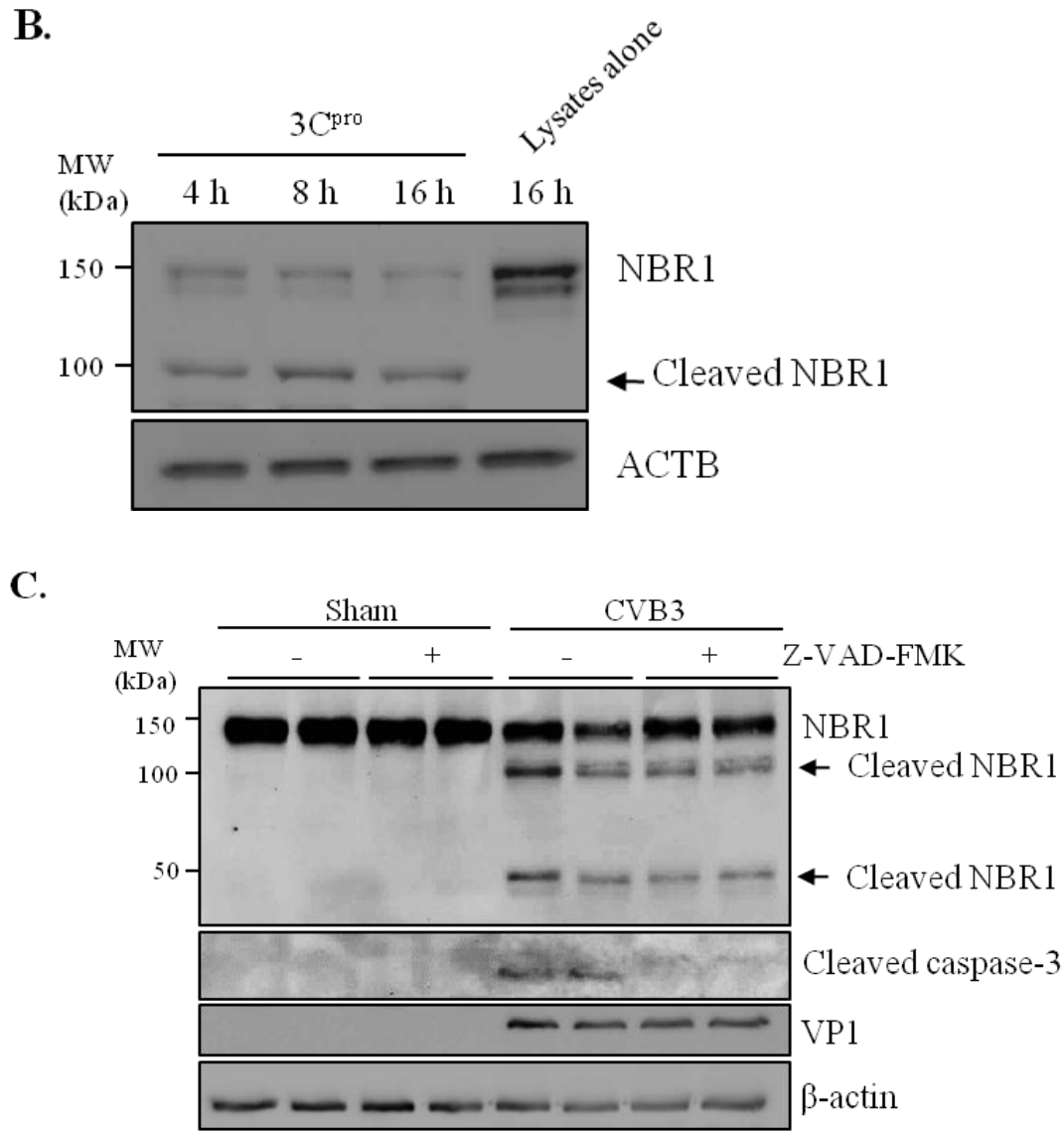

Figure 19. Cleavage of NBR1 by coxsackieviral proteinases $2A^{pro}$ and $3C^{pro}$.

(A, B) Effect of viral proteinase $2A^{pro}$ and $3C^{pro}$ on NBR1 cleavage by *in vitro* cleavage assay. Fifty microgram of protein extracts from HeLa cells were incubated with 0.1 μg of purified coxsackieviral $2A^{pro}$ (A), 0.1 μg of catalytic $2A^{pro}$ mutant (A), or 0.1 μg of $3C^{pro}$ (B) for increasing periods of time as indicated. **(C)** Effect of general caspase inhibition on CVB3-induced NBR1 cleavage. HeLa cells were infected with CVB3 for 7 h with or without pan caspase inhibitor Z-VAD-FMK (50 μM). Western blotting was performed to examine protein

expression of NBR1 using anti-N-terminal NBR1 antibody, VP1, cleaved caspase-3, and ACTB/β-actin (loading control). "–", vehicle control.

4.3.3 Identification of the cleavage sites on NBR1.

Using a computer server for prediction of cleavage sites by enteroviral proteinases (NetPicoRNA V1.0 algorithm), we found two potential cleavage sites by viral proteinase $3C^{pro}$ around the C-terminus of NBR1: residue 682 (FALPE/GPLG) and residue 612 (EEENE/GAGF), which result in the production of a protein of ~100kDa**,** consistent with the high molecular weight fragment detected in CVB3-infected cells. To determine the precise cleavage site, we constructed two NBR1 point mutants [NBR1-E682K and NBR1-E612K, in which glutamic acid (E) residue was replaced with lysine (K) residue]. **Fig. 20A** showed that the ~100kDa cleavage fragment disappeared, while the ~50kDa fragment remained in cells expressing NBR1-E682K, indicating that E682 is a cleavage site on NBR1 after CVB3 infection (**Fig. 20A**).

Amino acid sequence alignment of NBR1 with other known viral proteinase $2A^{pro}$ substrates, including SQSTM1, reveals a potential cleavage motif (MKNTG at residues 398-402) on NBR1. To determine whether NBR1 is cleaved at T/G, we constructed a point mutation plasmid NBR1-G402E, in which glycine (G) residue at position 402 was replaced with glutamic acid (E) residue. As shown in **Fig. 20B**, the cleavage fragment (~50kDa) disappeared and the level of the ~100kDa fragment was reduced in cells expressing mutant NBR1 comparing with cells expressing wildtype NBR1. This result suggests that NBR1 is primarily cleaved between T401 and G402, likely via the action of viral proteinase $2A^{pro}$. Schematic diagram presented in **Fig. 20C** shows NBR1 structural domains, the identified cleavage sites on NBR1, and the resulting cleavage fragments.

A.

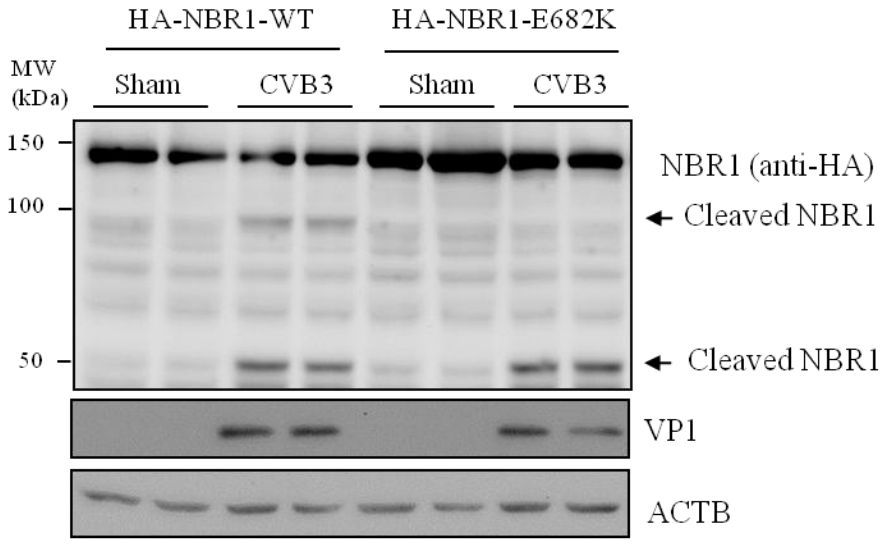
HA-NBR1-WT
HA-NBR1-E682K
MW (kDa)
Sham
CVB3
Sham
CVB3
150
100
50
NBR1 (anti-HA)
Cleaved NBR1
Cleaved NBR1
VP1
ACTB

B.

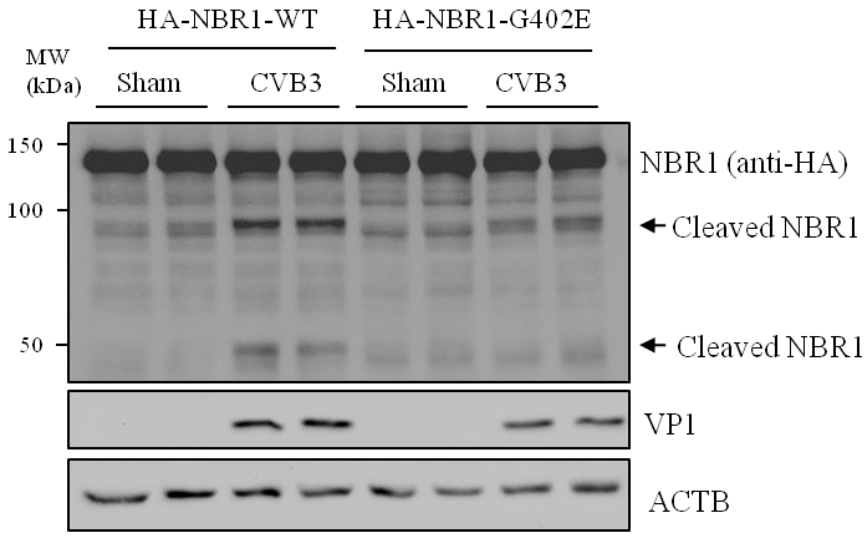
HA-NBR1-WT
HA-NBR1-G402E
MW (kDa)
Sham
CVB3
Sham
CVB3
150
100
50
NBR1 (anti-HA)
Cleaved NBR1
Cleaved NBR1
VP1
ACTB

C.

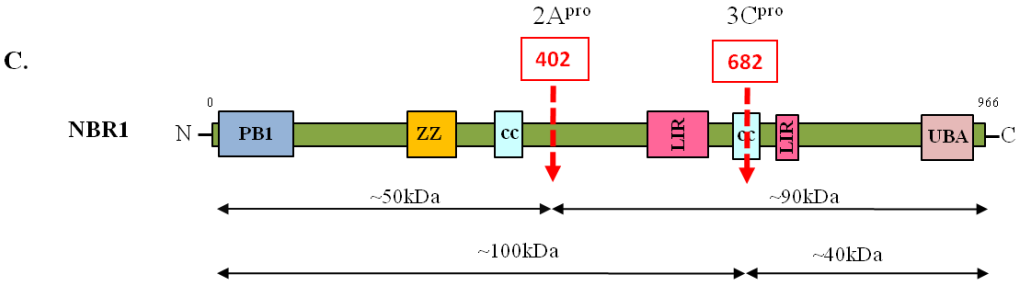
2A^pro
3C^pro
402
682
NBR1
N
0
PB1
ZZ
cc
LIR
cc
LIR
UBA
966
C
~50kDa
~90kDa
~100kDa
~40kDa

Figure 20. Identification of the cleavage sites on NBR1.

(A, B) Identification of NBR1 cleavage sites. HeLa cells were transiently transfected with HA-NBR1-WT, HA-NBR1-G402E [glycine (G) at amino acid 402 was replaced by glutamic acid (E)] (A), or HA-NBR1-E682K [glutamic acid (E) at amino acid 682 was replaced by lysine (K)] (B) for 24 h, followed by sham or CVB3 infection for 7h. Western blotting was performed to detect various forms of NBR1 using anti-HA antibody. Protein level of ACTB/β-actin was examined as a loading control. **(C)** Schematic diagram of the structural domains and the identified cleavage sites on NBR1. PB1, Phox/Bem1p domain; ZZ, zinc-finger domain; CC, coiled-coil domain; LIR, LC3-interacting region; UBA, ubiquitin association domain.

4.3.4 Dominant-negative effects of the C-terminal cleavage fragments of SQSTM1 and NBR1.

We have previously shown that cleavage of SQSTM1 as a consequence of CVB3 infection leads to the loss of the function of full-lengh SQSTM1 [219]. Here we further investigated whether the cleavage products have toxic gain-of-function properties. In this study, we focused on the C-terminal fragment of SQSTM1 (SQSTM1-C) since it retains intact LIR and UBA domains, but lacks the critical structures at the N-terminus which are essential for its function in selective autophagy (**Fig. 21A**). Our hypothesis was that the C-terminal cleavage product of SQSTM1 acts as a dominant-negative mutant by competing with the native SQSTM1 for LC3 and ubiquitin chain binding.

Misfolded proteins and damaged organelles in the cells usually undergo ubiquitination and are present in detergent-insoluble fractions of the cell extracts. Similar to our previous observation [219], triton-insoluble ubiquitin conjugates were accumulated in cells overexpressing SQSTM1-WT (**Fig. 21B & C**). Interestingly, we found that SQSTM1-WT-mediated insoluble

aggregate formation was blocked in the presence of SQSTM1-C (**Fig. 21B & C**). Consistent with this observation, we showed that SQSTM1-WT was translocated from the triton-insoluble fractions to triton-soluble parts in cells overexpressing SQSTM1-C (**Fig. 21B & C**).

We further explored the impacts of SQSTM1-C on the ability of native SQSTM1 to form aggregates. HeLa cells were co-transfected with GFP-SQSTM1-WT together with Flag-SQSTM1-WT, Flag-SQSTM1-N, or Flag-SQSTM1-C. **Fig. 21D** showed that the number of cells with GFP puncta was greatly reduced in cells co-expressing Flag-SQSTM1-C compared with cells co-expressing Flag-SQSTM1-WT, i.e., 29.93% versus 79.19% ($p<0.05$). SQSTM1-N appeared to have no effects on WT-SQSTM1-induced protein aggregate formation, i.e., 74.82% versus 79.19% ($p>0.05$) (**Fig. 21D**). Together, our results suggest a dominant-negative effect of SQSTM1-C on the function of native SQSTM1 in ubiquitin aggregate formation.

Finally, we examined the effects of the SQSTM1-C on selective autophagy. Since both SQSTM1 and NBR1 are targets of selective autophagy themselves, we then assessed protein levels of endogenous SQSTM1 and NBR1 in cells expressing SQSTM1-C. The results shown in **Fig. 21E** demonstrated that expression of SQSTM1-C led to an accumulation of full-length SQSTM1 and NBR1, indicating an inhibitory effect of the SQSTM1-C on selective autophagy.

Similarly, we found that overexpression of 3C-NBR1-C ($3C^{pro}$-induced C-terminal fragment of NBR1) resulted in an increased accumulation of endogenous SQSTM1 (**Fig. 22**). However, this effect appeared to be specific for 3C-NBR1-C as 2A-NBR1-C ($2A^{pro}$-induced C-terminal fragment of NBR1) failed to induce the accumulation of SQSTM1 (**Fig. 22**).

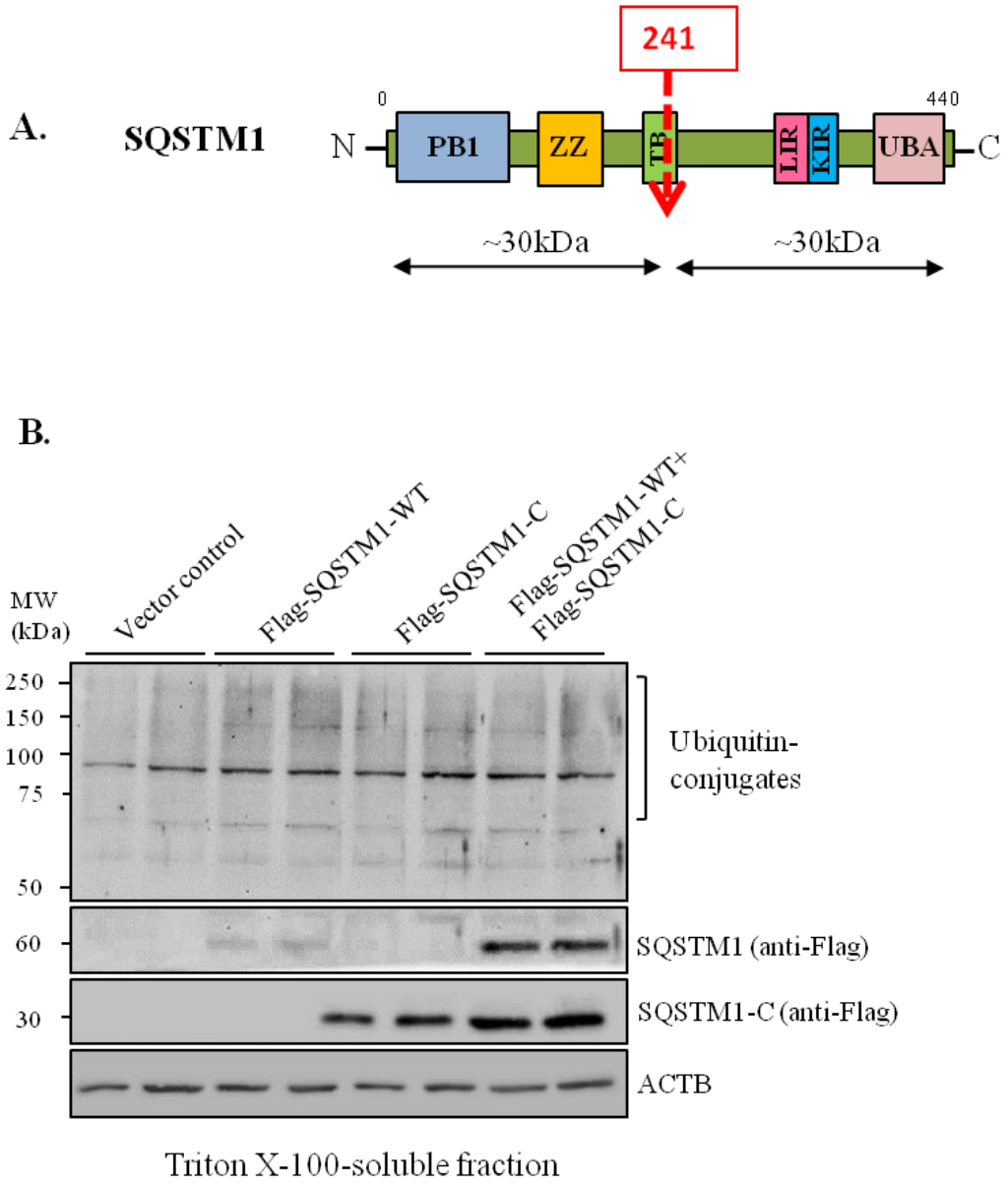
A.
SQSTM1
241
0
440
N
PB1
ZZ
TB
LIR
KIR
UBA
C
~30kDa
~30kDa
B.
MW
(kDa)
Vector control
Flag-SQSTM1-WT
Flag-SQSTM1-C
Flag-SQSTM1-WT+
Flag-SQSTM1-C
250
150
100
75
50
60
30
Ubiquitin-
conjugates
SQSTM1 (anti-Flag)
SQSTM1-C (anti-Flag)
ACTB
Triton X-100-soluble fraction

C.

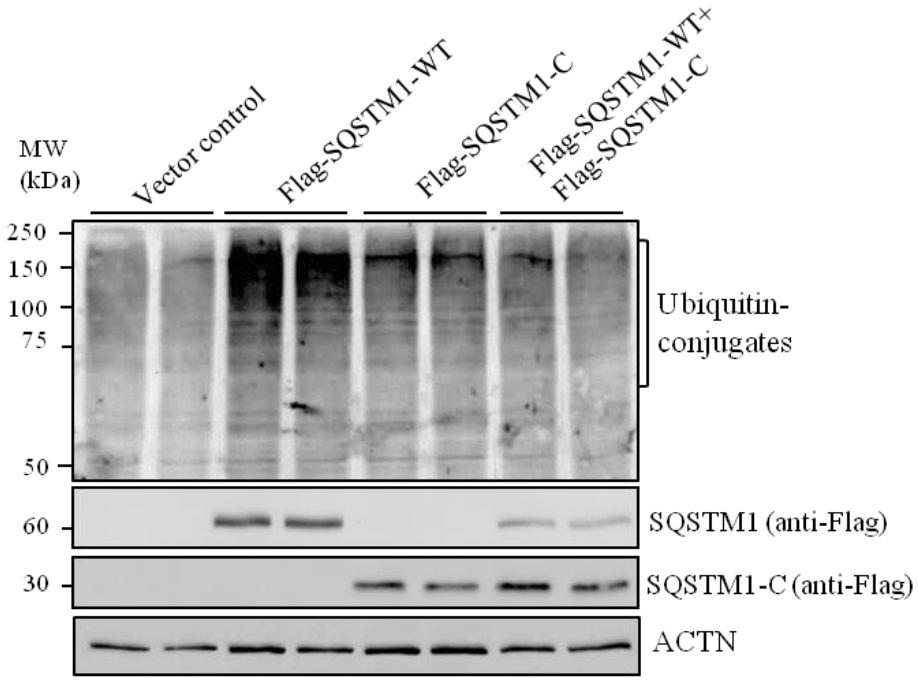

Triton X-100-insoluble fraction

D.

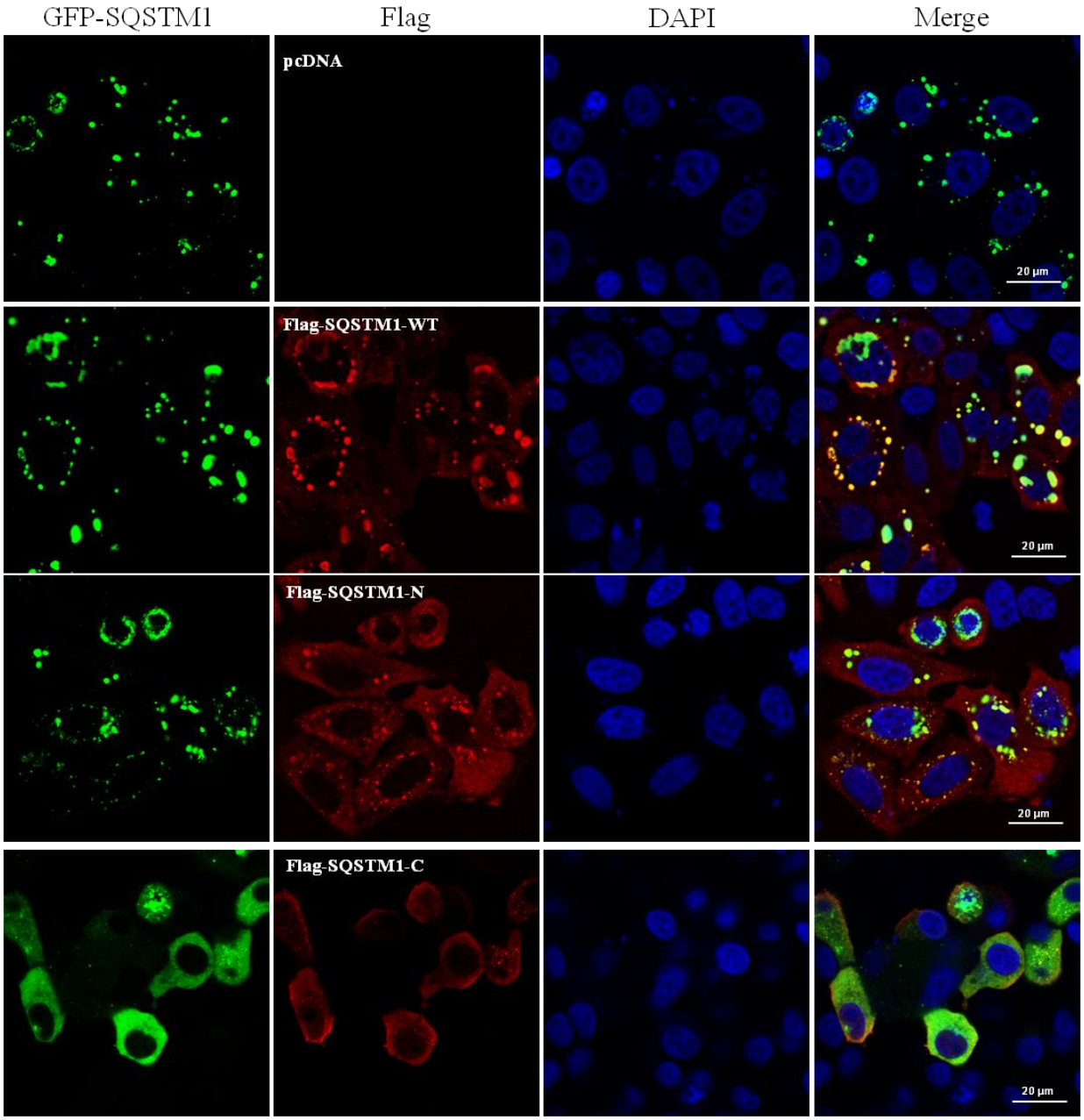
GFP-SQSTM1
Flag
DAPI
Merge
pcDNA
Flag-SQSTM1-WT
Flag-SQSTM1-N
Flag-SQSTM1-C
20 μm
20 μm
20 μm
20 μm

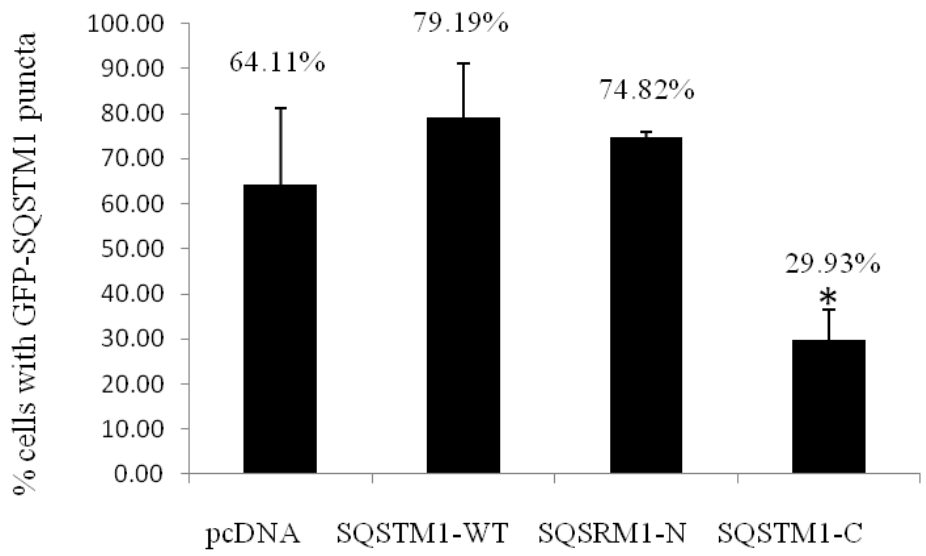

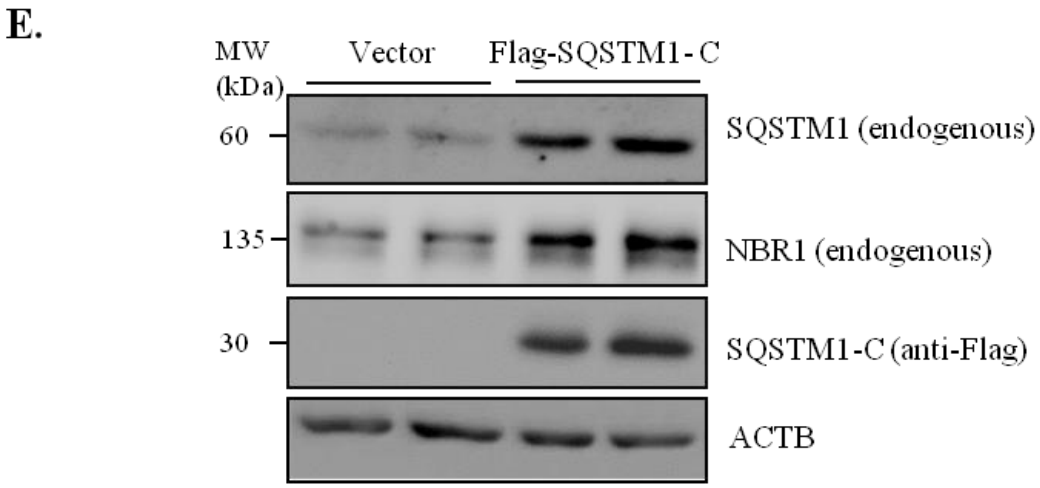

Figure 21. Dominant-negative effect of SQSTM1-C on native SQSTM1-mediated selective autophagy.

(A) Schematic diagram of the structural domains and the identified cleavage site on SQSTM1. PB1, Phox/Bem1p domain; ZZ, zinc-finger domain; TB, tumor necrosis-associated factor 6 binding domain; CC, coiled-coil domain; LIR, LC3-interacting region; KIR, keap1-interacting region; UBA, ubiquitin association domain. **(B, C)** SQSTM1-C inhibits native SQSTM1-mediated formation of insoluble ubiquitin conjugates. HeLa cells were transiently transfected

with an empty vector, SQSTM1-WT, SQSTM1-C alone, or SQSTM1-WT together with SQSTM1-C for 48 h as indicated, followed by isolation of Triton X-100-soluble and -insoluble fractions. The levels of ubiquitin conjugates in Triton X-100-soluble (B) and -insoluble fractions (C) were analyzed by Western blotting using anti-ubiquitin antibody. Protein expressions of ACTB/β-actin (B) and ACTN/α-actinin (C) were examined as loading controls for Triton X-100-soluble and -insoluble fractions, respectively. **(D)** SQSTM1-C blocks the function of native SQSTM1 in promoting protein aggregate formation. HeLa cells were co-transfected with GFP-SQSTM1-WT, together with pcDNA empty vector, Flag-SQSTM1-WT, Flag-SQSTM1-N, or Flag-SQSTM1-C for 48 h. Immunocytochemical staining was performed using anti-Flag antibody. The nucleus was counterstained with DAPI. Cell images were captured by confocal microscopy. The percentage represents the ratio of cells with GFP-SQSTM1 puncta relative to Flag-SQSTM1-WT, -N, or –C co-expressing cells (mean ± SD, n=3~5 images, with 35 to 90 co-expressing cells in total in each image). *, p=0.002 compared to SQSTM-WT control, by Student's *t* test. **(E)** Expression of SQSTM1-C results in an increased accumulation of endogenous full-length SQSTM1 and NBR1. HeLa cells were transiently transfected with empty vector or SQSTM1-C for 48 h. Western blot analysis was performed to examine the expression of endogenous SQSTM1 and NBR1, as well as SQSTM1-C as indicated. Expression of ACTB/β-actin was measured as the loading control.

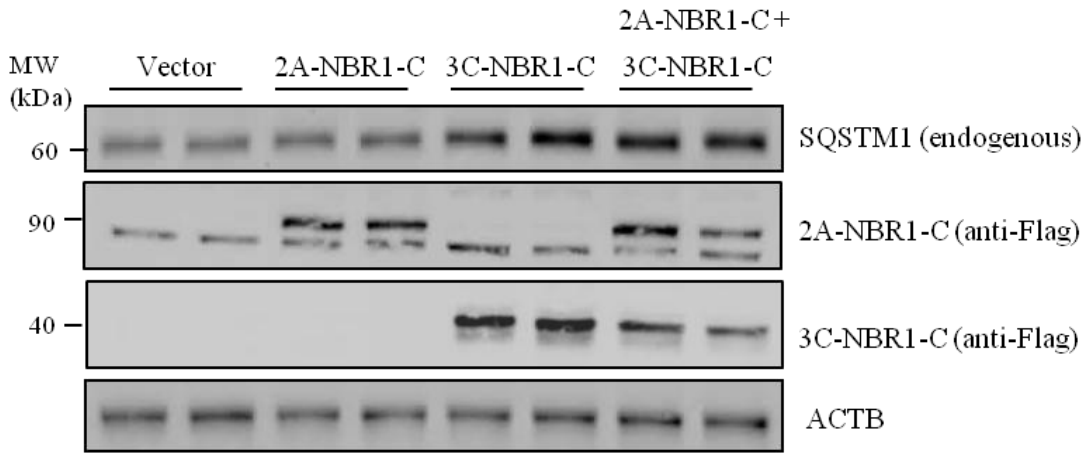

Figure 22. Overexpression of the C-terminal 3C^{pro}-mediated cleavage product of NBR1 causes an accumulation of native SQSTM1.

HeLa cells were transiently transfected with an empty vector, Flag-2A-NBR1-C (C-terminal cleavage fragment of NBR1 induced by $2A^{pro}$), Flag-3C-NBR1-C (C-terminal cleavage fragment of NBR1 induced by $3C^{pro}$), alone or in combination for 48 h. Western blot analysis was performed to examine the expression of endogenous SQSTM1, NBR1-C and ACTB/β (loading control).

4.3.5 Mutual regulation of SQSTM1 and NBR1 expression.

The similarities in the structure and function between SQSTM1 and NBR1 prompted us to question whether SQSTM1 and NBR1 are reciprocally regulated during CVB3 infection and if depletion of SQSTM1 results in a compensatory upregulation of NBR1 protein. The data presented in **Fig. 23** demonstrated that overexpression of SQSTM1 (or NBR1) resulted in increased protein level of NBR1 (or SQSTM1) (both non-cleaved and cleaved forms) (**Fig. 23A & C**), whereas knockdown of SQSTM1 (or NBR1) led to reduced protein expression of NBR1 (or SQSTM1) (both non-cleaved and cleaved forms) (**Fig. 23B & D**). To further determine whether the mutual regulation of SQSTM1 and NBR1 occurs at the transcriptional level, we examined mRNA expression of SQSTM1 and NBR1. We showed that the mRNA level of SQSTM1 (or NBR1) was not significantly altered when NBR1 (or SQSTM1) was overexpressed or knocked down (**Fig. 23E-H**), suggesting that SQSTM1 and NBR1 are reciprocally regulated at the post-transcriptional level. Together, these results suggest that the loss of the function of one autophagic adapter protein during CVB3 infection is unlikely to be compensated by the other.

A.

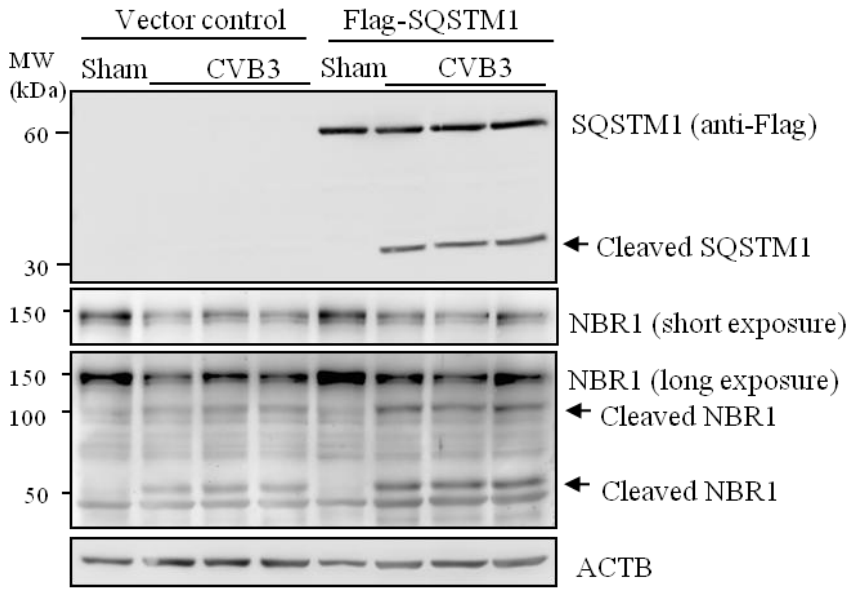
Vector control
Flag-SQSTM1
MW (kDa)
Sham
CVB3
Sham
CVB3
60
30
150
150
100
50
SQSTM1 (anti-Flag)
Cleaved SQSTM1
NBR1 (short exposure)
NBR1 (long exposure)
Cleaved NBR1
Cleaved NBR1
ACTB

B.

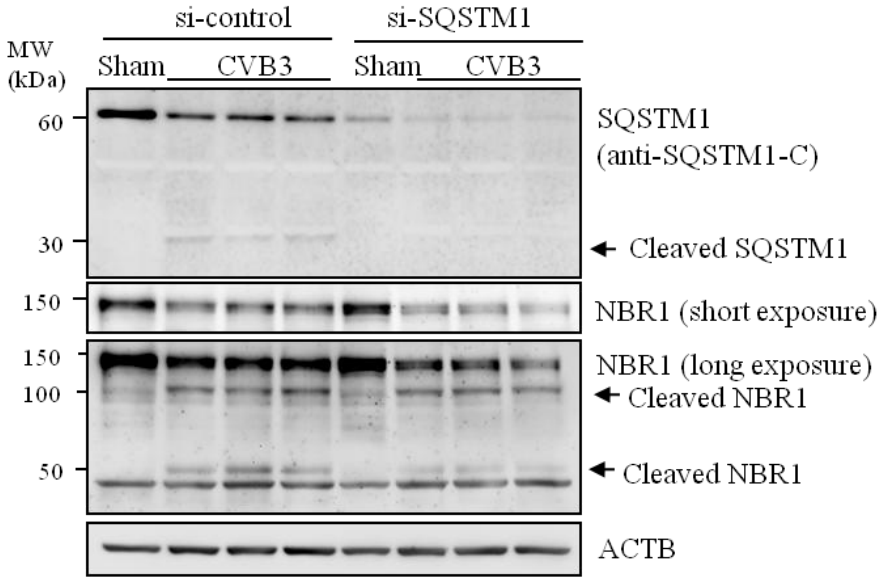
si-control
si-SQSTM1
MW (kDa)
Sham
CVB3
Sham
CVB3
60
30
150
150
100
50
SQSTM1 (anti-SQSTM1-C)
Cleaved SQSTM1
NBR1 (short exposure)
NBR1 (long exposure)
Cleaved NBR1
Cleaved NBR1
ACTB

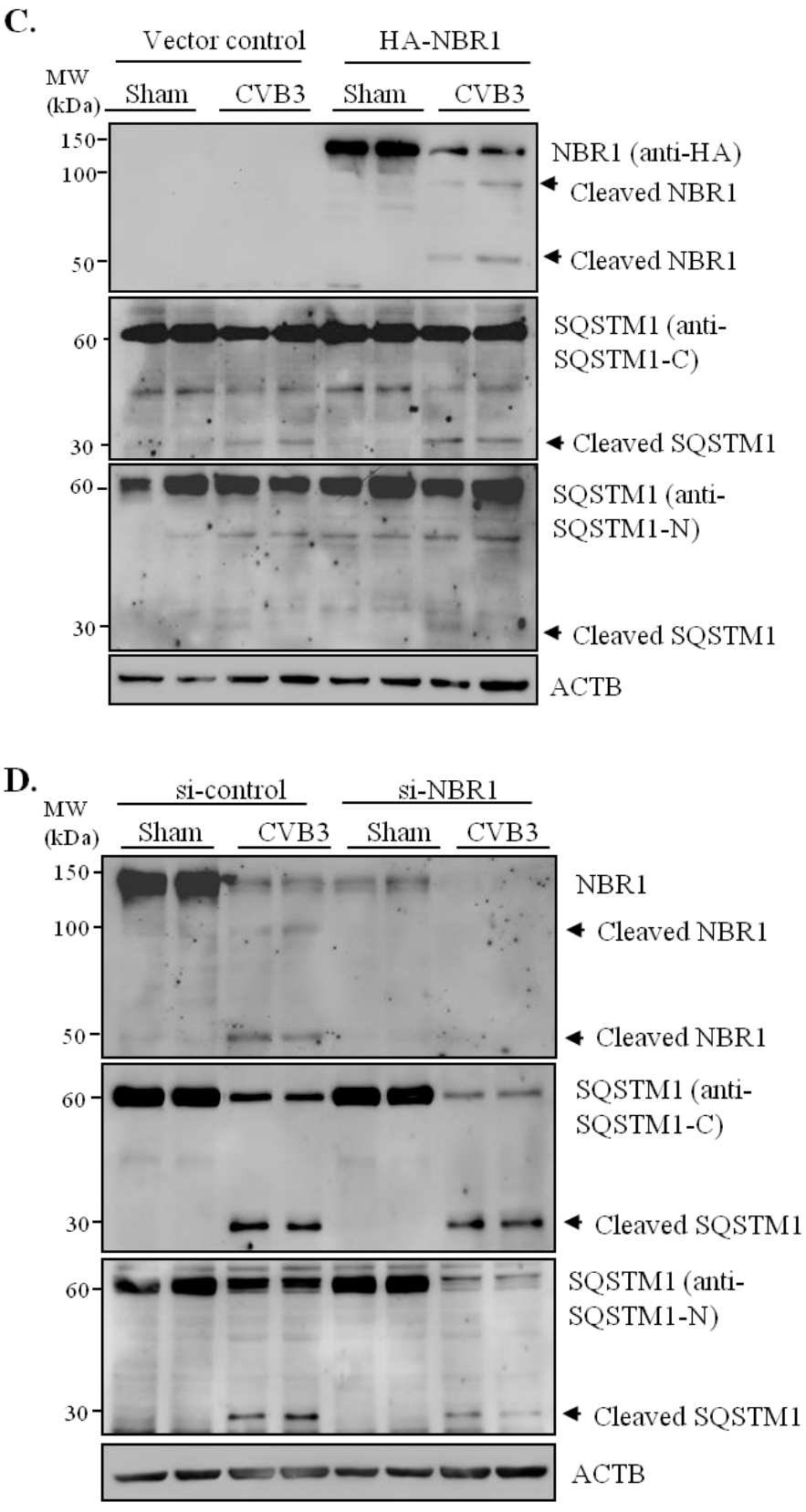
C.
Vector control
HA-NBR1
MW (kDa)
Sham
CVB3
Sham
CVB3
150
100
50
60
30
60
30
NBR1 (anti-HA)
Cleaved NBR1
Cleaved NBR1
SQSTM1 (anti-SQSTM1-C)
Cleaved SQSTM1
SQSTM1 (anti-SQSTM1-N)
Cleaved SQSTM1
ACTB
D.
si-control
si-NBR1
MW (kDa)
Sham
CVB3
Sham
CVB3
150
100
50
60
30
60
30
NBR1
Cleaved NBR1
Cleaved NBR1
SQSTM1 (anti-SQSTM1-C)
Cleaved SQSTM1
SQSTM1 (anti-SQSTM1-N)
Cleaved SQSTM1
ACTB

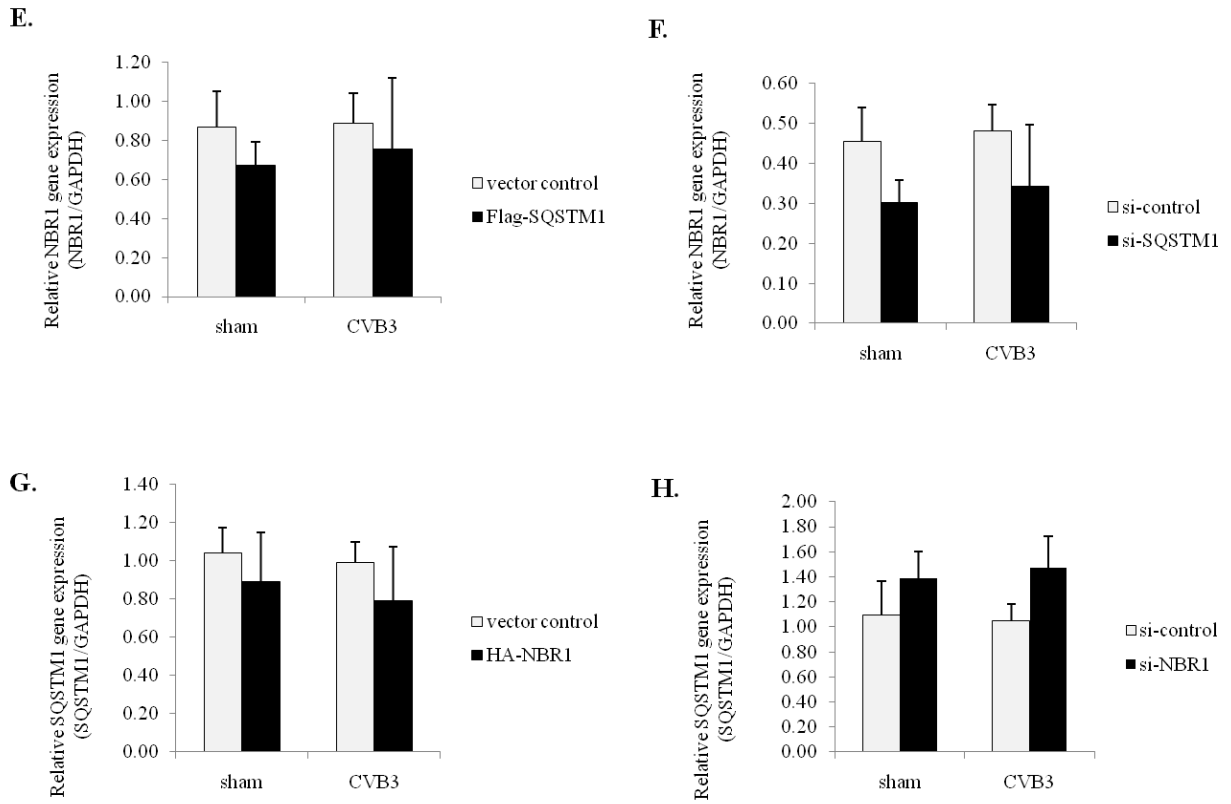

Figure 23. Reciprocal regulation of SQSTM1 and NBR1.

(A, B) Effects of overexpression or knockdown of SQSTM1 on NBR1 protein expression. HeLa cells were transiently transfected with Flag-SQSTM1 construct (A) or SQSTM1 siRNA (si-SQSTM1, Dharmacon, 100 nM) (B) for 24 h, followed by CVB3 infection for 7 h. Western blotting was performed to examine the expression of SQSTM1 using an anti-Flag antibody which recognizes the N-terminus of SQSTM1 (A) or using an anti-C-terminal SQSTM1 antibody (B), NBR1 using anti-N-terminal NBR1 antibody, and ACTB/β-actin (loading control). **(C, D)** Effects of overexpression or knockdown of NBR1 on SQSTM1 protein expression. HeLa cells were transiently transfected with HA-NBR1 construct (C) or NBR1 siRNA (si-NBR1, Dharmacon, 100 nM) (D) for 24 h, following by CVB3 infection for 7 h. Western blotting was performed to examine the expression of NBR1 using an anti-HA antibody which recognizes the N-terminus of NBR1 (C) or using an anti-N-terminal NBR1 antibody (D), and SQSTM1 using either anti-C-terminal or anti-N-terminal SQSTM1 antibody as indicated. Protein expression of

ACTB/β-actin was examined as a loading control. Si-control, scramble siRNA control. (**E, F**) Effects of overexpression or knockdown of SQSTM1 on NBR1 mRNA expression. HeLa cells were transiently transfected with Flag-SQSTM1 construct (E) or si-SQSTM1 (F) for 24 h, followed by CVB3 infection for 7 h. RT-qPCR was performed to examine mRNA levels of NBR1 and GAPDH (internal control). Results are presented as mean ± SD (n=4). **(G, H)** Effects of overexpression or knockdown of NBR1 on SQSTM1 mRNA expression. HeLa cells were transiently transfected with HA-NBR1 construct (G) or si-NBR1 (H) for 24 h, followed by CVB3 infection for 7 h. RT-qPCR was performed to examine mRNA levels of SQSTM1 and GAPDH (internal control). Results are presented as mean ± SD (n=4).

4.4 Discussion

Accumulating evidence has revealed that disruption of protein homeostasis is a key contributor to the development and pathogenesis of many human diseases, including those related to coxsackievirus infection [221, 222, 223]. Protein homeostasis is achieved through the function of protein quality control system. Autophagy-mediated selective recycling of the terminally-misfolded proteins/aggregates serves as a key component of protein quality control and defects in this pathway have been linked to protein conformation diseases, such as bone, liver, heart, and neurodegenerative diseases [124, 224, 225, 226, 227, 228, 229, 230, 231].

Misfolded and ubiquitinated proteins are commonly detected in CVB3-infected cells and tissues, suggesting that dysfunction of the protein degradation pathway may have a role in viral pathogenesis [60, 232]. We have previously demonstrated that autophagy adapter protein SQSTM1 is cleaved following CVB3 infection, resulting in the loss of the function of SQSTM1 in selective autophagy [219]. The present research extends our previous study to investigate the interaction between NBR1 and coxsackievirus infection. NBR1 is a SQSTM1-like cargo receptor and has been suggested to have a compensatory effect when SQSTM1 is malfunctioning [124]. In this

study, we showed that NBR1 is also cleaved after viral infection and the cleavage is catalyzed by both viral proteinase $2A^{pro}$ and $3C^{pro}$. More interestingly, we demonstrated that, in addition to loss-of-function, the C-terminal truncated mutants of SQSTM1 and NBR1 also exhibit a dominant-negative regulatory effect against the function of native proteins in the clearance of ubiquitin conjugates. First, we showed that the SQSTM1-C mutant inhibits full-length SQSTM1-dependent protein aggregate formation, a prerequisite step for SQSTM1-mediated selective degradation by autophagosome [120]. Second, we demonstrated that overexpression of SQSTM1-C results in elevated accumulation of both SQSTM1 and NBR1, two known substrate targets of selective autophagy. The mechanism of such action of SQSTM1-C remains unclear. We speculate that SQSTM1-C stabilizes full-length SQSTM1 and NBR1 by blocking their degradation through competing for the binding of ubiquitin chain and/or LC3.

Unlike SQSTM1, we found NBR1 by itself does not facilitate the formation of protein aggregates and promote the accumulation of insoluble ubiquitin conjugates (data not shown). This is presumably due to the difference in the function of the PB1 domains of these two proteins. The PB1 domain enables SQSTM1 to form self-aggregates which is a crucial step for SQSTM1-mediated selective autophagy [233]; however, NBR1 requires the coiled-coil (cc) domain, but not the PB1 domain, for its dimerization [122]. Our hypothesis is that cc domain-mediated NBR1 dimerization is not sufficient to induce the formation of large protein aggregates. In other words, the step of protein aggregate formation is dispensable for NBR1-mediated selective autophagy. Interestingly, we found that coexpression of SQSTM1 and NBR1 facilitates the formation of the punctate structures of NBR1 (data not shown). This is likely a result of the interaction between NBR1 and SQSTM1 and the ability of SQSTM1 to polymerize.

Another interesting observation of this study is that the cleavage product 3C-NBR1-C, but not 2A-NBR1-C, induces the accumulation of endogenous SQSTM1. As shown in the schematic diagram (**Fig. 20C**), as compared to 3C-NBR1-C, 2A-NBR1-C contains extra 280 amino acids at its N-terminus which include a second LIR and probably other undefined functional domains. It is postulated that the presence of additional domains may cause the failure to interfere with the function of native proteins. Future investigation is required to dissect the molecular basis of this assumption.

In this study, we reported a positive regulatory relationship between SQSTM1 and NBR1. The observation that knockdown of SQSTM1 results in a downregulation, rather than an upregulation of NBR1, implies that NBR1 may not play a compensatory role for the absence of SQSTM1. What are the possible mechanisms of the mutual regulation of SQSTM1 and NBR1? Our results demonstrated that overexpression or knockdown of NBR1 does not affect mRNA expression of SQSTM1, and vice versa, indicating that mutual regulation between SQSTM1 and NBR1 takes place at the post-transcriptional level. It has been previously demonstrated that NBR1 and SQSTM1 interact directly to form a heterodimer through respective PB1 domain [234]. GST pull-down assay also showed that the UBA domain of NBR1 can bind directly with SQSTM1 [235]. These findings raise the possibility that interaction between these two proteins prevents them from being recognized and degraded through autophagy. We speculate that overexpressed SQSTM1 interacts and stabilizes its binding partner, NBR1, whereas depletion of SQSTM1 results in the release of NBR1 from the binding complex and subsequent degradation, and vice versa. In line with this hypothesis, it was recently reported that the N-terminal truncated form of NBR1 (aa1-135) that contains an intact PB1 domain stabilizes SQSTM1 and reduce its turnover through autophagy pathway [235]. The other possible explanation for the reciprocal

regulation of NBR1 and SQSTM1 is that they compete for degradation through the shared autophagic pathway. For example, the decrease in NBR1 protein levels when SQSTM1 is silenced could be a result of accelerated disposal of NBR1 when there is less competition from SQSTM1. It was previously reported that SQSTM1 can also be degraded through the proteasome pathway [236]; however in the presence of proteasome inhibitors, we found a minimal increase in SQSTM1 and NBR1 protein levels compared to the treatment with lysosome inhibitors (data not shown), suggesting that proteasome pathway is not a major route for the degradation of SQSTM1 and NBR1.

In addition to NBR1 and SQSTM1, CVB3 proteinases were reported to target a number of other host proteins as introduced in **Section 1.2.3**, **Chapter 1**. Through modulating cellular processes and disrupting host innate immune response, viral proteinases play a crucial role in viral infection. SQSTM1 has been shown to have an antiviral effect against Sindbis viral infection by directing viral capsid protein for autophagic degradation [173]. However, in the present study and our previous report [219], we found that overexpression or knockdown of NBR1 and SQSTM1 had little impact on viral replication (data not shown), suggesting that loss of functional SQSTM1/NBR1 alone is not sufficient enough to benefit viral replication. We postulate that other cellular mechineries manipulated by viral proteinases are also needed to work in concordance with the cleavage of SQSTM1/NBR1 to ensure successful viral replication. Another speculation is that the cleavage of NBR1 and SQSTM1 are by-products due to the coincidence of possessing consensus sequences of viral proteinase-targeted subtrates. Therefore, the consequences of protein cleavage are not necessarily to benefit viral replication and proliferation, but depend on the native functions of these proteins. In other words, although the

cleavage of SQSTM1 and NBR1 does not favor viral replication, it contributes to overall viral pathogensis through disruption of selective degradation of protein aggregates.

Chapter 5: NBR1 is dispensable for PARK2-mediated mitophagy regardless of the presence or absence of SQSTM1

5.1 Background

Impaired mitochondrial function has been implicated in a number of human diseases, especially neurodegenerative and heart diseases [237, 238, 239]. Mitochondria dysfunction not only causes defects in energy-generation, but also results in an elevated production of reactive oxygen species and increased apoptosis [240]. Therefore, mitochondrial quality control (MQC), a process to preserve functional mitochondria, is extremely important for the maintenance of cellular homeostasis [241].

MQC depends on a balance between biogenesis and degradation of mitochondria. Efficient clearance of damaged mitochondria by autophagy, termed mitophagy, constitutes a critical component of MQC. Although multiple mechanisms have been suggested to be involved in the regulation of mitophagy [242, 243, 244, 245], the PTEN-induced putative kinase 1 (PINK1)/PARK2 pathway is the best characterized and most extensively studied signaling mechanism of mitophagy, partly due to the recognized significance of these two molecules in the pathogenesis of Parkinson Disease [246, 247, 248]. In healthy non-depolarized mitochondria, the serine/threonine kinase PINK1 is constantly and rapidly turned over by mitochondrial proteinases. Upon mitochondrial damage, PINK1 accumulates on the outer membrane of mitochondria and recruits the E3 ubiquitin ligase PARK2/Parkin from the cytosol to depolarized mitochondria, where PARK2 subsequently targets damaged mitochondrial proteins for ubiquitination and bulk degradation by autophagy [246, 247, 249, 250, 251, 252].

In addition to the removal of protein aggregates as alluded to previous chapters, SQSTM1 has been reported to be involved in PARK2-mediated mitophagy [252]. Although available data are still controversial, recent evidence supports the notion that SQSTM1 participates in the regulation of mitophagy, yet it is not absolutely required for this process since deletion of SQSTM1 does not block PARK2-dependent disposal of damaged mitochondria. The general assumption is that redundant autophagy receptors, for instance, NBR1, which shares similar functional domains with SQSTM1, have a compensatory role in mitophagy when SQSTM1 is deficient [122, 253]. However, definitive evidence is lacking.

5.2 Specific aims

In this chapter, we aim to investigate whether NBR1 plays a role in PARK2-dependent mitophagy, either alone or as a compensatory mechanism to overcome SQSTM1 depletion.

The **SPECIFIC AIMS** include:

Aim 1. To detect mitochondrial clustering and mitochondrial protein degradation after early and prolonged CCCP (a mitochondrial uncoupler to trigger mitophagy) treatment, respectively

Aim 2. To test whether NBR1 has any effects in mitochondrial clustering upon CCCP treatment

Aim 3. To investigate whether NBR1 alone or in concert with SQSTM1 plays a role in PARK2-mediated mitophagy

5.3 Results

5.3.1 CCCP treatment induces PARK2-dependent perinuclear clustering and degradation of mitochondrial proteins.

CCCP causes mitochondrial depolarization by increasing membrane permeability to protons and is a widely used mitochondrial uncoupler for the study of mitophagy [254, 255, 256, 257]. In this study, CCCP was used to investigate the functional role of NBR1 in PARK2-dependent mitophagy. Since regular HeLa cells express low levels of PARK2, HeLa cells stably expressing EGFP-Myc-PARK2 were established and used to examine the dynamics of mitochondria after CCCP treatment. The demonstrated features of PARK-mediated mitophagy include the translocation of PARK2 from cytosol to perinuclear region and the subsequent degradation of mitochondrial proteins [258]. In consistent with previous observations[254, 255], we showed that following 3 h of CCCP treatment, PARK2 translocated to the perinuclear regions and co-localized with mitochondrial outer membrane protein TOMM20 (mitochondrial import receptor subunit TOM20 homology) in clusters (**Fig. 24A, middle panel**). Ubiquitination of PARK2 was detected after 3 h of CCCP treatment, supporting previous report that PARK2 is self-ubiquitinated in the early stage of mitophagy (**Fig. 24B**)[252]. Furthermore, we found that the expression level of mitochondrial outer membrane protein, voltage-dependent anion channel 1 (VDAC1), but not other mitochondria proteins examined, including TOMM20, MAVS, and cytochrome C (CYCS), was markedly reduced after CCCP treatment for 3 h, indicating a specific protein degradation process during early mitochondrial damage (**Fig. 24B and C**). After a prolonged CCCP treatment (24 h), protein levels of all the tested mitochondrial proteins were dramatically decreased (**Fig. 24A-bottom panel, D, and E**), suggesting the bulk clearance of damaged mitochondria.

A.

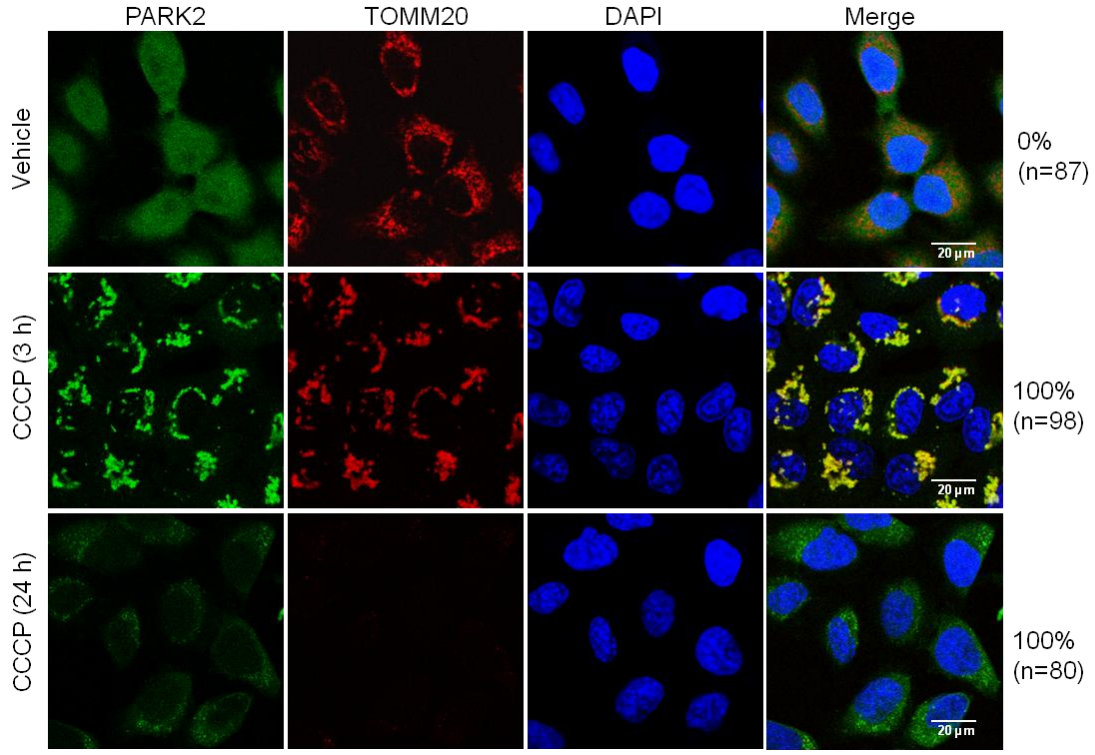
PARK2
TOMM20
DAPI
Merge
Vehicle
CCCP (3 h)
CCCP (24 h)
0%
(n=87)
100%
(n=98)
100%
(n=80)
20 µm
20 µm
20 µm

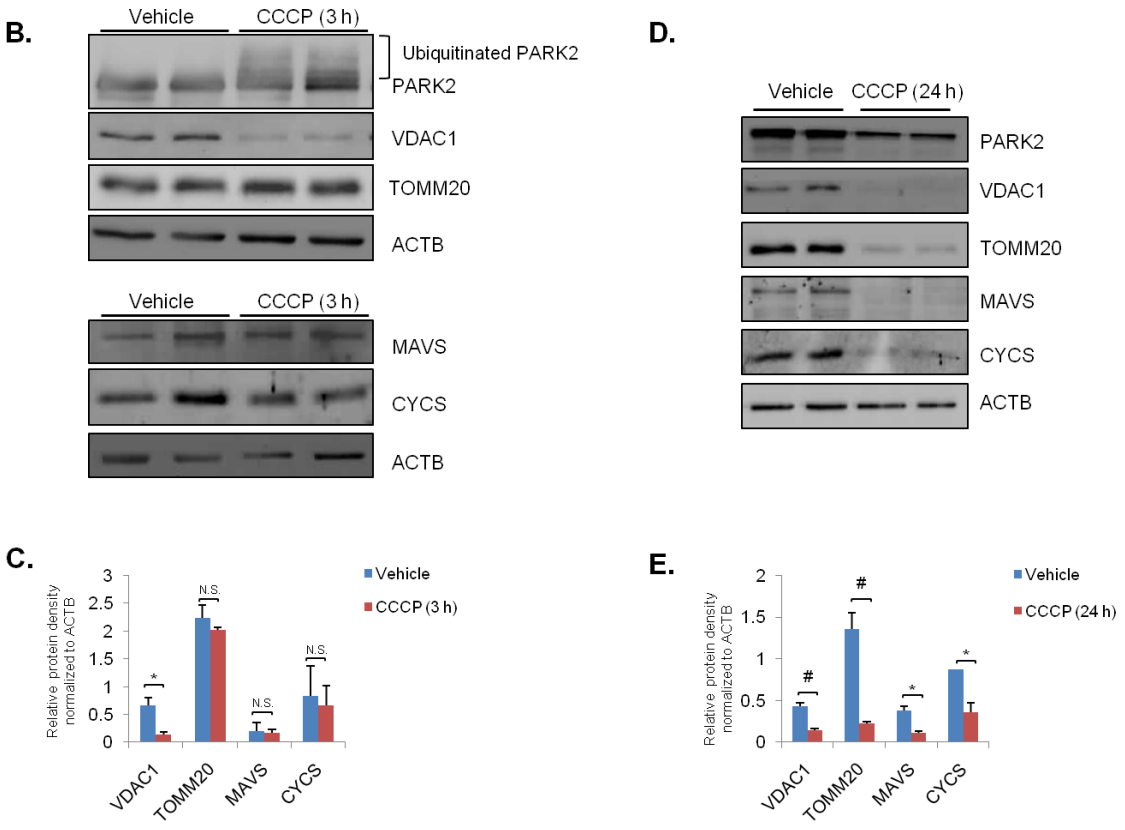

Figure 24. CCCP treatment induces perinuclear aggregation and degradation of mitochondrial proteins in HeLa cells stably expressing PARK2.

(**A, B, and D**) HeLa cells stably expressing EGFP-Myc-PARK2 were treated with either vehicle or CCCP (10 μM) for 3 h or 24 h as indicated. PARK2 signal was shown in green. Cells were immunostained for TOMM20 (red). Nuclei were counterstained with DAPI (blue). The percentage of cells with PARK2 translocation or TOMM20 degradation relative to the total number of cells counted (n) was presented **(A)**. Western blotting was performed to examine the levels of various mitochondrial proteins as indicated at 3 h (**B**) and 24 h **(D)** post CCCP treatment. ACTB/β-actin was probed as a loading control. **(C and E)** Densitometric analysis of protein levels after normalized to ACTB in **(B)** and **(D)**, respectively. *, $p<0.05$; #, $p<0.01$; N.S., not significant.

5.3.2 NBR1 is dispensable for CCCP-induced mitochondrial clustering.

It has been previously reported that SQSTM1 is required for PARK2-dependent mitochondrial perinuclear clustering triggered by CCCP treatment [253, 259]. We therefore questioned whether NBR1, a functional homolog of SQSTM1, has a similar role. HeLa cells stably expressing PARK2 were transiently transfected with HA-tagged NBR1 for 24 h, followed by vehicle or CCCP (10 μM) treatment for 3 h. As shown in **Fig. 25A**, NBR1 was evenly distributed throughout the cytoplasm in vehicle-treated cells. Upon CCCP treatment, NBR1 was recruited to the depolarized mitochondria that are characterized by perinuclear accumulation of PARK2 and TOMM20, suggesting a possible role for NBR1 in the formation of mitochondrial aggregates. To determine the definitive function of NBR1 in mitochondrial clustering, NBR1 in PARK2 stable HeLa cells was knocked down using siRNA technique. Confocal microscopy showed that gene-silencing of NBR1 had essentially no effect on CCCP-induced mitochondrial translocation of PARK2 and formation of mitochondrial aggregates (**Fig. 25B**). Together, our data suggest that NBR1 is not a necessary mediator in mitochondrial clustering.

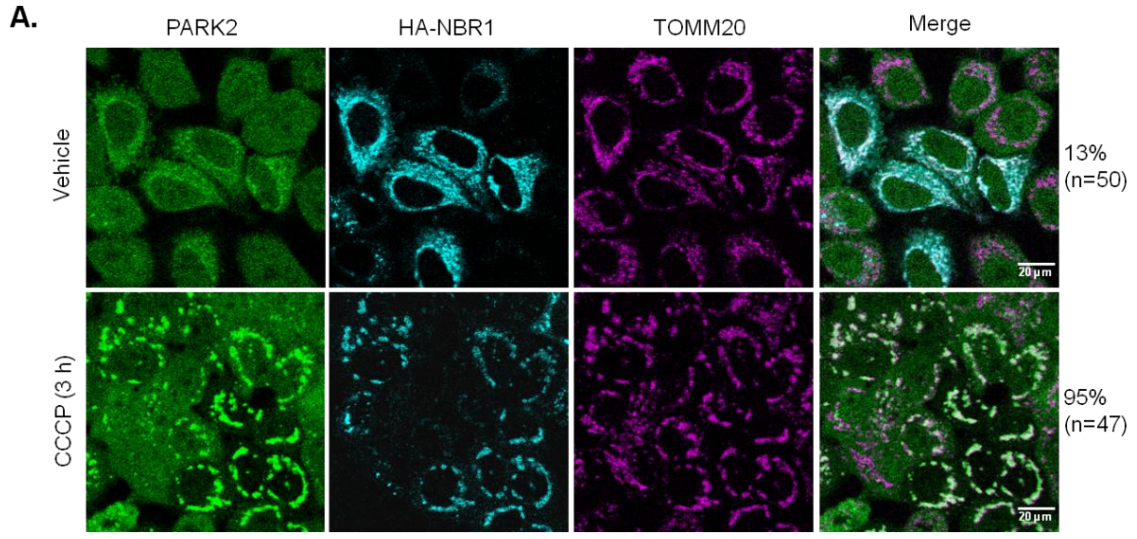

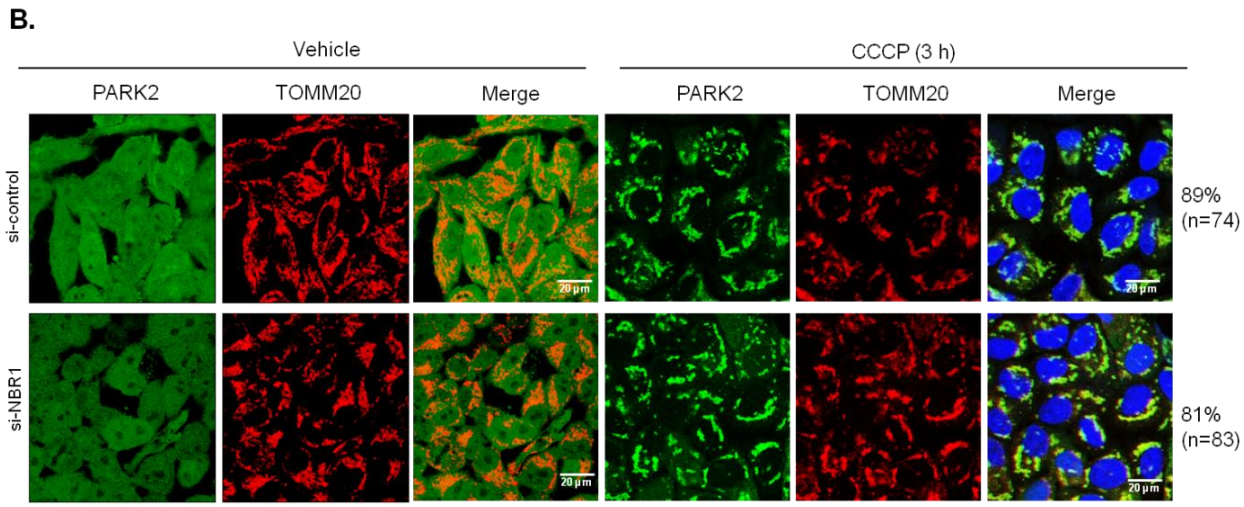

Figure 25. NBR1 is not required for CCCP-induced, PARK2-dependent mitochondrial clustering.

(**A**) HeLa cells stably expressing EGFP-Myc-PARK2 were transiently transfected with HA-NBR1 for 24 h, followed by vehicle or CCCP (10 µM) treatment for 3 h. PARK2 signal was shown in green. Cells were double immunostained with anti-HA (cyan) and anti-TOMM20 (magenta) antibodies. Quantification was presented as the percentage of cells with NBR1 clustering over total number of HA-NBR1 expressing cells (n). **(B)** PARK2 stably expressing HeLa cells were transiently transfected with control siRNA (si-control) or siRNA against *NBR1* (si-*NBR1*) for 48 h, followed by vehicle or CCCP (10 µM) treatment for 3 h. Cells were immunostained with anti-TOMM20 antibody (red). Nuclei were counterstained with DAPI (blue). Immunostaining results were quantified as the percentage of cells with PARK2 translocation over total number of cells counted (n) after CCCP treatment.

5.3.3 PARK2-dependent degradation of VDAC1 is mediated through the proteasome pathway.

We next determined whether NBR1 plays a role in CCCP-triggered early downregulation of VDAC1 (**Fig. 24B**). The results presented in **Fig. 26A-D** demonstrated that either knockdown or overexpression of NBR1 alone or in combination with SQSTM1 had no significant impact on CCCP-induced reduction of VDAC1 protein level. Furthermore, we showed that CCCP-induced

accumulation of PINK1 and ubiquitination of PARK2 were not influenced by modulation of SQSTM1 and/or NBR1 (**Fig. 26A and C**).

To understand whether PARK2 is required for decreased VDAC1 expression following CCCP treatment, regular HeLa cells that do not express PARK2 were treated with CCCP for 3 h. As shown in **Fig. 26E and F**, protein levels of VDAC1 remained unchanged after CCCP treatment, suggesting that downregulation of VDAC1 is PARK2-dependent. To further explore the underlying mechanism of VDAC1 degradation, PARK2 stable HeLa cells were treated with either proteasome inhibitor lactacystin or lysosome inhibitor BAF. We found that addition of LAC, but not BAF, inhibited CCCP-induced downregulation of VDAC1, indicating a proteasome-dependent mechanism of VDAC1 degradation (**Fig. 26G and H**). Taken together, our results suggest that CCCP treatment induces PARK2-dependent VDAC1 degradation through the ubiquitin-proteasome pathway. Both NBR1 and SQSTM1 do not appear to be involved in this process.

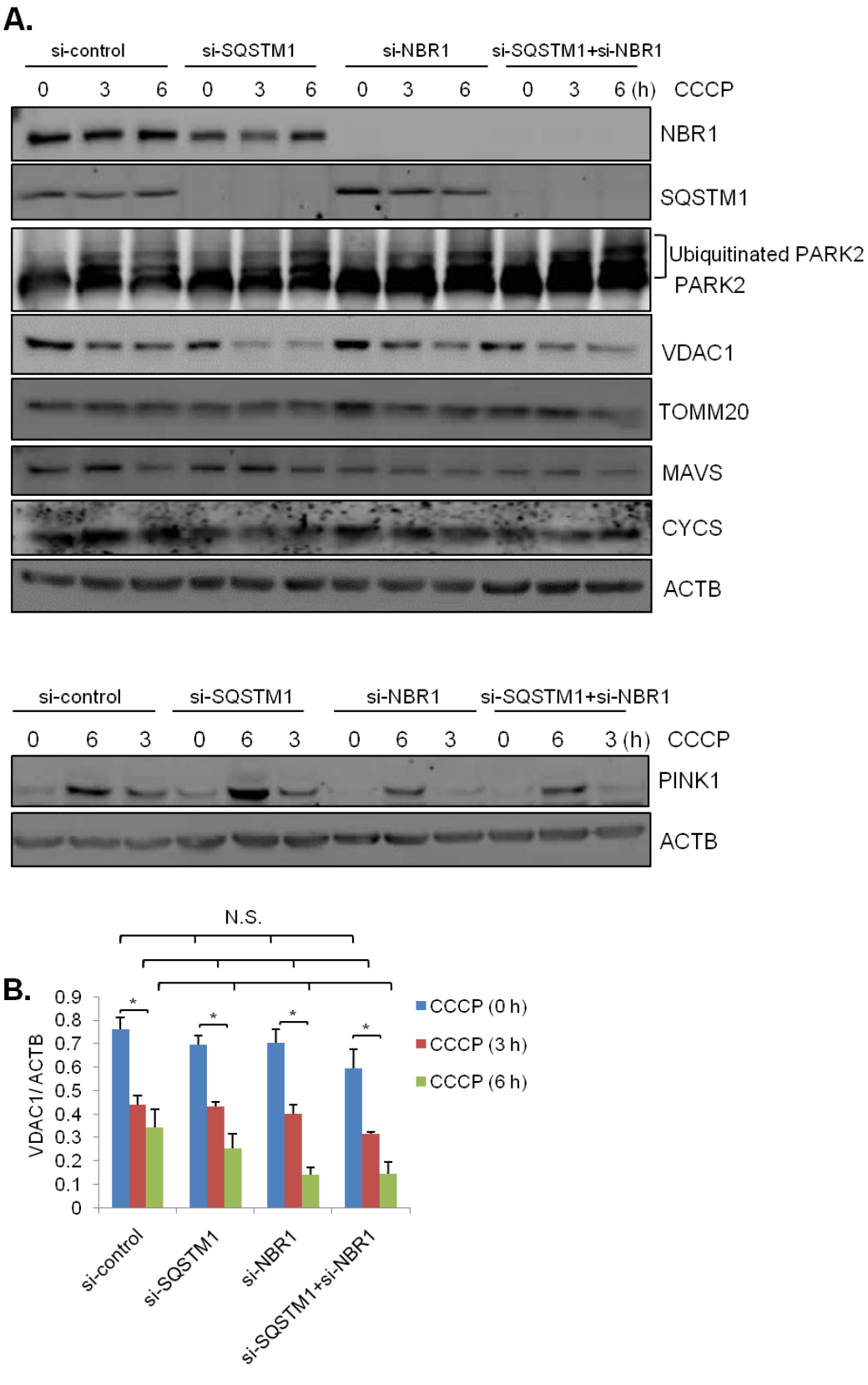
A.
si-control
si-SQSTM1
si-NBR1
si-SQSTM1+si-NBR1
0 3 6 0 3 6 0 3 6 0 3 6 (h) CCCP
NBR1
SQSTM1
Ubiquitinated PARK2
PARK2
VDAC1
TOMM20
MAVS
CYCS
ACTB
si-control
si-SQSTM1
si-NBR1
si-SQSTM1+si-NBR1
0 6 3 0 6 3 0 6 3 0 6 3 (h) CCCP
PINK1
ACTB
B.
N.S.
VDAC1/ACTB
0.9
0.8
0.7
0.6
0.5
0.4
0.3
0.2
0.1
0
CCCP (0 h)
CCCP (3 h)
CCCP (6 h)
si-control
si-SQSTM1
si-NBR1
si-SQSTM1+si-NBR1

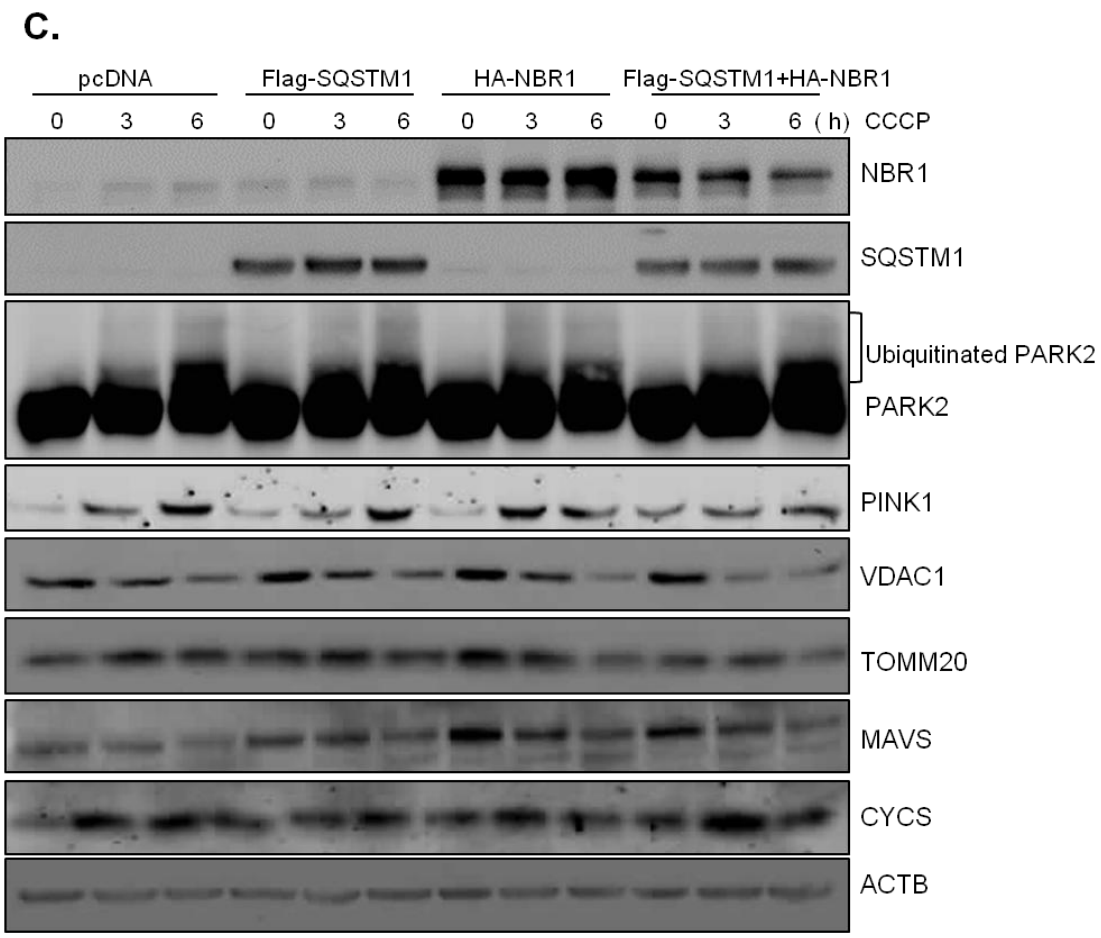
C.
pcDNA
Flag-SQSTM1
HA-NBR1
Flag-SQSTM1+HA-NBR1
0 3 6 0 3 6 0 3 6 0 3 6 (h) CCCP
NBR1
SQSTM1
Ubiquitinated PARK2
PARK2
PINK1
VDAC1
TOMM20
MAVS
CYCS
ACTB

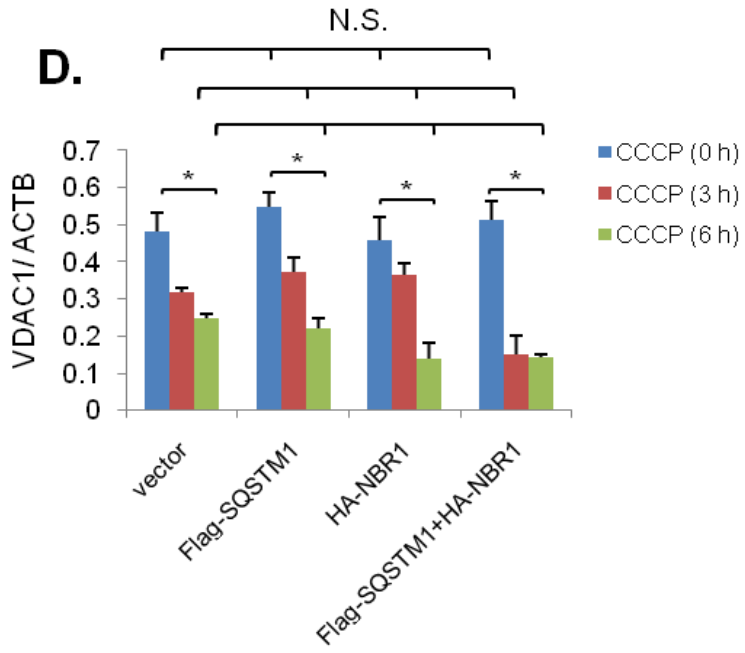
D.
N.S.
VDAC1/ACTB
0.7
0.6
0.5
0.4
0.3
0.2
0.1
0
*
CCCP (0 h)
CCCP (3 h)
CCCP (6 h)
vector
Flag-SQSTM1
HA-NBR1
Flag-SQSTM1+HA-NBR1

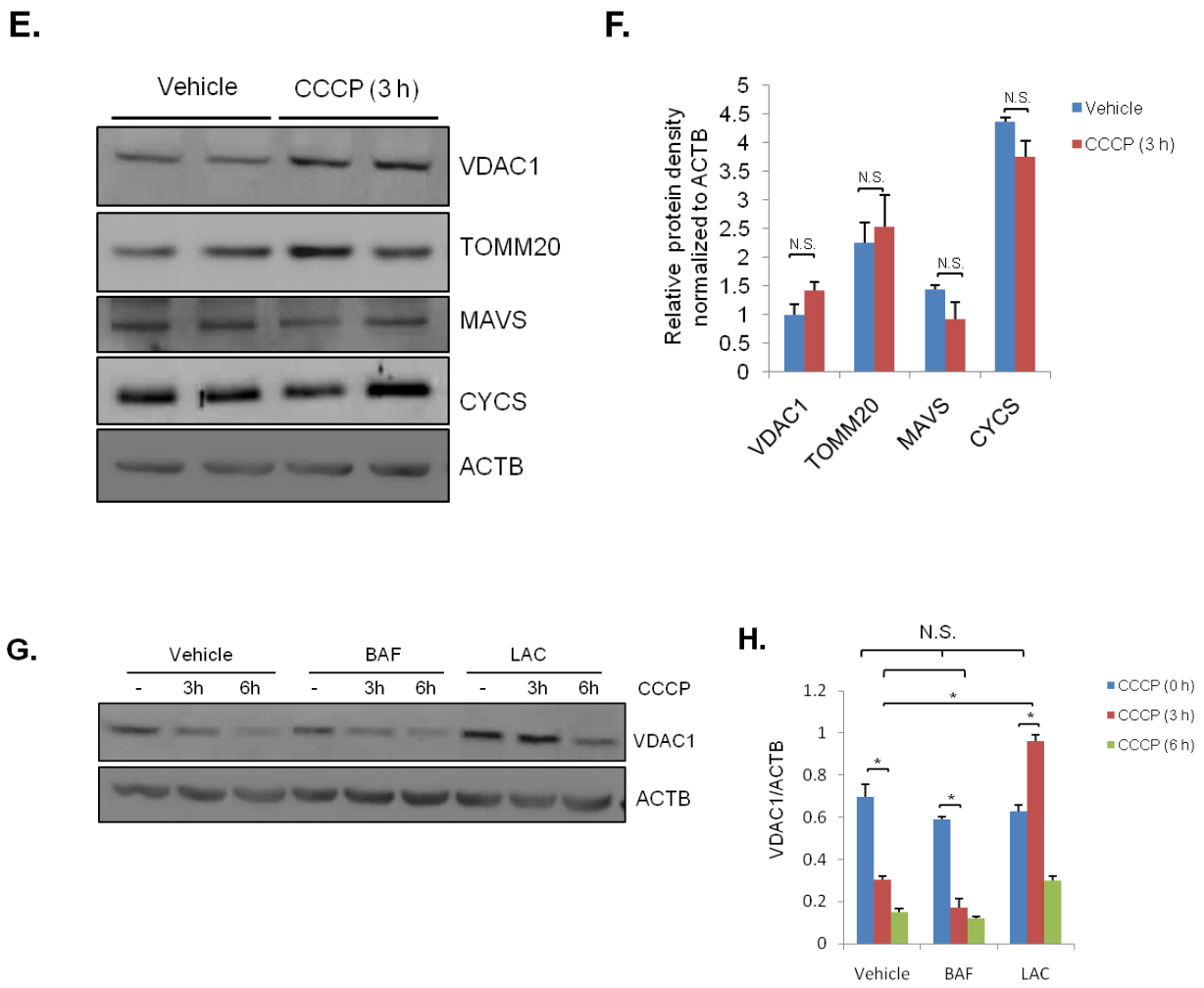

Figure 26. PARK2-dependent early degradation of VDAC1 is mediated through the ubiquitin-proteasome pathway.

(A) HeLa cells stably expressing PARK2 were transiently transfected with si-*NBR1* and si-*SQSTM1* alone or in combination as indicated for 48 h, followed by vehicle or CCCP (10 μM) treatment for 3 or 6 h. Cells transfected with si-control were used as controls. Western blotting was performed to examine protein expression of NBR1, SQSTM1, and various mitochondrial proteins as indicated. **(B)** Densitometric analysis of VDAC1 after normalized to ACTB in **(A).** **(C)** PARK2 stably expressing HeLa cells were transiently transfected with HA-NBR1 and Flag-SQSTM1 alone or in combination as indicated for 24 h, followed by vehicle or CCCP (10 μM) treatment for 3 or 6 h. Cells transfected with empty vector were used as controls. Protein levels of NBR1 (using anti-NBR1 antibody), SQSTM1 (using anti-FLAG antibody), and various

mitochondrial proteins were examined as described above. **(D)** Densitometric analysis of VDAC1 after normalized to ACTB in **(C)**. **(E)** Regular HeLa cells were treated with CCCP (10 μM) for 3 h. Western blot analysis was carried out to examine the expression of various mitochondrial proteins as indicated. **(F**) Densitometric analysis of protein levels after normalized to ACTB in **(E)**. **(G)** HeLa cells stably expressing PARK2 were treated with CCCP (10 μM) for indicated time periods in the presence or absence of lysosomal inhibitor bafilomycin A1 (BAF, 200 nM) or proteasome inhibitor lactacystin (LAC, 10 μM). Protein level of VDAC1 was examined by Western blotting. **(H)** Densitometric analysis of protein levels after normalized to ACTB in **(G)**. *, $p<0.05$; N.S., not significant.

5.3.4 NBR1 is dispensable for CCCP-induced mitophagy regardless of the presence or absence of SQSTM1.

Finally, we examined the role of NBR1 in CCCP-induced mitophagy. As mentioned earlier, the function of SQSTM1 in regulating mitophagy is still controversial. Here we first utilized the *Sqstm*1$^{-/-}$ MEFs to evaluate the effects of depletion of SQSTM1 on CCCP-induced mitophagy. Since MEFs express very low levels of PARK2, we transiently transfected exogenous PARK2 into these cells, then treated them with CCCP for 24 h. Confocal microscopy data showed that as compared to vehicle-treated cells where TOMM20 was stained in red, after CCCP treatment, TOMM20 signal was barely detectable in PARK2 expressing cells independent of SQSTM1 (**Fig. 27A**), implying that SQSTM1 is not an essential modulator in the removal of damaged mitochondria.

We next examined the role of NBR1 in mitophagy in the presence or absence of SQSTM1. As shown in **Fig. 27B**, following CCCP treatment, TOMM20 signal was undetectable either in MEFs with knockdown of NBR1 alone (*Sqstm*1$^{+/+}$ MEFs + si-*Nbr1*) or in combination with SQSTM1 (*Sqstm*1$^{-/-}$ MEFs + si-*Nbr1*). Similar results were obtained using regular HeLa cells

transfected with si-*NBR1* alone or together with si-*SQSTM1* (**Fig. 27C**). Consistent with the Immunofluorescence results, Western blot analysis demonstrated that neither knockdown nor overexpression of NBR1 alone or in combination with SQSTM1 has significant impacts on CCCP-induced degradation of mitochondrial proteins (**Fig. 27D-G**). Collectively, our results suggest that NBR1 is dispensable for the final removal of damaged mitochondria regardless of the presence or absence of SQSTM1.

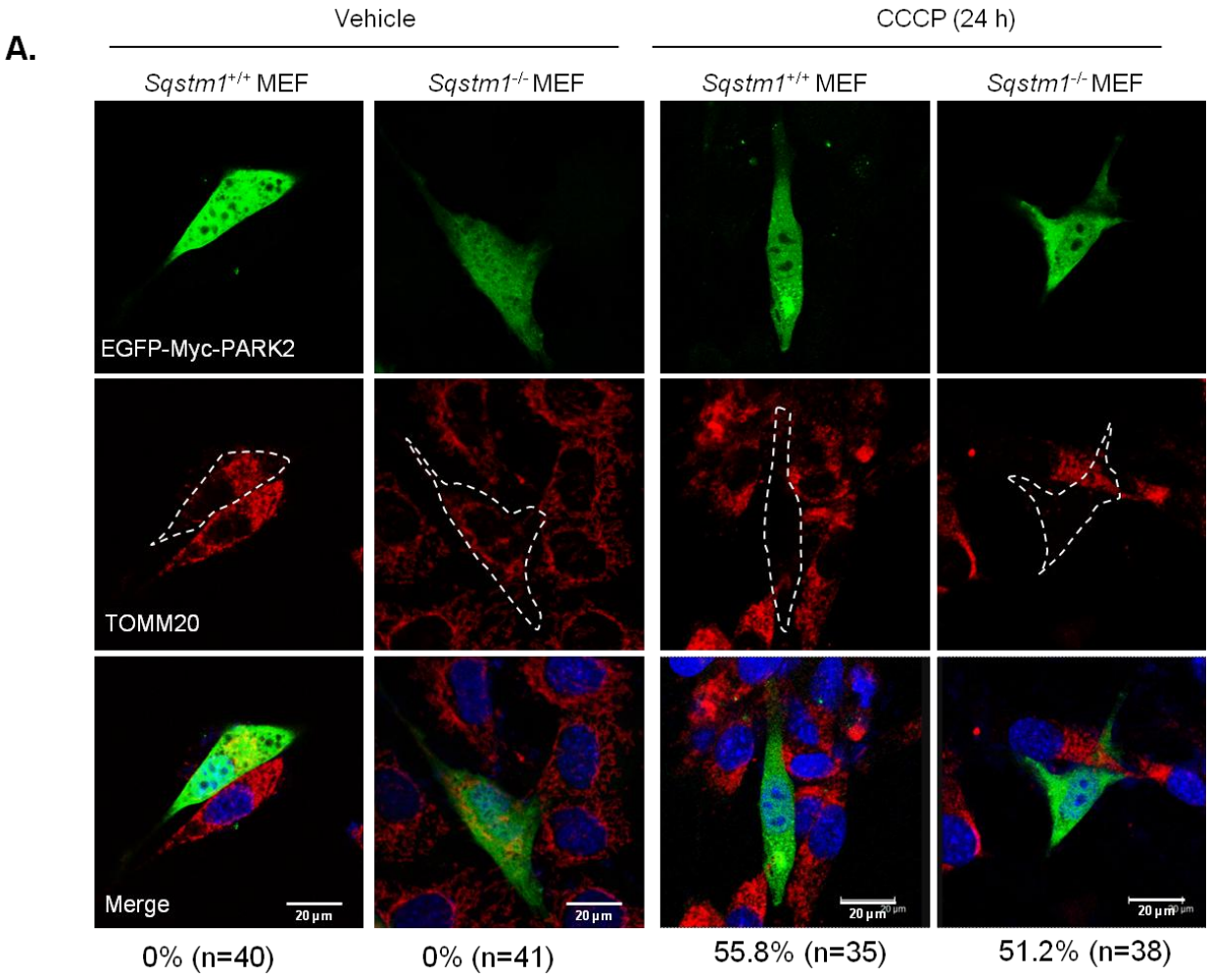

B.

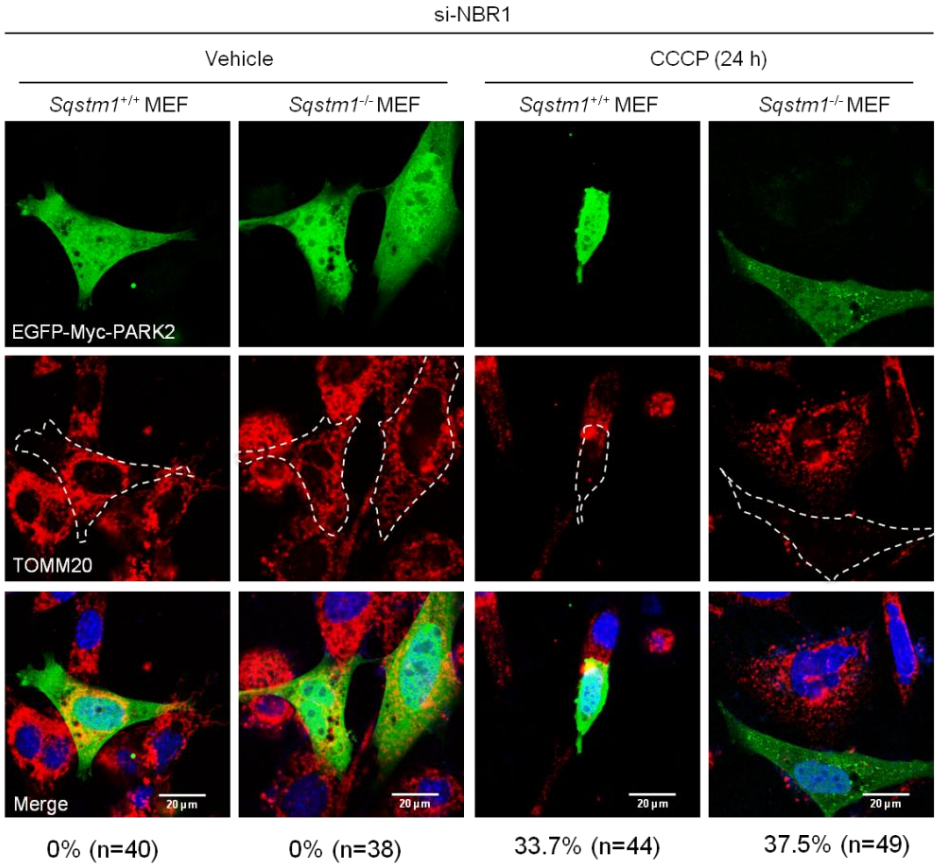
si-NBR1
Vehicle
CCCP (24 h)
Sqstm1+/+ MEF
Sqstm1-/- MEF
Sqstm1+/+ MEF
Sqstm1-/- MEF
EGFP-Myc-PARK2
TOMM20
Merge
20 μm
0% (n=40)
0% (n=38)
33.7% (n=44)
37.5% (n=49)

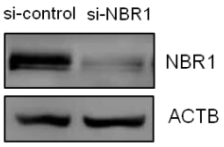
si-control
si-NBR1
NBR1
ACTB

C.

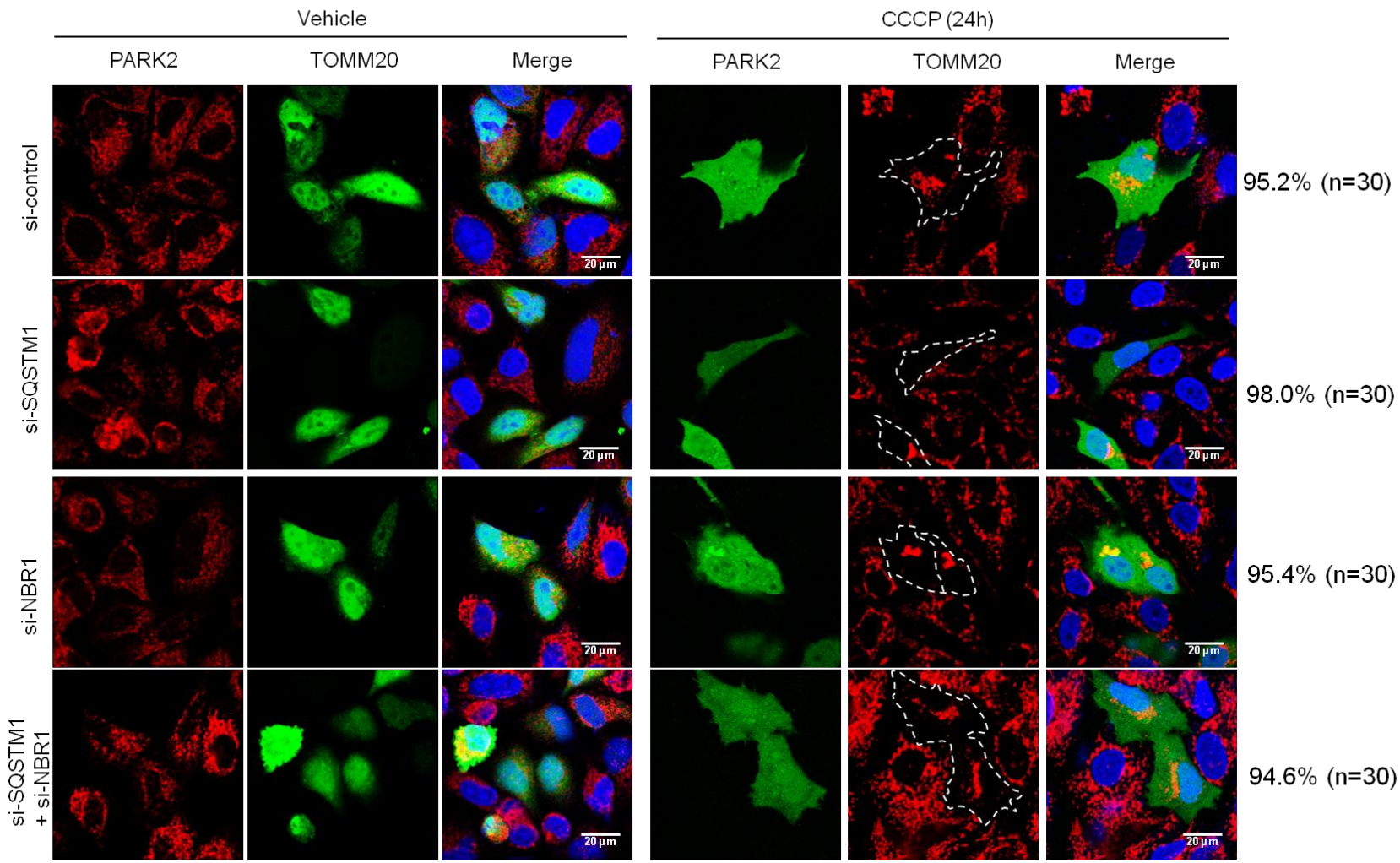
Vehicle
CCCP (24h)
PARK2
TOMM20
Merge
PARK2
TOMM20
Merge
si-control
si-SQSTM1
si-NBR1
si-SQSTM1 + si-NBR1
20 μm
95.2% (n=30)
98.0% (n=30)
95.4% (n=30)
94.6% (n=30)

D.

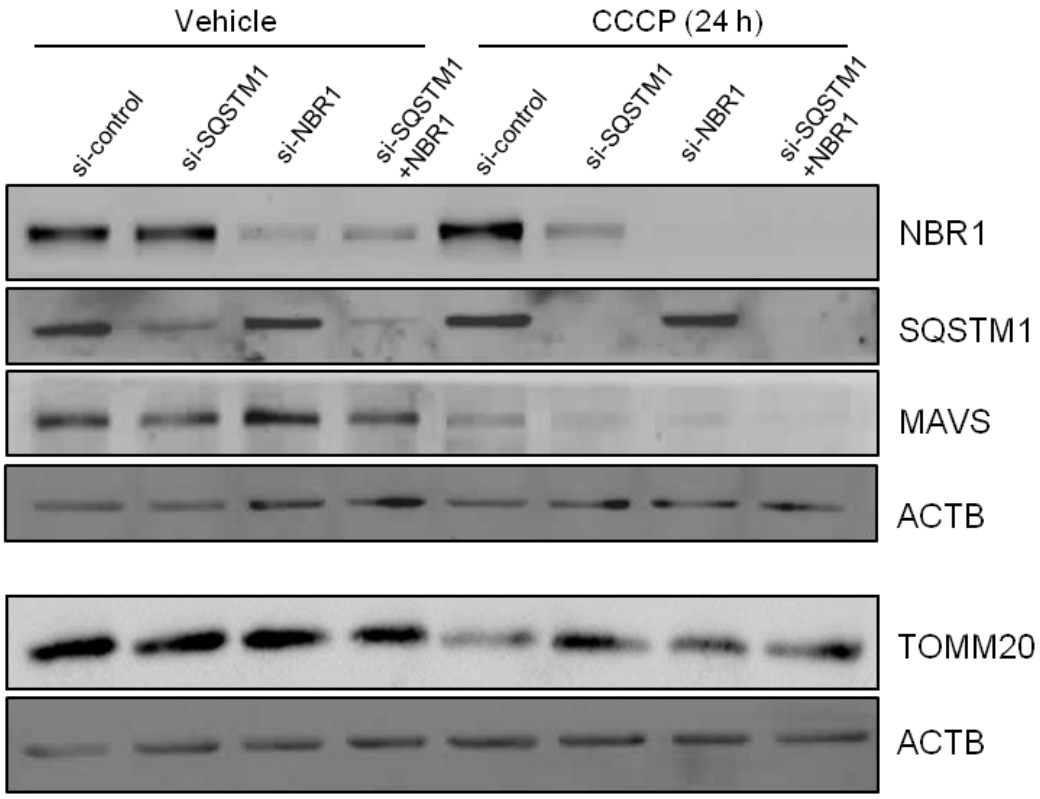
Vehicle
CCCP (24 h)
si-control
si-SQSTM1
si-NBR1
si-SQSTM1 +NBR1
si-control
si-SQSTM1
si-NBR1
si-SQSTM1 +NBR1
NBR1
SQSTM1
MAVS
ACTB
TOMM20
ACTB

E.

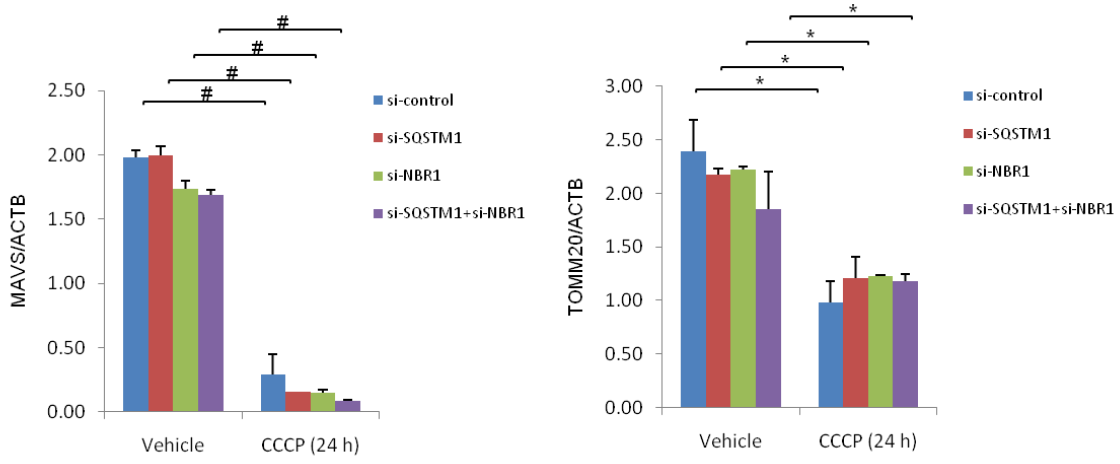
MAVS/ACTB
2.50
2.00
1.50
1.00
0.50
0.00
#
#
#
#
Vehicle
CCCP (24 h)
si-control
si-SQSTM1
si-NBR1
si-SQSTM1+si-NBR1
TOMM20/ACTB
3.00
2.50
2.00
1.50
1.00
0.50
0.00
*
*
*
*
Vehicle
CCCP (24 h)
si-control
si-SQSTM1
si-NBR1
si-SQSTM1+si-NBR1

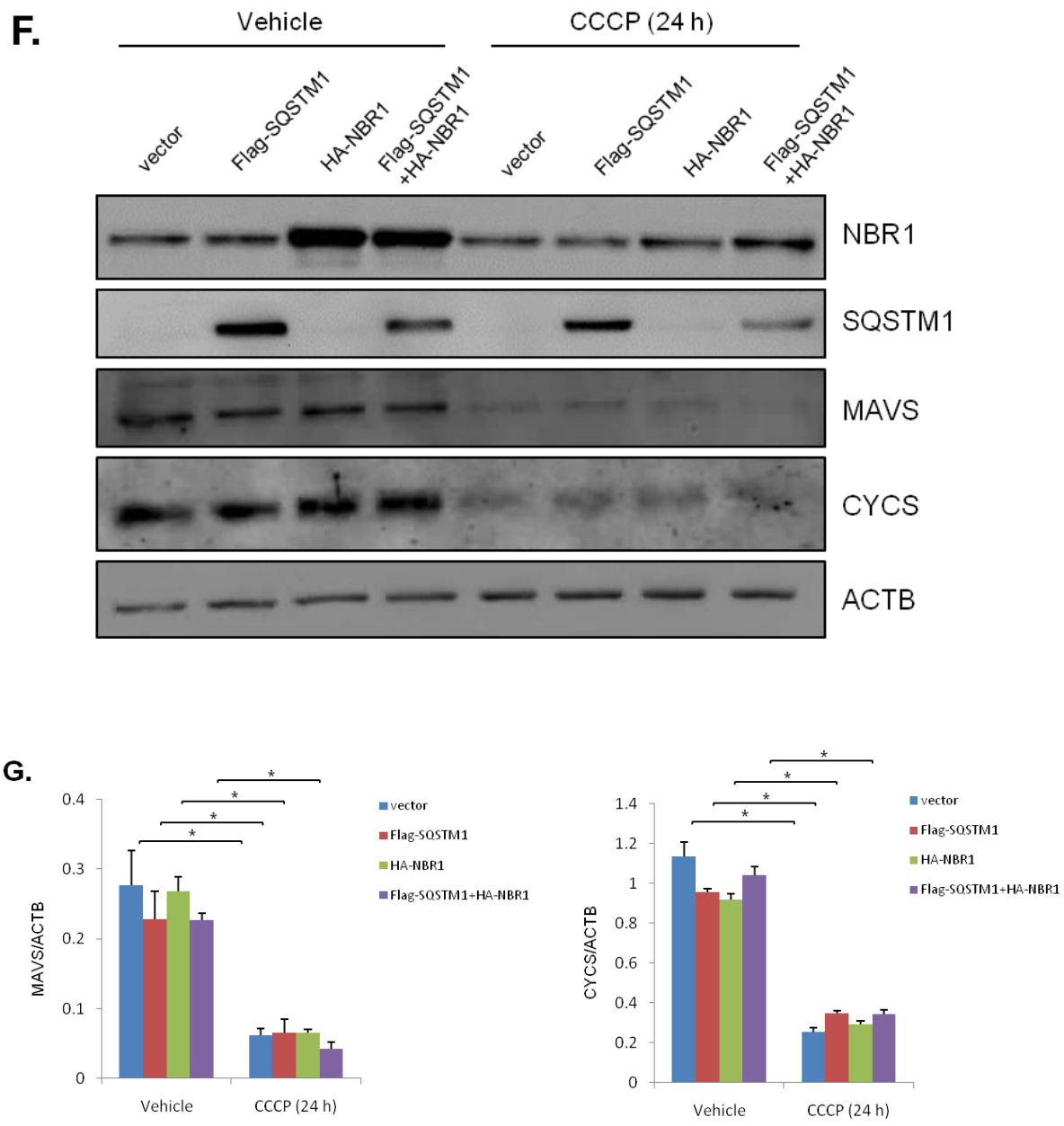

Figure 27. NBR1 is dispensable for CCCP-induced mitophagy regardless of the presence or absence of SQSTM1.

(**A**) *Sqstm1* wide-type (*Sqstm1*$^{+/+}$) or deficient (*Sqstm1*$^{-/-}$) MEFs were transiently transfected with a plasmid expressing EGFP-Myc-PARK2 for 24 h. Cells were then treated with vehicle or CCCP (10 μM) for 24 h. PARK2 was displayed in green, and TOMM20 was stained in red. The percentage of cells with TOMM20 degradation relative to total counted cells expressing PARK2

(n) was presented. (**B and C**) *Sqstm1* wide-type or deficient MEFs **(B)** and regular HeLa cells **(C)** were transiently transfected with si-*NBR1* for 24 h, followed by second transfection with EGFP-Myc-PARK2 plasmid for additional 24 h. Cells were then treated with vehicle or CCCP for 24 h. PARK2 signal was shown in green, and TOMM20 was stained in red. Quantification was performed as described above. The si-NBR1 knockdown efficiency in MEFs was evaluated by Western blotting. **(D)** PARK2 stably expressing HeLa cells were transiently transfected with si-*NBR1* and si-*SQSTM1* alone or in combination as indicated for 48 h, followed by vehicle or CCCP (10 μM) treatment for 24 h. The knockdown efficiency of si-*NBR1* and si-*SQSTM1* and protein levels of mitochondrial proteins were examined by Western blotting. **(E)** Densitometric analysis of protein levels of MAVS and TOMM20 after normalized to ACTB. #, $p<0.01$; *, $p<0.05$. **(F)** HeLa cells stably expressing PARK2 were transiently transfected with HA-NBR1 and Flag-SQSTM1 alone or in combination as indicated for 24 h, followed by vehicle or CCCP (10 μM) treatment for 24 h. The cDNA transfection efficiency and protein levels of mitochondrial proteins were examined by Western blotting. **(G)** Densitometric analysis of protein levels of MAVS and CYCS after normalized to ACTB. #, $p<0.01$.

5.4 Discussion

Selective removal of terminally damaged organelles that are highly toxic to the cells through autophagy represents an important self-defense mechanism to protect against cell damage. Autophagy adaptor proteins, including SQSTM1 and NBR1, have been revealed to be essential in mediating selective autophagy [130, 131, 260, 261, 262]. SQSTM1 and NBR1 share similar functional domains, including the PB1 domain, the LC3-interacting regions (LIR), and the ubiquitin association (UBA) domain [121]. Through interacting with both LC3 and ubiquitin chains, they function as autophagy receptors targeting ubiquitinated proteins/organelles to autophagosomes for degradation. Functional redundancy of these two proteins has been proposed in the clearance of ubiquitinated proteins and damaged mitochondria [122, 131, 253]; however, direct experimental evidence is still missing.

The major findings of the current study are two-fold. First, NBR1 alone does not seem to play a key role in PARK2-mediated mitophagy as neither knockdown nor overexpression of NBR1 affects CCCP-induced mitochondrial clearance. Second, NBR1 does not appear to serve as a compensatory mechanism for the loss of function of SQSTM1 in regulating mitophagy as deletion of both SQSTM1 and NBR1 fails to rescue mitochondrial degradation triggered by CCCP. Our results in this study suggest that additional autophagic adaptor proteins are responsible for the regulation of PARK2-dependent mitophagy. Alternatively, depletion of SQSTM1 results in the activation and recruitment of redundant proteins other than NBR1 to dysfunctional mitochondria. It was previously shown that outer mitochondrial membrane protein BCL2/adenovirus E1B 19kDa interacting protein 3-like (Nix/BNIP3) and FUN14 domain containing 1 (FUNDC1) act as a receptor for CCCP and hypoxia-induced mitophagy, respectively [255, 263]. Moreover, it was recently reported that upon depolarization or oxidative stress, optineurin is recruited to depolarized mitochondria to facilitate mitochondrial degradation by autophagy [264]. Most recently, autophagy/beclin-1 regulator 1 (AMBRA1) was identified as a novel autophagy receptor for impaired mitochondria through binding to autophagosome LC3 in both PARK2- and SQSTM1-dependent and independent manners [265]. Whether these proteins play a compensatory role in mitophagy in SQSTM1 and NBR1 deficient cells warrants further investigation.

In this study we demonstrated that NBR1 is recruited to the depolarized mitochondria upon injury although it may not be a necessary mediator for mitophagy. Together with early reports that SQSTM1 co-localizes with mitochondria marker TOMM20 and PARK2 upon stress [252, 253, 259], our results suggest that both NBR1 and SQSTM1 are likely targets of mitophagy themselves.

This hypothesis was supported by the data presented in **Fig. 27D and F** that protein levels of NBR1 and SQSTM1 are markedly decreased in CCCP-treated cells as compared to control.

Another interesting observation of this study is PARK2-dependent selective proteasomal degradation of VDAC1 at the early stage of mitochondrial damage. This result is consistent with previous reports that mitochondrial proteins, such as TOMM20, TOMM40, TOMM70, Omp25, and mitofusins, undergo proteasomal degradation before the entire damaged mitochondria are destined for autophagic degradation [254, 266, 267]. These findings point to important cellular strategies to maintain a functional network of mitochondria at different phases of organ damage. During the early stage of mitochondrial damage, the proteasome pathway plays a key role in quality control through disposal of individual damaged proteins. However, an extended injury results in a massive accumulation of misfolded proteins that exceed the proteolytic capacity of the proteasome. Under this condition, the mitophagy pathway is therefore activated to remove the whole damaged organelles from the cells to restore homeostasis.

In summary, our results reveal that NBR1 is neither an essential protein in PARK2-mediated mitophagy nor does it play a major compensatory role in mitochondrial degradation in SQSTM1 depletion cells.

Chapter 6: Closing remarks

6.1 Research summary and conclusions

A **summary** of the major findings in my study is listed below:

Chapter 3: Cleavage of sequestosome 1/p62 results in disrupted selective autophagy

1. SQSTM1 is cleaved at glycine 241 (G241) following CVB3 infection through the activity of viral proteinase $2A^{pro}$.

2. The cleavage fragments of SQSTM1 are no longer the substrates of autophagy, and their ability to form protein aggregates is greatly compromised.

3. The cleavage fragments of SQSTM1 lose the function of native SQSTM1 in activating NFKB pathway.

4. In addition to the disruption of selective autophagy, CVB3 infection results in an incomplete general autophagy pathway due to the blockage of autophagic flux.

Chapter 4: Dominant-negative function of the C-terminal fragments of NBR1 and SQSTM1 generated during CVB3 infection

1. NBR1 is also cleaved during CVB3 infection by virus-encoded proteinase $2A^{pro}$ and $3C^{pro}$ at glycine 402 (G402) and glutamic acid 682 (E682), respectively.

2. In addition to the loss-of-function, the cleavage of SQSTM1/NBR1 leads to the generation of toxic mutants. The C-terminal fragments of SQSTM1 and NBR1 exhibit a dominant-negative effect against native SQSTM1/NBR1, probably by competing for LC3 and ubiquitin chain binding.

3. SQSTM1 and NBR1 are positively and mutually regulated during viral infection.

Chapter 5: NBR1 is dispensable for PARK2-mediated mitophagy regardless of the presence or absence of SQSTM1

1. NBR1 does not appear to be required for mitochondrial clustering following mitochondrial depolarization induced by mitochondrial uncoupler CCCP.

2. NBR1 alone or together with SQSTM1 does not prevent the degradation of damaged mitochondria.

In **conclusion**, my research demonstrated that CVB3 infection results in disrupted aggrephagy, autophagic flux and host defense signaling, suggesting novel mechanisms through which coxsackievirus infection induces abnormal accumulation of ubiquitin conjugates and benefits its own replication. The disruption of aggrephagy and host defense signaling is due to the proteolytic cleavage of autophagy adaptor proteins SQSTM1 and NBR1. SQSTM1 and NBR1 do not appear to play an indispensable role in mitophagy.

6.2 Research significance

To date, there is no effective treatment to viral myocarditis and its chronic complication, DCM. Understanding the pathogenesis of this disease from different perspectives will facilitate the discovery of novel therapeutic targets and the development of new drugs. Virus-induced cardiomyopathy is accompanied by abnormal accumulation of ubiquitin conjugates observed in both animal models and patients. Proteotoxicity generated by protein aggregates has emerged to play a key role in the pathogenesis of proteinopathies, such as neurodegenerative and heart diseases. Thus, elucidation of the biological process of ubiquitin conjugates formation is the first step to understand the disease. Our findings that CVB3 induces the cleavage of the two functionally similar autophagy adapter proteins and subsequent impairment of selective

clearance of ubiquitin aggregates suggest a novel mechanism contributing to the pathogenesis of CVB3 infection. Knowledge gained in this study offers a potential for the development of new drugs targeting the loss of SQSTM1 and NBR1 function for the treatment of CVB3-induced diseases.

From a broader perspective, the extended list of host proteins targeted by viral proteinases provides valuable information for screening and developing viral proteinase inhibitors. A compilation of verified substrates has revealed a core consensus sequence [L/I/M•X•T/S•X|G•X•X•X] for enteroviral proteinase $2A^{pro}$ and [A•X•X•Q|G•P•X•X] for enteroviral proteinase $3C^{pro}$ (L, leucine; I, isoleucine; M, methionine; T, threonine; S, serine; A, alanine; Q, glutamine; G, glycine; P, proline; X stands for any amino acid; |, stands for the scissile site); however, the characterization of viral proteinase substrates is still at an early stage. Identification of an increasing number of viral proteinase targets will assist in a better recognition of protein characteristics at primary and conformational levels and the development of viral proteinase inhibitors. A sample strategy is to design a small molecule that mimics viral substrates and has a higher affinity to viral proteinases. In this way, it interrupts the interaction of viral proteinases with its native substrates.

This study reveals a new mechanism of SQSTM1 and NBR1 regulation. It was previously reported that SQSTM1 protein level is controlled by autophagic degradation [185], as well as transcriptional and post-transcriptional regulation during autophagy [268, 269, 270, 271]. The current study provides the first proof that SQSTM1 is regulated by viral proteinases-targeted cleavage. This finding further emphasizes the notion that evaluation of autophagy flux cannot solely rely on the measurement of SQSTM1, and a combination of different methods is required.

Furthermore, my study provides a powerful model system to delineate the biological functions and mechanisms of SQSTM1 and NBR1. The study establishes a model to investigate the functional changes of toxic gain-of-function or dominant-negative effects of the cleavage mutants by generating cleavage fragments and the non-cleavable form. Given the importance of SQSTM1 and NBR1 in various cellular processes and the diversity of host proteinases, it is assumed that they may also be targeted by other proteinases [194]. In fact, a latest study showed that SQSTM1 cleavage can also be mediated by caspase 8 [272]. Thus, the functional consequences induced by distinct cleavage warrant further investigation using similar strategies.

6.3 Limitations and future directions

Although the cleavage of SQSTM1 and NBR1 has also been confirmed in HL-1 cells (a cell line derived from mouse cardiomyocytes) following CVB3 infection, the data would be more solid if the cleavage products were detected in CVB3-infected mouse hearts. Using tissue extracts from CVB3-infected mouse hearts, we were unable to detect significant downregulation and obvious cleavage of SQSTM1 and NBR1 by Western blot analysis. We believe that this is largely due to the nature of highly focal infection of the heart by CVB3 [273]. Unlike *in vitro* studies in which we can achieve 100% viral infection, in the *in vivo* mouse model the viral infection rate is much lower with an average ~30% of the cardiomyocytes being infected at 9d post-infection (the peak time for viral replication). In addition, cardiac fibroblasts and vascular smooth muscle cells in the heart are resistant to CVB3 infection. Thus, it is extremely challenging to detect changes of protein expression using extracts from virus-infected hearts. In fact, we found that even viral capsid protein VP1 was hardly detectable in CVB3-infected mouse hearts by Western blotting because this protein is much diluted in whole tissue lysates.

Fluorescence-activated cell sorting (FACS) may be instrumental to solve this problem. For example, susceptible mice can be infected with recombinant EGFP-CVB3 [274], followed by the separation and collection of EGFP-tagged and CVB3-infected cardiomyocytes using FACS. **Second**, the finding that viral proteinases induce the cleavage of SQSTM1 and NBR1 has been verified in both virus-infected cells and with the *in vitro* cleavage assay by incubating cell lysates with purified viral proteinases; however, we do not know whether viral proteinases induce the cleavage directly or with the involvement of other cellular factors. This point would be clarified using a purified SQSTM1 and NBR1 with intact tertiary structure. **Third**, the underlying mechanism through which CVB3 infection results in the blockage of autophagic flux remains to be elucidated. LAMP1, LAMP2, and the small GTP binding protein Rab7 are of functional importance in autophagic vacuole maturation [275, 276, 277]. Given that SQSTM1 colocalizes with Rab7 and LAMP2 as a component of mTOR complex 1 (mTORC1), and is required for mTOR recruitment to the lysosomal surface upon activation of mTORC1 pathway [278, 279], it is conceivable that reduction of SQSTM1 also affects the formation of the autophagosome (akin to mTOR inactivation) and autolysosome. Thus, it is worthy to further investigate whether these proteins may contribute to autophagic flux during CVB3 infection. **Fourth**, an interesting question that remains is what determines the assortment of ubiquitinated substrates to different types of selective autophagy. A variety of ubiquitin chains are generated by the sequential conjugation of ubiquitin moieties from the side chain or the main chain amide group to the C terminus of the succeeding ubiquitin module. It is possible that different forms of ubiquitin linkage are recognized by ubiquitin-binding domains of autophagic adaptor proteins, which translates divergent ubiquitin messages into different types of selective autophagy. **Moreover**, *in vivo* experiments are required to further study the effects of SQSTM1 and NBR1 cleavage on the

pathogenesis of viral myocarditis. It is intriguing to evaluate the functional significance of SQSTM1-N and SQSTM1-C in intact hearts. The potential pathogenic role of SQSTM1-N and SQSTM1-C in cardiac dysfunction and DCM can be examined using a transgenic mouse model with cardiac-specific expression of SQSTM1-N and SQSTM1-C. It is anticipated that overexpression of SQSTM1-N and SQSTM1-C in mouse hearts will reduce cardiac function, promoting the development of DCM based on the *in vitro* findings. Due to the high, basal levels of endogenous SQSTM1 in the heart, transgenic mice with cardiac expression of the non-cleavable form of SQSTM1 may not be a suitable model for studying the functional significance of SQSTM1 cleavage. In addition, overexpression of SQSTM1 in mouse hearts has been associated with cardiac hypertrophy[280]. Thus, in the future, we propose to establish a knockin mouse model expressing non-cleavable SQSTM1 (to replace the endogenous SQSTM1 gene) in the heart to determine whether this form of SQSTM1 can rescue the heart from CVB3-induced DCM. **Finally**, the widely used model to study mitochondrial dysfunction with the protonophore CCCP and overexpression of PARK2 are very practical to decipher the role of PARK2 and PINK1 in the removal of damaged mitochondria. However, it has been argued that it may not be a suitable model system to study mitochondrial dysfunction in which mitophagy is triggered in a physiological manner[281]. It is suggested that only when applying mild and transient oxidative stress, mitophagy is specifically induced in mammalian cells without triggering bulk autophagy[282]. This may also partly explain the discrepancies regarding the requirement of SQSTM1 in mitophagy in different studies. Thus, the development of a suitable model that mimics the physiological condition to the largest extent is greatly needed.

Bibliography

1. Feldman AM, McNamara D. Myocarditis. *N Engl J Med* 2000, **343**(19)**:** 1388-1398.

2. Baughman KL. Diagnosis of myocarditis: death of Dallas criteria. *Circulation* 2006, **113**(4)**:** 593-595.

3. Kawai C. From myocarditis to cardiomyopathy: mechanisms of inflammation and cell death: learning from the past for the future. *Circulation* 1999, **99**(8)**:** 1091-1100.

4. Kodama M, Hanawa H, Saeki M, Hosono H, Inomata T, Suzuki K, *et al.* Rat dilated cardiomyopathy after autoimmune giant cell myocarditis. *Circ Res* 1994, **75**(2)**:** 278-284.

5. Schultz JC, Hilliard AA, Cooper LT, Jr., Rihal CS. Diagnosis and treatment of viral myocarditis. *Mayo Clinic proceedings Mayo Clinic* 2009, **84**(11)**:** 1001-1009.

6. Felker GM, Hu W, Hare JM, Hruban RH, Baughman KL, Kasper EK. The spectrum of dilated cardiomyopathy. The Johns Hopkins experience with 1,278 patients. *Medicine (Baltimore)* 1999, **78**(4)**:** 270-283.

7. Magnani JW, Danik HJ, Dec GW, Jr., DiSalvo TG. Survival in biopsy-proven myocarditis: a long-term retrospective analysis of the histopathologic, clinical, and hemodynamic predictors. *Am Heart J* 2006, **151**(2)**:** 463-470.

8. Doolan A, Langlois N, Semsarian C. Causes of sudden cardiac death in young Australians. *Med J Aust* 2004, **180**(3)**:** 110-112.

9. Kearney MT, Cotton JM, Richardson PJ, Shah AM. Viral myocarditis and dilated cardiomyopathy: mechanisms, manifestations, and management. *Postgraduate medical journal* 2001, **77**(903)**:** 4-10.

10. Cooper LT, Jr. Myocarditis. *N Engl J Med* 2009, **360**(15)**:** 1526-1538.

11. Grumbach IM, Heim A, Pring-Akerblom P, Vonhof S, Hein WJ, Muller G, *et al.* Adenoviruses and enteroviruses as pathogens in myocarditis and dilated cardiomyopathy. *Acta cardiologica* 1999, **54**(2)**:** 83-88.

12. Liu PP, Mason JW. Advances in the understanding of myocarditis. *Circulation* 2001, **104**(9)**:** 1076-1082.

13. Martino TA, Petric M, Weingartl H, Bergelson JM, Opavsky MA, Richardson CD, *et al.* The coxsackie-adenovirus receptor (CAR) is used by reference strains and clinical isolates representing all six serotypes of coxsackievirus group B and by swine vesicular disease virus. *Virology* 2000, **271**(1)**:** 99-108.

14. Liu P, Aitken K, Kong YY, Opavsky MA, Martino T, Dawood F, *et al.* The tyrosine kinase p56lck is essential in coxsackievirus B3-mediated heart disease. *Nature medicine* 2000, **6**(4)**:** 429-434.

15. Deonarain R, Cerullo D, Fuse K, Liu PP, Fish EN. Protective role for interferon-beta in coxsackievirus B3 infection. *Circulation* 2004, **110**(23)**:** 3540-3543.

16. Negishi H, Osawa T, Ogami K, Ouyang X, Sakaguchi S, Koshiba R, *et al.* A critical link between Toll-like receptor 3 and type II interferon signaling pathways in antiviral innate immunity. *Proc Natl Acad Sci U S A* 2008, **105**(51)**:** 20446-20451.

17. Goubau D, Deddouche S, Reis e Sousa C. Cytosolic sensing of viruses. *Immunity* 2013, **38**(5)**:** 855-869.

18. Stark GR, Darnell JE, Jr. The JAK-STAT pathway at twenty. *Immunity* 2012, **36**(4)**:** 503-514.

19. Feng Q, Langereis MA, Lork M, Nguyen M, Hato SV, Lanke K, *et al.* Enteroviruses 2Apro targets MDA5 and MAVS in infected cells. *Journal of virology* 2014.

20. Huber SA, Lodge PA. Coxsackievirus B-3 myocarditis in Balb/c mice. Evidence for autoimmunity to myocyte antigens. *Am J Pathol* 1984, **116**(1)**:** 21-29.

21. Huber SA. Autoimmunity in myocarditis: relevance of animal models. *Clinical immunology and immunopathology* 1997, **83**(2)**:** 93-102.

22. Gauntt CJ, Arizpe HM, Higdon AL, Wood HJ, Bowers DF, Rozek MM, *et al.* Molecular mimicry, anti-coxsackievirus B3 neutralizing monoclonal antibodies, and myocarditis. *J Immunol* 1995, **154**(6)**:** 2983-2995.

23. Massilamany C, Huber SA, Cunningham MW, Reddy J. Relevance of molecular mimicry in the mediation of infectious myocarditis. *J Cardiovasc Transl Res* 2014, **7**(2)**:** 165-171.

24. Canter CE, Simpson KP. Diagnosis and treatment of myocarditis in children in the current era. *Circulation* 2014, **129**(1)**:** 115-128.

25. Rose NR. Learning from myocarditis: mimicry, chaos and black holes. *F1000prime reports* 2014, **6:** 25.

26. Seko Y, Takahashi N, Yagita H, Okumura K, Yazaki Y. Expression of cytokine mRNAs in murine hearts with acute myocarditis caused by coxsackievirus b3. *J Pathol* 1997, **183**(1)**:** 105-108.

27. Matsumori A, Yamada T, Suzuki H, Matoba Y, Sasayama S. Increased circulating cytokines in patients with myocarditis and cardiomyopathy. *Br Heart J* 1994, **72**(6)**:** 561-566.

28. Freeman GL, Colston JT, Zabalgoitia M, Chandrasekar B. Contractile depression and expression of proinflammatory cytokines and iNOS in viral myocarditis. *Am J Physiol* 1998, **274**(1 Pt 2)**:** H249-258.

29. Ono K, Matsumori A, Shioi T, Furukawa Y, Sasayama S. Cytokine gene expression after myocardial infarction in rat hearts: possible implication in left ventricular remodeling. *Circulation* 1998, **98**(2)**:** 149-156.

30. Feuer R, Whitton JL. Preferential coxsackievirus replication in proliferating/activated cells: implications for virus tropism, persistence, and pathogenesis. *Current topics in microbiology and immunology* 2008, **323:** 149-173.

31. Cohn JN, Ferrari R, Sharpe N. Cardiac remodeling--concepts and clinical implications: a consensus paper from an international forum on cardiac remodeling. Behalf of an International Forum on Cardiac Remodeling. *J Am Coll Cardiol* 2000, **35**(3)**:** 569-582.

32. Florea VG. Left ventricular remodelling: the chicken and egg story of structure and function. *International journal of cardiology* 1999, **71**(3)**:** 207-208.

33. Esfandiarei M, McManus BM. Molecular biology and pathogenesis of viral myocarditis. *Annual review of pathology* 2008, **3:** 127-155.

34. Gravanis MB, Sternby NH. Incidence of myocarditis. A 10-year autopsy study from Malmo, Sweden. *Archives of pathology & laboratory medicine* 1991, **115**(4)**:** 390-392.

35. Dec GW, Jr., Palacios IF, Fallon JT, Aretz HT, Mills J, Lee DC, *et al.* Active myocarditis in the spectrum of acute dilated cardiomyopathies. Clinical features, histologic correlates, and clinical outcome. *N Engl J Med* 1985, **312**(14)**:** 885-890.

36. Mason JW, O'Connell JB, Herskowitz A, Rose NR, McManus BM, Billingham ME, *et al.* A clinical trial of immunosuppressive therapy for myocarditis. The Myocarditis Treatment Trial Investigators. *N Engl J Med* 1995, **333**(5)**:** 269-275.

37. Chen YS, Wang MJ, Chou NK, Han YY, Chiu IS, Lin FY, *et al.* Rescue for acute myocarditis with shock by extracorporeal membrane oxygenation. *The Annals of thoracic surgery* 1999, **68**(6)**:** 2220-2224.

38. Schultz JC, Hilliard AA, Cooper LT, Jr., Rihal CS. Diagnosis and treatment of viral myocarditis. *Mayo Clinic proceedings* 2009, **84**(11)**:** 1001-1009.

39. Okada I, Matsumori A, Matoba Y, Tominaga M, Yamada T, Kawai C. Combination treatment with ribavirin and interferon for coxsackievirus B3 replication. *The Journal of laboratory and clinical medicine* 1992, **120**(4)**:** 569-573.

40. Matsumori A, Crumpacker CS, Abelmann WH. Prevention of viral myocarditis with recombinant human leukocyte interferon alpha A/D in a murine model. *J Am Coll Cardiol* 1987, **9**(6)**:** 1320-1325.

41. Kishimoto C, Takada H, Kawamata H, Umatake M, Ochiai H. Immunoglobulin treatment prevents congestive heart failure in murine encephalomyocarditis viral myocarditis associated with reduction of inflammatory cytokines. *J Pharmacol Exp Ther* 2001, **299**(2)**:** 645-651.

42. Yamada T, Matsumori A, Sasayama S. Therapeutic effect of anti-tumor necrosis factor-alpha antibody on the murine model of viral myocarditis induced by encephalomyocarditis virus. *Circulation* 1994, **89**(2)**:** 846-851.

43. Matsumori A, Nunokawa Y, Yamaki A, Yamamoto K, Hwang MW, Miyamoto T, *et al.* Suppression of cytokines and nitric oxide production, and protection against lethal endotoxemia and viral myocarditis by a new NF-kappaB inhibitor. *Eur J Heart Fail* 2004, **6**(2)**:** 137-144.

44. Cooper LT, Baughman KL, Feldman AM, Frustaci A, Jessup M, Kuhl U, *et al.* The role of endomyocardial biopsy in the management of cardiovascular disease: a scientific statement from the American Heart Association, the American College of Cardiology, and the European Society of Cardiology Endorsed by the Heart Failure Society of America and the Heart Failure Association of the European Society of Cardiology. *European heart journal* 2007, **28**(24)**:** 3076-3093.

45. Stanton C, Mookadam F, Cha S, McNamara D, Aukrust P, Wojnicz R, *et al.* Greater symptom duration predicts response to immunomodulatory therapy in dilated cardiomyopathy. *International journal of cardiology* 2008, **128**(1)**:** 38-41.

46. Wojnicz R, Nowalany-Kozielska E, Wojciechowska C, Glanowska G, Wilczewski P, Niklewski T, *et al.* Randomized, placebo-controlled study for immunosuppressive treatment of inflammatory dilated cardiomyopathy: two-year follow-up results. *Circulation* 2001, **104**(1)**:** 39-45.

47. Opavsky MA, Penninger J, Aitken K, Wen WH, Dawood F, Mak T, *et al.* Susceptibility to myocarditis is dependent on the response of alphabeta T lymphocytes to coxsackieviral infection. *Circ Res* 1999, **85**(6)**:** 551-558.

48. Ebrahimi-Fakhari D, Wahlster L, McLean PJ. Protein degradation pathways in Parkinson's disease: curse or blessing. *Acta Neuropathol* 2012, **124**(2)**:** 153-172.

49. Double KL. Neuronal vulnerability in Parkinson's disease. *Parkinsonism & related disorders* 2012, **18 Suppl 1:** S52-54.

50. Safar JG. Molecular pathogenesis of sporadic prion diseases in man. *Prion* 2012, **6**(2)**:** 108-115.

51. Guest WC, Silverman JM, Pokrishevsky E, O'Neill MA, Grad LI, Cashman NR. Generalization of the prion hypothesis to other neurodegenerative diseases: an imperfect fit. *Journal of toxicology and environmental health Part A* 2011, **74**(22-24)**:** 1433-1459.

52. Crippa V, Sau D, Rusmini P, Boncoraglio A, Onesto E, Bolzoni E, *et al.* The small heat shock protein B8 (HspB8) promotes autophagic removal of misfolded proteins involved in amyotrophic lateral sclerosis (ALS). *Hum Mol Genet* 2010, **19**(17)**:** 3440-3456.

53. Arrasate M, Finkbeiner S. Protein aggregates in Huntington's disease. *Experimental neurology* 2012, **238**(1)**:** 1-11.

54. Douglas PM, Summers DW, Cyr DM. Molecular chaperones antagonize proteotoxicity by differentially modulating protein aggregation pathways. *Prion* 2009, **3**(2)**:** 51-58.

55. Willis MS, Patterson C. Proteotoxicity and cardiac dysfunction--Alzheimer's disease of the heart? *N Engl J Med* 2013, **368**(5)**:** 455-464.

56. Weekes J, Morrison K, Mullen A, Wait R, Barton P, Dunn MJ. Hyperubiquitination of proteins in dilated cardiomyopathy. *Proteomics* 2003, **3**(2)**:** 208-216.

57. Sanbe A, Osinska H, Saffitz JE, Glabe CG, Kayed R, Maloyan A, *et al.* Desmin-related cardiomyopathy in transgenic mice: a cardiac amyloidosis. *Proc Natl Acad Sci U S A* 2004, **101**(27)**:** 10132-10136.

58. Gianni D, Li A, Tesco G, McKay KM, Moore J, Raygor K, *et al.* Protein aggregates and novel presenilin gene variants in idiopathic dilated cardiomyopathy. *Circulation* 2010, **121**(10)**:** 1216-1226.

59. Pattison JS, Sanbe A, Maloyan A, Osinska H, Klevitsky R, Robbins J. Cardiomyocyte expression of a polyglutamine preamyloid oligomer causes heart failure. *Circulation* 2008, **117**(21)**:** 2743-2751.

60. Si X, Gao G, Wong J, Wang Y, Zhang J, Luo H. Ubiquitination is required for effective replication of coxsackievirus B3. *PLoS One* 2008, **3**(7)**:** e2585.

61. Gao G, Zhang J, Si X, Wong J, Cheung C, McManus B, *et al.* Proteasome inhibition attenuates coxsackievirus-induced myocardial damage in mice. *Am J Physiol Heart Circ Physiol* 2008, **295**(1)**:** H401-408.

62. Crowell RL, Landau BJ. A short history and introductory background on the coxsackieviruses of group B. *Current topics in microbiology and immunology* 1997, **223:** 1-11.

63. Gauntt CJ, Paque RE, Trousdale MD, Gudvangen RJ, Barr DT, Lipotich GJ, *et al.* Temperature-sensitive mutant of coxsackievirus B3 establishes resistance in neonatal mice that protects them during adolescence against coxsackievirus B3-induced myocarditis. *Infect Immun* 1983, **39**(2)**:** 851-864.

64. Tapparel C, Siegrist F, Petty TJ, Kaiser L. Picornavirus and enterovirus diversity with associated human diseases. *Infection, genetics and evolution : journal of molecular epidemiology and evolutionary genetics in infectious diseases* 2013, **14:** 282-293.

65. Klump WM, Bergmann I, Muller BC, Ameis D, Kandolf R. Complete nucleotide sequence of infectious Coxsackievirus B3 cDNA: two initial 5' uridine residues are regained during plus-strand RNA synthesis. *J Virol* 1990, **64**(4)**:** 1573-1583.

66. Flanegan JB, Petterson RF, Ambros V, Hewlett NJ, Baltimore D. Covalent linkage of a protein to a defined nucleotide sequence at the 5'-terminus of virion and replicative intermediate RNAs of poliovirus. *Proc Natl Acad Sci U S A* 1977, **74**(3)**:** 961-965.

67. Toyoda H, Franco D, Fujita K, Paul AV, Wimmer E. Replication of poliovirus requires binding of the poly(rC) binding protein to the cloverleaf as well as to the adjacent C-rich spacer sequence between the cloverleaf and the internal ribosomal entry site. *Journal of virology* 2007, **81**(18)**:** 10017-10028.

68. He W, Lu H, Zhao K, Song D, Gai X, Gao F. Complete genome sequence of a coxsackievirus B3 isolated from a Sichuan snub-nosed monkey. *Journal of virology* 2012, **86**(23)**:** 13134-13135.

69. Belsham GJ. Divergent picornavirus IRES elements. *Virus research* 2009, **139**(2)**:** 183-192.

70. Fernandez-Miragall O, Lopez de Quinto S, Martinez-Salas E. Relevance of RNA structure for the activity of picornavirus IRES elements. *Virus research* 2009, **139**(2)**:** 172-182.

71. Huber SA, Gauntt CJ, Sakkinen P. Enteroviruses and myocarditis: viral pathogenesis through replication, cytokine induction, and immunopathogenicity. *Advances in virus research* 1998, **51:** 35-80.

72. Gradi A, Imataka H, Svitkin YV, Rom E, Raught B, Morino S, *et al.* A novel functional human eukaryotic translation initiation factor 4G. *Mol Cell Biol* 1998, **18**(1)**:** 334-342.

73. Lamphear BJ, Yan R, Yang F, Waters D, Liebig HD, Klump H, *et al.* Mapping the cleavage site in protein synthesis initiation factor eIF-4 gamma of the 2A proteases from human Coxsackievirus and rhinovirus. *J Biol Chem* 1993, **268**(26)**:** 19200-19203.

74. Badorff C, Lee GH, Lamphear BJ, Martone ME, Campbell KP, Rhoads RE, *et al.* Enteroviral protease 2A cleaves dystrophin: evidence of cytoskeletal disruption in an acquired cardiomyopathy. *Nature medicine* 1999, **5**(3)**:** 320-326.

75. Yalamanchili P, Weidman K, Dasgupta A. Cleavage of transcriptional activator Oct-1 by poliovirus encoded protease 3Cpro. *Virology* 1997, **239**(1)**:** 176-185.

76. Yalamanchili P, Banerjee R, Dasgupta A. Poliovirus-encoded protease 2APro cleaves the TATA-binding protein but does not inhibit host cell RNA polymerase II transcription in vitro. *Journal of virology* 1997, **71**(9)**:** 6881-6886.

77. Clark ME, Lieberman PM, Berk AJ, Dasgupta A. Direct cleavage of human TATA-binding protein by poliovirus protease 3C in vivo and in vitro. *Mol Cell Biol* 1993, **13**(2)**:** 1232-1237.

78. Yalamanchili P, Datta U, Dasgupta A. Inhibition of host cell transcription by poliovirus: cleavage of transcription factor CREB by poliovirus-encoded protease 3Cpro. *Journal of virology* 1997, **71**(2)**:** 1220-1226.

79. Clark ME, Hammerle T, Wimmer E, Dasgupta A. Poliovirus proteinase 3C converts an active form of transcription factor IIIC to an inactive form: a mechanism for inhibition of host cell polymerase III transcription by poliovirus. *Embo J* 1991, **10**(10)**:** 2941-2947.

80. Isoyama T, Kamoshita N, Yasui K, Iwai A, Shiroki K, Toyoda H, *et al.* Lower concentration of La protein required for internal ribosome entry on hepatitis C virus RNA than on poliovirus RNA. *The Journal of general virology* 1999, **80 (Pt 9):** 2319-2327.

81. Wong J, Zhang J, Yanagawa B, Luo Z, Yang X, Chang J, *et al.* Cleavage of serum response factor mediated by enteroviral protease 2A contributes to impaired cardiac function. *Cell Res* 2012, **22**(2)**:** 360-371.

82. Weidman MK, Yalamanchili P, Ng B, Tsai W, Dasgupta A. Poliovirus 3C protease-mediated degradation of transcriptional activator p53 requires a cellular activity. *Virology* 2001, **291**(2)**:** 260-271.

83. Lamphear BJ, Yan R, Yang F, Waters D, Liebig HD, Klump H, *et al.* Mapping the cleavage site in protein synthesis initiation factor eIF-4 gamma of the 2A proteases from human Coxsackievirus and rhinovirus. *J Biol Chem* 1993, **268**(26)**:** 19200-19203.

84. de Breyne S, Bonderoff JM, Chumakov KM, Lloyd RE, Hellen CU. Cleavage of eukaryotic initiation factor eIF5B by enterovirus 3C proteases. *Virology* 2008, **378**(1)**:** 118-122.

85. Joachims M, Van Breugel PC, Lloyd RE. Cleavage of poly(A)-binding protein by enterovirus proteases concurrent with inhibition of translation in vitro. *J Virol* 1999, **73**(1)**:** 718-727.

86. White JP, Cardenas AM, Marissen WE, Lloyd RE. Inhibition of cytoplasmic mRNA stress granule formation by a viral proteinase. *Cell host & microbe* 2007, **2**(5)**:** 295-305.

87. Fung G, Ng CS, Zhang J, Shi J, Wong J, Piesik P, *et al.* Production of a dominant-negative fragment due to G3BP1 cleavage contributes to the disruption of mitochondria-associated protective stress granules during CVB3 infection. *PLoS One* 2013, **8**(11)**:** e79546.

88. Perera R, Daijogo S, Walter BL, Nguyen JH, Semler BL. Cellular protein modification by poliovirus: the two faces of poly(rC)-binding protein. *Journal of virology* 2007, **81**(17)**:** 8919-8932.

89. Mukherjee A, Morosky SA, Delorme-Axford E, Dybdahl-Sissoko N, Oberste MS, Wang T, *et al.* The coxsackievirus B 3C protease cleaves MAVS and TRIF to attenuate host type I interferon and apoptotic signaling. *PLoS pathogens* 2011, **7**(3)**:** e1001311.

90. Neznanov N, Chumakov KM, Neznanova L, Almasan A, Banerjee AK, Gudkov AV. Proteolytic cleavage of the p65-RelA subunit of NF-kappaB during poliovirus infection. *J Biol Chem* 2005, **280**(25)**:** 24153-24158.

91. Back SH, Kim YK, Kim WJ, Cho S, Oh HR, Kim JE, *et al.* Translation of polioviral mRNA is inhibited by cleavage of polypyrimidine tract-binding proteins executed by polioviral 3C(pro). *Journal of virology* 2002, **76**(5)**:** 2529-2542.

92. Badorff C, Berkely N, Mehrotra S, Talhouk JW, Rhoads RE, Knowlton KU. Enteroviral protease 2A directly cleaves dystrophin and is inhibited by a dystrophin-based substrate analogue. *J Biol Chem* 2000, **275**(15)**:** 11191-11197.

93. Seipelt J, Liebig HD, Sommergruber W, Gerner C, Kuechler E. 2A proteinase of human rhinovirus cleaves cytokeratin 8 in infected HeLa cells. *J Biol Chem* 2000, **275**(26)**:** 20084-20089.

94. Joachims M, Harris KS, Etchison D. Poliovirus protease 3C mediates cleavage of microtubule-associated protein 4. *Virology* 1995, **211**(2)**:** 451-461.

95. Weng KF, Li ML, Hung CT, Shih SR. Enterovirus 71 3C protease cleaves a novel target CstF-64 and inhibits cellular polyadenylation. *PLoS pathogens* 2009, **5**(9)**:** e1000593.

96. Wong J, Si X, Angeles A, Zhang J, Shi J, Fung G, *et al.* Cytoplasmic redistribution and cleavage of AUF1 during coxsackievirus infection enhance the stability of its viral genome. *FASEB journal : official publication of the Federation of American Societies for Experimental Biology* 2013, **27**(7)**:** 2777-2787.

97. Fung G, Shi J, Deng H, Hou J, Wang C, Hong A, *et al.* Cytoplasmic translocation, aggregation, and cleavage of TDP-43 by enteroviral proteases modulate viral pathogenesis. *Cell Death Differ* 2015.

98. Choi AM, Ryter SW, Levine B. Autophagy in human health and disease. *N Engl J Med* 2013, **368**(7)**:** 651-662.

99. Massey AC, Zhang C, Cuervo AM. Chaperone-mediated autophagy in aging and disease. *Current topics in developmental biology* 2006, **73:** 205-235.

100. Mijaljica D, Prescott M, Devenish RJ. Microautophagy in mammalian cells: revisiting a 40-year-old conundrum. *Autophagy* 2011, **7**(7)**:** 673-682.

101. Cuervo AM, Wong E. Chaperone-mediated autophagy: roles in disease and aging. *Cell Res* 2014, **24**(1)**:** 92-104.

102. Fader CM, Colombo MI. Autophagy and multivesicular bodies: two closely related partners. *Cell Death Differ* 2009, **16**(1)**:** 70-78.

103. He C, Klionsky DJ. Regulation mechanisms and signaling pathways of autophagy. *Annu Rev Genet* 2009, **43:** 67-93.

104. Klionsky DJ. Autophagy: from phenomenology to molecular understanding in less than a decade. *Nat Rev Mol Cell Biol* 2007, **8**(11)**:** 931-937.

105. Mizushima N, Levine B. Autophagy in mammalian development and differentiation. *Nature cell biology* 2010, **12**(9)**:** 823-830.

106. Noguchi S, Keira Y, Murayama K, Ogawa M, Fujita M, Kawahara G, *et al.* Reduction of UDP-N-acetylglucosamine 2-epimerase/N-acetylmannosamine kinase activity and sialylation in distal myopathy with rimmed vacuoles. *J Biol Chem* 2004, **279**(12)**:** 11402-11407.

107. Ogier-Denis E, Codogno P. Autophagy: a barrier or an adaptive response to cancer. *Biochim Biophys Acta* 2003, **1603**(2)**:** 113-128.

108. Ohsumi Y. Molecular dissection of autophagy: two ubiquitin-like systems. *Nat Rev Mol Cell Biol* 2001, **2**(3)**:** 211-216.

109. Kabeya Y, Mizushima N, Ueno T, Yamamoto A, Kirisako T, Noda T, *et al.* LC3, a mammalian homologue of yeast Apg8p, is localized in autophagosome membranes after processing. *Embo J* 2000, **19**(21)**:** 5720-5728.

110. Kihara A, Kabeya Y, Ohsumi Y, Yoshimori T. Beclin-phosphatidylinositol 3-kinase complex functions at the trans-Golgi network. *EMBO Rep* 2001, **2**(4)**:** 330-335.

111. Zeng X, Overmeyer JH, Maltese WA. Functional specificity of the mammalian Beclin-Vps34 PI 3-kinase complex in macroautophagy versus endocytosis and lysosomal enzyme trafficking. *J Cell Sci* 2006, **119**(Pt 2)**:** 259-270.

112. Codogno P, Meijer AJ. Autophagy and signaling: their role in cell survival and cell death. *Cell Death Differ* 2005, **12 Suppl 2:** 1509-1518.

113. Talloczy Z, Jiang W, Virgin HWt, Leib DA, Scheuner D, Kaufman RJ, *et al.* Regulation of starvation- and virus-induced autophagy by the eIF2alpha kinase signaling pathway. *Proc Natl Acad Sci U S A* 2002, **99**(1)**:** 190-195.

114. Levine B, Kroemer G. Autophagy in the pathogenesis of disease. *Cell* 2008, **132**(1)**:** 27-42.

115. Mizushima N, Levine B, Cuervo AM, Klionsky DJ. Autophagy fights disease through cellular self-digestion. *Nature* 2008, **451**(7182)**:** 1069-1075.

116. Shintani T, Klionsky DJ. Autophagy in health and disease: a double-edged sword. *Science* 2004, **306**(5698)**:** 990-995.

117. Alexander DE, Leib DA. Xenophagy in herpes simplex virus replication and pathogenesis. *Autophagy* 2008, **4**(1)**:** 101-103.

118. Levine B. Eating oneself and uninvited guests: autophagy-related pathways in cellular defense. *Cell* 2005, **120**(2)**:** 159-162.

119. Virgin HW, Levine B. Autophagy genes in immunity. *Nature immunology* 2009, **10**(5)**:** 461-470.

120. Kirkin V, McEwan DG, Novak I, Dikic I. A role for ubiquitin in selective autophagy. *Mol Cell* 2009, **34**(3)**:** 259-269.

121. Kraft C, Peter M, Hofmann K. Selective autophagy: ubiquitin-mediated recognition and beyond. *Nat Cell Biol* 2010, **12**(9)**:** 836-841.

122. Johansen T, Lamark T. Selective autophagy mediated by autophagic adapter proteins. *Autophagy* 2011, **7**(3)**:** 279-296.

123. Bjorkoy G, Lamark T, Brech A, Outzen H, Perander M, Overvatn A, *et al.* p62/SQSTM1 forms protein aggregates degraded by autophagy and has a protective effect on huntingtin-induced cell death. *J Cell Biol* 2005, **171**(4)**:** 603-614.

124. Kirkin V, Lamark T, Sou YS, Bjorkoy G, Nunn JL, Bruun JA, *et al.* A role for NBR1 in autophagosomal degradation of ubiquitinated substrates. *Mol Cell* 2009, **33**(4)**:** 505-516.

125. Kim PK, Hailey DW, Mullen RT, Lippincott-Schwartz J. Ubiquitin signals autophagic degradation of cytosolic proteins and peroxisomes. *Proc Natl Acad Sci U S A* 2008, **105**(52)**:** 20567-20574.

126. Thurston TL, Ryzhakov G, Bloor S, von Muhlinen N, Randow F. The TBK1 adaptor and autophagy receptor NDP52 restricts the proliferation of ubiquitin-coated bacteria. *Nat Immunol* 2009, **10**(11)**:** 1215-1221.

127. Rogov V, Dotsch V, Johansen T, Kirkin V. Interactions between autophagy receptors and ubiquitin-like proteins form the molecular basis for selective autophagy. *Mol Cell* 2014, **53**(2)**:** 167-178.

128. Wild P, Farhan H, McEwan DG, Wagner S, Rogov VV, Brady NR, *et al.* Phosphorylation of the autophagy receptor optineurin restricts Salmonella growth. *Science* 2011, **333**(6039)**:** 228-233.

129. Tumbarello DA, Waxse BJ, Arden SD, Bright NA, Kendrick-Jones J, Buss F. Autophagy receptors link myosin VI to autophagosomes to mediate Tom1-dependent autophagosome maturation and fusion with the lysosome. *Nat Cell Biol* 2012, **14**(10)**:** 1024-1035.

130. Pankiv S, Clausen TH, Lamark T, Brech A, Bruun JA, Outzen H, *et al.* p62/SQSTM1 binds directly to Atg8/LC3 to facilitate degradation of ubiquitinated protein aggregates by autophagy. *J Biol Chem* 2007, **282**(33)**:** 24131-24145.

131. Kirkin V, Lamark T, Sou YS, Bjorkoy G, Nunn JL, Bruun JA, *et al.* A role for NBR1 in autophagosomal degradation of ubiquitinated substrates. *Mol Cell* 2009, **33**(4)**:** 505-516.

132. Birgisdottir AB, Lamark T, Johansen T. The LIR motif - crucial for selective autophagy. *J Cell Sci* 2013, **126**(Pt 15)**:** 3237-3247.

133. Nakai A, Yamaguchi O, Takeda T, Higuchi Y, Hikoso S, Taniike M, *et al.* The role of autophagy in cardiomyocytes in the basal state and in response to hemodynamic stress. *Nature medicine* 2007, **13**(5)**:** 619-624.

134. Taneike M, Yamaguchi O, Nakai A, Hikoso S, Takeda T, Mizote I, *et al.* Inhibition of autophagy in the heart induces age-related cardiomyopathy. *Autophagy* 2010, **6**(5)**:** 600-606.

135. Pattison JS, Osinska H, Robbins J. Atg7 induces basal autophagy and rescues autophagic deficiency in CryABR120G cardiomyocytes. *Circ Res* 2011, **109**(2)**:** 151-160.

136. Cheng Z, Fang Q. Danon disease: focusing on heart. *Journal of human genetics* 2012, **57**(7)**:** 407-410.

137. Malicdan MC, Nishino I. Autophagy in lysosomal myopathies. *Brain Pathol* 2012, **22**(1)**:** 82-88.

138. Malicdan MC, Noguchi S, Nonaka I, Saftig P, Nishino I. Lysosomal myopathies: an excessive build-up in autophagosomes is too much to handle. *Neuromuscular disorders : NMD* 2008, **18**(7)**:** 521-529.

139. Ruivo R, Anne C, Sagne C, Gasnier B. Molecular and cellular basis of lysosomal transmembrane protein dysfunction. *Biochim Biophys Acta* 2009, **1793**(4)**:** 636-649.

140. Hein S, Arnon E, Kostin S, Schonburg M, Elsasser A, Polyakova V, *et al.* Progression from compensated hypertrophy to failure in the pressure-overloaded human heart: structural deterioration and compensatory mechanisms. *Circulation* 2003, **107**(7)**:** 984-991.

141. Rothermel BA, Hill JA. Autophagy in load-induced heart disease. *Circ Res* 2008, **103**(12)**:** 1363-1369.

142. Zhu H, Tannous P, Johnstone JL, Kong Y, Shelton JM, Richardson JA, *et al.* Cardiac autophagy is a maladaptive response to hemodynamic stress. *The Journal of clinical investigation* 2007, **117**(7)**:** 1782-1793.

143. Guo R, Ren J. Deficiency in AMPK attenuates ethanol-induced cardiac contractile dysfunction through inhibition of autophagosome formation. *Cardiovasc Res* 2012, **94**(3)**:** 480-491.

144. Cho MW, Teterina N, Egger D, Bienz K, Ehrenfeld E. Membrane rearrangement and vesicle induction by recombinant poliovirus 2C and 2BC in human cells. *Virology* 1994, **202**(1)**:** 129-145.

145. Goldsmith CS, Tatti KM, Ksiazek TG, Rollin PE, Comer JA, Lee WW, *et al.* Ultrastructural characterization of SARS coronavirus. *Emerg Infect Dis* 2004, **10**(2)**:** 320-326.

146. Gosert R, Kanjanahaluethai A, Egger D, Bienz K, Baker SC. RNA replication of mouse hepatitis virus takes place at double-membrane vesicles. *Journal of virology* 2002, **76**(8)**:** 3697-3708.

147. Pedersen KW, van der Meer Y, Roos N, Snijder EJ. Open reading frame 1a-encoded subunits of the arterivirus replicase induce endoplasmic reticulum-derived double-membrane vesicles which carry the viral replication complex. *Journal of virology* 1999, **73**(3)**:** 2016-2026.

148. Miller S, Krijnse-Locker J. Modification of intracellular membrane structures for virus replication. *Nat Rev Microbiol* 2008, **6**(5)**:** 363-374.

149. Jackson WT, Giddings TH, Jr., Taylor MP, Mulinyawe S, Rabinovitch M, Kopito RR, *et al.* Subversion of cellular autophagosomal machinery by RNA viruses. *PLoS biology* 2005, **3**(5)**:** e156.

150. Khakpoor A, Panyasrivanit M, Wikan N, Smith DR. A role for autophagolysosomes in dengue virus 3 production in HepG2 cells. *The Journal of general virology* 2009, **90**(Pt 5)**:** 1093-1103.

151. Panyasrivanit M, Khakpoor A, Wikan N, Smith DR. Co-localization of constituents of the dengue virus translation and replication machinery with amphisomes. *The Journal of general virology* 2009, **90**(Pt 2)**:** 448-456.

152. Huang SC, Chang CL, Wang PS, Tsai Y, Liu HS. Enterovirus 71-induced autophagy detected in vitro and in vivo promotes viral replication. *J Med Virol* 2009, **81**(7)**:** 1241-1252.

153. Zhang Y, Li Z, Xinna G, Xin G, Yang H. Autophagy promotes the replication of encephalomyocarditis virus in host cells. *Autophagy* 2011, **7**(6)**:** 613-628.

154. O'Donnell V, Pacheco JM, LaRocco M, Burrage T, Jackson W, Rodriguez LL, *et al.* Foot-and-mouth disease virus utilizes an autophagic pathway during viral replication. *Virology* 2011, **410**(1)**:** 142-150.

155. Krejbich-Trotot P, Gay B, Li-Pat-Yuen G, Hoarau JJ, Jaffar-Bandjee MC, Briant L, *et al.* Chikungunya triggers an autophagic process which promotes viral replication. *Virology journal* 2011, **8:** 432.

156. Ferraris P, Blanchard E, Roingeard P. Ultrastructural and biochemical analyses of hepatitis C virus-associated host cell membranes. *The Journal of general virology* 2010, **91**(Pt 9)**:** 2230-2237.

157. Ait-Goughoulte M, Kanda T, Meyer K, Ryerse JS, Ray RB, Ray R. Hepatitis C virus genotype 1a growth and induction of autophagy. *Journal of virology* 2008, **82**(5)**:** 2241-2249.

158. Dreux M, Gastaminza P, Wieland SF, Chisari FV. The autophagy machinery is required to initiate hepatitis C virus replication. *Proc Natl Acad Sci U S A* 2009, **106**(33)**:** 14046-14051.

159. Sir D, Chen WL, Choi J, Wakita T, Yen TS, Ou JH. Induction of incomplete autophagic response by hepatitis C virus via the unfolded protein response. *Hepatology* 2008, **48**(4)**:** 1054-1061.

160. Tanida I, Fukasawa M, Ueno T, Kominami E, Wakita T, Hanada K. Knockdown of autophagy-related gene decreases the production of infectious hepatitis C virus particles. *Autophagy* 2009, **5**(7)**:** 937-945.

161. Ke PY, Chen SS. Activation of the unfolded protein response and autophagy after hepatitis C virus infection suppresses innate antiviral immunity in vitro. *The Journal of clinical investigation* 2011, **121**(1)**:** 37-56.

162. Prentice E, Jerome WG, Yoshimori T, Mizushima N, Denison MR. Coronavirus replication complex formation utilizes components of cellular autophagy. *J Biol Chem* 2004, **279**(11)**:** 10136-10141.

163. Zhao Z, Thackray LB, Miller BC, Lynn TM, Becker MM, Ward E, *et al.* Coronavirus replication does not require the autophagy gene ATG5. *Autophagy* 2007, **3**(6)**:** 581-585.

164. Wong J, Zhang J, Si X, Gao G, Mao I, McManus BM, *et al.* Autophagosome supports coxsackievirus B3 replication in host cells. *Journal of virology* 2008, **82**(18)**:** 9143-9153.

165. Panyasrivanit M, Khakpoor A, Wikan N, Smith DR. Linking dengue virus entry and translation/replication through amphisomes. *Autophagy* 2009, **5**(3)**:** 434-435.

166. Su WC, Chao TC, Huang YL, Weng SC, Jeng KS, Lai MM. Rab5 and class III phosphoinositide 3-kinase Vps34 are involved in hepatitis C virus NS4B-induced autophagy. *Journal of virology* 2011, **85**(20)**:** 10561-10571.

167. Kirkegaard K, Jackson WT. Topology of double-membraned vesicles and the opportunity for non-lytic release of cytoplasm. *Autophagy* 2005, **1**(3)**:** 182-184.

168. Shrivastava S, Raychoudhuri A, Steele R, Ray R, Ray RB. Knockdown of autophagy enhances the innate immune response in hepatitis C virus-infected hepatocytes. *Hepatology* 2011, **53**(2)**:** 406-414.

169. Singh R, Kaushik S, Wang Y, Xiang Y, Novak I, Komatsu M, *et al.* Autophagy regulates lipid metabolism. *Nature* 2009, **458**(7242)**:** 1131-1135.

170. Dong H, Czaja MJ. Regulation of lipid droplets by autophagy. *Trends in endocrinology and metabolism: TEM* 2011, **22**(6)**:** 234-240.

171. Heaton NS, Randall G. Dengue virus-induced autophagy regulates lipid metabolism. *Cell host & microbe* 2010, **8**(5)**:** 422-432.

172. Liang XH, Kleeman LK, Jiang HH, Gordon G, Goldman JE, Berry G, *et al.* Protection against fatal Sindbis virus encephalitis by beclin, a novel Bcl-2-interacting protein. *Journal of virology* 1998, **72**(11)**:** 8586-8596.

173. Orvedahl A, MacPherson S, Sumpter R, Jr., Talloczy Z, Zou Z, Levine B. Autophagy protects against Sindbis virus infection of the central nervous system. *Cell host & microbe* 2010, **7**(2)**:** 115-127.

174. Yajima T, Knowlton KU. Viral myocarditis: from the perspective of the virus. *Circulation* 2009, **119**(19)**:** 2615-2624.

175. Gorbea C, Makar KA, Pauschinger M, Pratt G, Bersola JL, Varela J, *et al.* A role for Toll-like receptor 3 variants in host susceptibility to enteroviral myocarditis and dilated cardiomyopathy. *J Biol Chem* 2010, **285**(30)**:** 23208-23223.

176. Wong J, Zhang J, Si X, Gao G, Mao I, McManus BM, *et al.* Autophagosome supports coxsackievirus B3 replication in host cells. *J Virol* 2008, **82**(18)**:** 9143-9153.

177. Zhang J, Wong J, Gao G, Luo H. Tripeptidyl peptidase II serves as an alternative to impaired proteasome to maintain viral growth in the host cells. *FEBS Lett* 2011, **585**(1)**:** 261-265.

178. Salonen A, Ahola T, Kaariainen L. Viral RNA replication in association with cellular membranes. *Current topics in microbiology and immunology* 2005, **285:** 139-173.

179. Jackson WT, Giddings TH, Jr., Taylor MP, Mulinyawe S, Rabinovitch M, Kopito RR, *et al.* Subversion of cellular autophagosomal machinery by RNA viruses. *PLoS biology* 2005, **3**(5)**:** e156.

180. Suhy DA, Giddings TH, Jr., Kirkegaard K. Remodeling the endoplasmic reticulum by poliovirus infection and by individual viral proteins: an autophagy-like origin for virus-induced vesicles. *J Virol* 2000, **74**(19)**:** 8953-8965.

181. Kirkegaard K, Taylor MP, Jackson WT. Cellular autophagy: surrender, avoidance and subversion by microorganisms. *Nat Rev Microbiol* 2004, **2**(4)**:** 301-314.

182. Kemball CC, Alirezaei M, Flynn CT, Wood MR, Harkins S, Kiosses WB, *et al.* Coxsackievirus infection induces autophagy-like vesicles and megaphagosomes in pancreatic acinar cells in vivo. *Journal of virology* 2010, **84**(23)**:** 12110-12124.

183. Bjorkoy G, Lamark T, Pankiv S, Overvatn A, Brech A, Johansen T. Monitoring autophagic degradation of p62/SQSTM1. *Methods Enzymol* 2009, **452:** 181-197.

184. Jiang P, Mizushima N. LC3- and p62-based biochemical methods for the analysis of autophagy progression in mammalian cells. *Methods* 2015, **75:** 13-18.

185. Mizushima N, Yoshimori T, Levine B. Methods in mammalian autophagy research. *Cell* 2010, **140**(3)**:** 313-326.

186. Ichimura Y, Komatsu M. Selective degradation of p62 by autophagy. *Semin Immunopathol* 2010, **32**(4)**:** 431-436.

187. Komatsu M, Ichimura Y. Selective autophagy regulates various cellular functions. *Genes Cells* 2010, **15**(9)**:** 923-933.

188. Ichimura Y, Kumanomidou T, Sou YS, Mizushima T, Ezaki J, Ueno T, *et al.* Structural basis for sorting mechanism of p62 in selective autophagy. *J Biol Chem* 2008, **283**(33)**:** 22847-22857.

189. Duran A, Linares JF, Galvez AS, Wikenheiser K, Flores JM, Diaz-Meco MT, *et al.* The signaling adaptor p62 is an important NF-kappaB mediator in tumorigenesis. *Cancer Cell* 2008, **13**(4)**:** 343-354.

190. Komatsu M, Waguri S, Koike M, Sou YS, Ueno T, Hara T, *et al.* Homeostatic levels of p62 control cytoplasmic inclusion body formation in autophagy-deficient mice. *Cell* 2007, **131**(6)**:** 1149-1163.

191. Moscat J, Diaz-Meco MT. p62 at the crossroads of autophagy, apoptosis, and cancer. *Cell* 2009, **137**(6)**:** 1001-1004.

192. Komatsu M, Kurokawa H, Waguri S, Taguchi K, Kobayashi A, Ichimura Y, *et al.* The selective autophagy substrate p62 activates the stress responsive transcription factor Nrf2 through inactivation of Keap1. *Nat Cell Biol* 2010, **12**(3)**:** 213-223.

193. Lau A, Wang XJ, Zhao F, Villeneuve NF, Wu T, Jiang T, *et al.* A noncanonical mechanism of Nrf2 activation by autophagy deficiency: direct interaction between Keap1 and p62. *Mol Cell Biol* 2010, **30**(13)**:** 3275-3285.

194. Norman JM, Cohen GM, Bampton ET. The in vitro cleavage of the hAtg proteins by cell death proteases. *Autophagy* 2010, **6**(8)**:** 1042-1056.

195. Seibenhener ML, Babu JR, Geetha T, Wong HC, Krishna NR, Wooten MW. Sequestosome 1/p62 is a polyubiquitin chain binding protein involved in ubiquitin proteasome degradation. *Mol Cell Biol* 2004, **24**(18)**:** 8055-8068.

196. Zhou C, Zhong W, Zhou J, Sheng F, Fang Z, Wei Y, *et al.* Monitoring autophagic flux by an improved tandem fluorescent-tagged LC3 (mTagRFP-mWasabi-LC3) reveals that high-dose rapamycin impairs autophagic flux in cancer cells. *Autophagy* 2012, **8**(8)**:** 1215-1226.

197. Tanida I, Ueno T, Uchiyama Y. A super-ecliptic, pHluorin-mKate2, tandem fluorescent protein-tagged human LC3 for the monitoring of mammalian autophagy. *PLoS One* 2014, **9**(10)**:** e110600.

198. Kimura S, Noda T, Yoshimori T. Dissection of the autophagosome maturation process by a novel reporter protein, tandem fluorescent-tagged LC3. *Autophagy* 2007, **3**(5)**:** 452-460.

199. Delorme-Axford E, Morosky S, Bomberger J, Stolz DB, Jackson WT, Coyne CB. BPIFB3 regulates autophagy and coxsackievirus B replication through a noncanonical pathway independent of the core initiation machinery. *mBio* 2014, **5**(6)**:** e02147.

200. Xi X, Zhang X, Wang B, Wang T, Wang J, Huang H, *et al.* The interplays between autophagy and apoptosis induced by enterovirus 71. *PLoS One* 2013, **8**(2)**:** e56966.

201. Richards AL, Jackson WT. Intracellular vesicle acidification promotes maturation of infectious poliovirus particles. *PLoS pathogens* 2012, **8**(11)**:** e1003046.

202. Rubinsztein DC. The roles of intracellular protein-degradation pathways in neurodegeneration. *Nature* 2006, **443**(7113)**:** 780-786.

203. Takamura A, Komatsu M, Hara T, Sakamoto A, Kishi C, Waguri S, *et al.* Autophagy-deficient mice develop multiple liver tumors. *Genes Dev* 2011, **25**(8)**:** 795-800.

204. Luo H, Wong J, Wong B. Protein degradation systems in viral myocarditis leading to dilated cardiomyopathy. *Cardiovasc Res* 2010, **85**(2)**:** 347-356.

205. Zatloukal K, Stumptner C, Fuchsbichler A, Heid H, Schnoelzer M, Kenner L, *et al.* p62 Is a common component of cytoplasmic inclusions in protein aggregation diseases. *Am J Pathol* 2002, **160**(1)**:** 255-263.

206. Lelouard H, Gatti E, Cappello F, Gresser O, Camosseto V, Pierre P. Transient aggregation of ubiquitinated proteins during dendritic cell maturation. *Nature* 2002, **417**(6885)**:** 177-182.

207. Itakura E, Mizushima N. p62 Targeting to the autophagosome formation site requires self-oligomerization but not LC3 binding. *J Cell Biol* 2011, **192**(1)**:** 17-27.

208. Lamark T, Perander M, Outzen H, Kristiansen K, Overvatn A, Michaelsen E, *et al.* Interaction codes within the family of mammalian Phox and Bem1p domain-containing proteins. *J Biol Chem* 2003, **278**(36)**:** 34568-34581.

209. Deng L, Wang C, Spencer E, Yang L, Braun A, You J, *et al.* Activation of the IkappaB kinase complex by TRAF6 requires a dimeric ubiquitin-conjugating enzyme complex and a unique polyubiquitin chain. *Cell* 2000, **103**(2)**:** 351-361.

210. Sanz L, Diaz-Meco MT, Nakano H, Moscat J. The atypical PKC-interacting protein p62 channels NF-kappaB activation by the IL-1-TRAF6 pathway. *EMBO J* 2000, **19**(7)**:** 1576-1586.

211. Sanz L, Sanchez P, Lallena MJ, Diaz-Meco MT, Moscat J. The interaction of p62 with RIP links the atypical PKCs to NF-kappaB activation. *EMBO J* 1999, **18**(11)**:** 3044-3053.

212. Le Negrate G. Viral interference with innate immunity by preventing NF-kappaB activity. *Cell Microbiol* 2012, **14**(2)**:** 168-181.

213. Shi J, Luo H. Interplay between the cellular autophagy machinery and positive-stranded RNA viruses. *Acta Biochim Biophys Sin (Shanghai)* 2012, **44**(5)**:** 375-384.

214. Levine B, Deretic V. Unveiling the roles of autophagy in innate and adaptive immunity. *Nat Rev Immunol* 2007, **7**(10)**:** 767-777.

215. Schmid D, Munz C. Innate and adaptive immunity through autophagy. *Immunity* 2007, **27**(1)**:** 11-21.

216. Lamark T, Kirkin V, Dikic I, Johansen T. NBR1 and p62 as cargo receptors for selective autophagy of ubiquitinated targets. *Cell Cycle* 2009, **8**(13)**:** 1986-1990.

217. Cemma M, Kim PK, Brumell JH. The ubiquitin-binding adaptor proteins p62/SQSTM1 and NDP52 are recruited independently to bacteria-associated microdomains to target Salmonella to the autophagy pathway. *Autophagy* 2011, **7**(3)**:** 341-345.

218. Deosaran E, Larsen KB, Hua R, Sargent G, Wang Y, Kim S, *et al.* NBR1 acts as an autophagy receptor for peroxisomes. *J Cell Sci* 2013, **126**(Pt 4)**:** 939-952.

219. Shi J, Wong J, Piesik P, Fung G, Zhang J, Jagdeo J, *et al.* Cleavage of sequestosome 1/p62 by an enteroviral protease results in disrupted selective autophagy and impaired NFKB signaling. *Autophagy* 2013, **9**(10).

220. Carthy CM, Yanagawa B, Luo H, Granville DJ, Yang D, Cheung P, *et al.* Bcl-2 and Bcl-xL overexpression inhibits cytochrome c release, activation of multiple caspases, and virus release following coxsackievirus B3 infection. *Virology* 2003, **313**(1)**:** 147-157.

221. Willis MS, Patterson C. Proteotoxicity and cardiac dysfunction--Alzheimer's disease of the heart? *N Engl J Med* 2013, **368**(5)**:** 455-464.

222. Toyama BH, Hetzer MW. Protein homeostasis: live long, won't prosper. *Nat Rev Mol Cell Biol* 2013, **14**(1)**:** 55-61.

223. Luo H, Wong J, Wong B. Protein degradation systems in viral myocarditis leading to dilated cardiomyopathy. *Cardiovasc Res* 2010, **85**(2)**:** 347-356.

224. Ding WX. Role of autophagy in liver physiology and pathophysiology. *World J Biol Chem* 2010, **1**(1)**:** 3-12.

225. Rue L, Lopez-Soop G, Gelpi E, Martinez-Vicente M, Alberch J, Perez-Navarro E. Brain region- and age-dependent dysregulation of p62 and NBR1 in a mouse model of Huntington's disease. *Neurobiol Dis* 2013, **52:** 219-228.

226. Mori F, Tanji K, Odagiri S, Toyoshima Y, Yoshida M, Kakita A, *et al.* Autophagy-related proteins (p62, NBR1 and LC3) in intranuclear inclusions in neurodegenerative diseases. *Neurosci Lett* 2012, **522**(2)**:** 134-138.

227. Mori F, Tanji K, Odagiri S, Toyoshima Y, Yoshida M, Ikeda T, *et al.* Ubiquilin immunoreactivity in cytoplasmic and nuclear inclusions in synucleinopathies, polyglutamine diseases and intranuclear inclusion body disease. *Acta Neuropathol* 2012, **124**(1)**:** 149-151.

228. Odagiri S, Tanji K, Mori F, Kakita A, Takahashi H, Wakabayashi K. Autophagic adapter protein NBR1 is localized in Lewy bodies and glial cytoplasmic inclusions and is involved in aggregate formation in alpha-synucleinopathy. *Acta Neuropathol* 2012, **124**(2)**:** 173-186.

229. Willis MS, Townley-Tilson WH, Kang EY, Homeister JW, Patterson C. Sent to destroy: the ubiquitin proteasome system regulates cell signaling and protein quality control in cardiovascular development and disease. *Circ Res* 2010, **106**(3)**:** 463-478.

230. Zheng Q, Wang X. Autophagy and the ubiquitin-proteasome system in cardiac dysfunction. *Panminerva Med* 2010, **52**(1)**:** 9-25.

231. Zheng Q, Su H, Ranek MJ, Wang X. Autophagy and p62 in cardiac proteinopathy. *Circ Res* 2011, **109**(3)**:** 296-308.

232. Gao G, Zhang J, Si X, Wong J, Cheung C, McManus B, *et al.* Proteasome inhibition attenuates coxsackievirus-induced myocardial damage in mice. *Am J Physiol Heart Circ Physiol* 2008, **295**(1)**:** H401-408.

233. Itakura E, Mizushima N. p62 Targeting to the autophagosome formation site requires self-oligomerization but not LC3 binding. *J Cell Biol* 2011, **192**(1)**:** 17-27.

234. Lamark T, Perander M, Outzen H, Kristiansen K, Overvatn A, Michaelsen E, *et al.* Interaction codes within the family of mammalian Phox and Bem1p domain-containing proteins. *J Biol Chem* 2003, **278**(36)**:** 34568-34581.

235. Whitehouse CA, Waters S, Marchbank K, Horner A, McGowan NW, Jovanovic JV, *et al.* Neighbor of Brca1 gene (Nbr1) functions as a negative regulator of postnatal osteoblastic bone formation and p38 MAPK activity. *Proc Natl Acad Sci U S A* 2010, **107**(29)**:** 12913-12918.

236. Seibenhener ML, Babu JR, Geetha T, Wong HC, Krishna NR, Wooten MW. Sequestosome 1/p62 is a polyubiquitin chain binding protein involved in ubiquitin proteasome degradation. *Molecular and cellular biology* 2004, **24**(18)**:** 8055-8068.

237. Schiavi A, Ventura N. The interplay between mitochondria and autophagy and its role in the aging process. *Experimental gerontology* 2014, **56:** 147-153.

238. Ryan BJ, Hoek S, Fon EA, Wade-Martins R. Mitochondrial dysfunction and mitophagy in Parkinson's: from familial to sporadic disease. *Trends Biochem Sci* 2015.

239. Shires SE, Gustafsson AB. Mitophagy and heart failure. *Journal of molecular medicine* 2015, **93**(3)**:** 253-262.

240. Kubli DA, Gustafsson AB. Mitochondria and mitophagy: the yin and yang of cell death control. *Circ Res* 2012, **111**(9)**:** 1208-1221.

241. Jin S. Autophagy, mitochondrial quality control, and oncogenesis. *Autophagy* 2006, **2**(2)**:** 80-84.

242. Kageyama Y, Hoshijima M, Seo K, Bedja D, Sysa-Shah P, Andrabi SA, *et al.* Parkin-independent mitophagy requires Drp1 and maintains the integrity of mammalian heart and brain. *Embo J* 2014, **33**(23)**:** 2798-2813.

243. Melser S, Chatelain EH, Lavie J, Mahfouf W, Jose C, Obre E, *et al.* Rheb regulates mitophagy induced by mitochondrial energetic status. *Cell Metab* 2013, **17**(5)**:** 719-730.

244. Shi RY, Zhu SH, Li V, Gibson SB, Xu XS, Kong JM. BNIP3 interacting with LC3 triggers excessive mitophagy in delayed neuronal death in stroke. *CNS neuroscience & therapeutics* 2014, **20**(12)**:** 1045-1055.

245. Novak I, Kirkin V, McEwan DG, Zhang J, Wild P, Rozenknop A, *et al.* Nix is a selective autophagy receptor for mitochondrial clearance. *EMBO Rep* 2010, **11**(1)**:** 45-51.

246. Narendra D, Tanaka A, Suen DF, Youle RJ. Parkin-induced mitophagy in the pathogenesis of Parkinson disease. *Autophagy* 2009, **5**(5)**:** 706-708.

247. Narendra DP, Jin SM, Tanaka A, Suen DF, Gautier CA, Shen J, *et al.* PINK1 is selectively stabilized on impaired mitochondria to activate Parkin. *PLoS biology* 2010, **8**(1)**:** e1000298.

248. Vives-Bauza C, Zhou C, Huang Y, Cui M, de Vries RL, Kim J, *et al.* PINK1-dependent recruitment of Parkin to mitochondria in mitophagy. *Proc Natl Acad Sci U S A* 2010, **107**(1)**:** 378-383.

249. Gegg ME, Cooper JM, Chau KY, Rojo M, Schapira AH, Taanman JW. Mitofusin 1 and mitofusin 2 are ubiquitinated in a PINK1/parkin-dependent manner upon induction of mitophagy. *Hum Mol Genet* 2010, **19**(24)**:** 4861-4870.

250. Ziviani E, Tao RN, Whitworth AJ. Drosophila parkin requires PINK1 for mitochondrial translocation and ubiquitinates mitofusin. *Proc Natl Acad Sci U S A* 2010, **107**(11)**:** 5018-5023.

251. Poole AC, Thomas RE, Yu S, Vincow ES, Pallanck L. The mitochondrial fusion-promoting factor mitofusin is a substrate of the PINK1/parkin pathway. *PLoS One* 2010, **5**(4)**:** e10054.

252. Geisler S, Holmstrom KM, Skujat D, Fiesel FC, Rothfuss OC, Kahle PJ, *et al.* PINK1/Parkin-mediated mitophagy is dependent on VDAC1 and p62/SQSTM1. *Nat Cell Biol* 2010, **12**(2)**:** 119-131.

253. Narendra D, Kane LA, Hauser DN, Fearnley IM, Youle RJ. p62/SQSTM1 is required for Parkin-induced mitochondrial clustering but not mitophagy; VDAC1 is dispensable for both. *Autophagy* 2010, **6**(8)**:** 1090-1106.

254. Tanaka A, Cleland MM, Xu S, Narendra DP, Suen DF, Karbowski M, *et al.* Proteasome and p97 mediate mitophagy and degradation of mitofusins induced by Parkin. *J Cell Biol* 2010, **191**(7)**:** 1367-1380.

255. Ding WX, Ni HM, Li M, Liao Y, Chen X, Stolz DB, *et al.* Nix is critical to two distinct phases of mitophagy, reactive oxygen species-mediated autophagy induction and Parkin-ubiquitin-p62-mediated mitochondrial priming. *J Biol Chem* 2010, **285**(36)**:** 27879-27890.

256. Granot Z, Silverman E, Friedlander R, Melamed-Book N, Eimerl S, Timberg R, *et al.* The life cycle of the steroidogenic acute regulatory (StAR) protein: from transcription through proteolysis. *Endocrine research* 2002, **28**(4)**:** 375-386.

257. Norman SG, Johnson GV. Compromised mitochondrial function results in dephosphorylation of tau through a calcium-dependent process in rat brain cerebral cortical slices. *Neurochemical research* 1994, **19**(9)**:** 1151-1158.

258. Youle RJ, Narendra DP. Mechanisms of mitophagy. *Nat Rev Mol Cell Biol* 2011, **12**(1)**:** 9-14.

259. Okatsu K, Saisho K, Shimanuki M, Nakada K, Shitara H, Sou YS, *et al.* p62/SQSTM1 cooperates with Parkin for perinuclear clustering of depolarized mitochondria. *Genes Cells* 2010, **15**(8)**:** 887-900.

260. Shi J, Fung G, Piesik P, Zhang J, Luo H. Dominant-negative function of the C-terminal fragments of NBR1 and SQSTM1 generated during enteroviral infection. *Cell Death Differ* 2014, **21**(9)**:** 1432-1441.

261. Shi J, Wong J, Piesik P, Fung G, Zhang J, Jagdeo J, *et al.* Cleavage of sequestosome 1/p62 by an enteroviral protease results in disrupted selective autophagy and impaired NFKB signaling. *Autophagy* 2013, **9**(10)**:** 1591-1603.

262. Deosaran E, Larsen KB, Hua R, Sargent G, Wang Y, Kim S, *et al.* NBR1 acts as an autophagy receptor for peroxisomes. *Journal of cell science* 2013, **126**(Pt 4)**:** 939-952.

263. Liu L, Feng D, Chen G, Chen M, Zheng Q, Song P, *et al.* Mitochondrial outer-membrane protein FUNDC1 mediates hypoxia-induced mitophagy in mammalian cells. *Nat Cell Biol* 2012, **14**(2)**:** 177-185.

264. Wong YC, Holzbaur EL. Optineurin is an autophagy receptor for damaged mitochondria in parkin-mediated mitophagy that is disrupted by an ALS-linked mutation. *Proc Natl Acad Sci U S A* 2014, **111**(42)**:** E4439-4448.

265. Strappazzon F, Nazio F, Corrado M, Cianfanelli V, Romagnoli A, Fimia GM, *et al.* AMBRA1 is able to induce mitophagy via LC3 binding, regardless of PARKIN and p62/SQSTM1. *Cell Death Differ* 2015, **22**(3)**:** 419-432.

266. Yoshii SR, Kishi C, Ishihara N, Mizushima N. Parkin mediates proteasome-dependent protein degradation and rupture of the outer mitochondrial membrane. *J Biol Chem* 2011, **286**(22)**:** 19630-19640.

267. Karbowski M, Youle RJ. Regulating mitochondrial outer membrane proteins by ubiquitination and proteasomal degradation. *Curr Opin Cell Biol* 2011, **23**(4)**:** 476-482.

268. He C, Klionsky DJ. Regulation mechanisms and signaling pathways of autophagy. *Annual review of genetics* 2009, **43:** 67-93.

269. Nakaso K, Yoshimoto Y, Nakano T, Takeshima T, Fukuhara Y, Yasui K, *et al.* Transcriptional activation of p62/A170/ZIP during the formation of the aggregates: possible mechanisms and the role in Lewy body formation in Parkinson's disease. *Brain research* 2004, **1012**(1-2)**:** 42-51.

270. Matsumoto G, Wada K, Okuno M, Kurosawa M, Nukina N. Serine 403 phosphorylation of p62/SQSTM1 regulates selective autophagic clearance of ubiquitinated proteins. *Mol Cell* 2011, **44**(2)**:** 279-289.

271. Tanji K, Miki Y, Ozaki T, Maruyama A, Yoshida H, Mimura J, *et al.* Phosphorylation of serine 349 of p62 in Alzheimer's disease brain. *Acta neuropathologica communications* 2014, **2:** 50.

272. Matsuzawa Y, Oshima S, Nibe Y, Kobayashi M, Maeyashiki C, Nemoto Y, *et al.* RIPK3 regulates p62-LC3 complex formation via the caspase-8-dependent cleavage of p62. *Biochem Biophys Res Commun* 2015, **456**(1)**:** 298-304.

273. Althof N, Harkins S, Kemball CC, Flynn CT, Alirezaei M, Whitton JL. In vivo ablation of type I interferon receptor from cardiomyocytes delays coxsackieviral clearance and accelerates myocardial disease. *Journal of virology* 2014, **88**(9)**:** 5087-5099.

274. Feuer R, Mena I, Pagarigan R, Slifka MK, Whitton JL. Cell cycle status affects coxsackievirus replication, persistence, and reactivation in vitro. *Journal of virology* 2002, **76**(9)**:** 4430-4440.

275. Eskelinen EL. Roles of LAMP-1 and LAMP-2 in lysosome biogenesis and autophagy. *Molecular aspects of medicine* 2006, **27**(5-6)**:** 495-502.

276. Jager S, Bucci C, Tanida I, Ueno T, Kominami E, Saftig P, *et al.* Role for Rab7 in maturation of late autophagic vacuoles. *J Cell Sci* 2004, **117**(Pt 20)**:** 4837-4848.

277. Gutierrez MG, Munafo DB, Beron W, Colombo MI. Rab7 is required for the normal progression of the autophagic pathway in mammalian cells. *J Cell Sci* 2004, **117**(Pt 13)**:** 2687-2697.

278. Duran A, Amanchy R, Linares JF, Joshi J, Abu-Baker S, Porollo A, *et al.* p62 is a key regulator of nutrient sensing in the mTORC1 pathway. *Mol Cell* 2011, **44**(1)**:** 134-146.

279. Sancak Y, Peterson TR, Shaul YD, Lindquist RA, Thoreen CC, Bar-Peled L, *et al.* The Rag GTPases bind raptor and mediate amino acid signaling to mTORC1. *Science* 2008, **320**(5882)**:** 1496-1501.

280. Zhang X, Azhar G, Chai J, Sheridan P, Nagano K, Brown T, *et al.* Cardiomyopathy in transgenic mice with cardiac-specific overexpression of serum response factor. *Am J Physiol Heart Circ Physiol* 2001, **280**(4)**:** H1782-1792.

281. Figge MT, Osiewacz HD, Reichert AS. Quality control of mitochondria during aging: is there a good and a bad side of mitochondrial dynamics? *BioEssays : news and reviews in molecular, cellular and developmental biology* 2013, **35**(4)**:** 314-322.

282. Frank M, Duvezin-Caubet S, Koob S, Occhipinti A, Jagasia R, Petcherski A, *et al.* Mitophagy is triggered by mild oxidative stress in a mitochondrial fission dependent manner. *Bba-Mol Cell Res* 2012, **1823**(12)**:** 2297-2310.